Role of methyltransferases in fungal development and secondary metabolite production

Dissertation
for the award of the degree
"**Doctor rerum naturalium**"
Division of Mathematics and Natural Sciences
of the Georg-August University Göttingen

submitted by
Özlem Sarikaya Bayram
from Istanbul / Turkey

Göttingen 2013

Member of the Thesis Committee: **Prof. Dr. Gerhard H. Braus** (Reviewer I)

Department of Molecular Microbiology and Genetics, Institute of Microbiology and Genetics, Georg-August University Göttingen

Member of the Thesis Committee: **Prof. Dr. Stefanie Pöggeler** (Reviewer II)

Department of Genetics of Eukaryotic Microorganisms, Institute of Microbiology and Genetics, Georg-August University Göttingen

Member of the Thesis Committee: **Prof. Dr. Heike Krebber**

Department of Molecular Genetics, Institute of Microbiology and Genetics, Georg-August University Göttingen

Date of oral examination: 17.01.2014

Affirmation

I hereby declare that this thesis was written independently and with no other sources and aids than quoted.

Göttingen, 20.11.2013

Özlem Sarikaya Bayram

This doctoral study was performed in the group of Prof. Dr. Gerhard H. Braus, at the Department of Molecular Microbiology and Genetics at the Institute of Microbiology and Genetics, Georg-August University, Göttingen.

Some of the results of this doctoral study was peer-reviewed and published in the journal *PLoS Genetics* and some more results are currently under review for publication in a scientific journal.

Sarikaya Bayram O, Bayram O, Valerius O, Park H.S, Irniger S, Gerke J, Ni M, Han K.H, Yu J.H, and Braus G.H. (**2010**). LaeA control of velvet family regulatory proteins for light-dependent development and fungal cell-type specificity. ***PLoS Genet** 6*, e1001226.

Sarikaya Bayram O, Bayram O, Feussner K, Kim J.H, Kim H.S, Kaever A, Feussner I, Chae K.S, Han D.M, Han K.H, and Braus G.H. (**2013**). Membrane-bound methyltransferase complex VapA-VipC-VapB guides epigenetic control of fungal development. (under review)

To the memory of my beloved mother Mrs. Gülten Sarikaya

Table of contents

Summary

Fungal development and secondary metabolism are controlled by environmental signals through regulatory proteins. VeA protein is the founding member of the velvet superfamily of fungal regulators. It is involved in light response and coordinates sexual reproduction and secondary metabolism in *Aspergillus nidulans*. In the dark, VeA bridges VelB and LaeA proteins to form the VelB-VeA-LaeA (velvet) complex. The VeA-like protein VelB is a developmental regulator, whereas LaeA has been known as global regulator of secondary metabolism. In the first part of this study, it was shown that VelB forms a second light-regulated complex together with VosA, another member of the velvet family, which represses asexual development. LaeA directs the formation of the VelB-VosA and VelB-VeA-LaeA complexes and coordinates secondary metabolism during development. The *laeA* null mutant results in constitutive sexual differentiation, indicating that LaeA plays a pivotal role in inhibiting sexual development in response to light. Moreover, the absence of LaeA results in formation of significantly smaller fruiting bodies, which is due to the lack of a specific globose cell type (Hülle cells) that nurses the young fruiting body during development. This suggests that LaeA plays a dynamic role in fungal morphological and chemical development, and controls expression, interactions and modification of the velvet regulators. VeA represents a platform for protein-protein interactions for regulation of development and secondary metabolism. VeA platform function was further studied in the second part of this study, which focused on novel VeA interacting proteins (Vips) and their interaction partners. A yeast two-hybrid screen using VeA as bait led to the identification of a trimeric methyltransferase complex that connects signal transduction to epigenetic control. The novel complex contains the plasma membrane associated trimeric VapA-VipC-VapB proteins. The VipC-VapB heterodimeric methyltransferases of the complex are tethered to the plasma membrane by the FYVE-like zinc finger protein VapA allowing the nuclear VelB-VeA-LaeA complex to activate transcription for sexual development. Once the release from VapA is triggered, VipC-VapB is transported into the nucleus. VipC-VapB physically interacts with VeA, impairs its nuclear import and protein stability, which in consequence reduces the level of nuclear VelB-VeA-LaeA complex. Nuclear VapB methyltransferase diminishes the establishment of facultative heterochromatin by decreasing histone 3 lysine 9 trimethylation (H3K9 me3). This favors the activation of early regulatory genes *flbA* and *flbC,* which promotes the asexual program in presence of light. The VapA-VipC-VapB methyltransferase pathway combines control of nuclear import and stability of transcription factors with histone modification to foster appropriate differentiation responses.

Zusammenfassung

Pilzentwicklung und Sekundärmetabolismus werden durch Einwirkung von Umwelteinflüssen von Regulatorproteinen kontrolliert. Das VeA Protein repräsentiert die velvet-Domänen-Familie der Pilzregulatoren. VeA passt die sexuelle Entwicklung und den dazu gehörenden Sekundärmetabolismus von *Aspergillus nidulans* an die Lichtverhältnisse an. VeA bindet im Dunkeln an VelB und bildet schließlich den trimeren VelB-VeA-LaeA (velvet) Komplex. VeA dient als Brückenprotein für das velvet-Domänen-Protein VelB als Regulator der Entwicklung und die Methyltransferase LaeA als Regulator des Sekundärmetabolismus. VelB kann mit VosA einen zweiten licht-regulierten Komplex bilden, der die asexuelle Entwicklung reprimiert. Auch VosA gehört zur Familie der Velvet-Proteine. LaeA kontrolliert die Bildung der VelB-VosA und VelB-VeA-LaeA Komplexe während der Entwicklung. *laeA* Nullmutationen können nicht mehr auf Licht reagieren, was ihre Schlüsselrolle als Regulatoren der Entwicklung unterstreicht. Die Abwesenheit von LaeA führt zur Bildung von wesentlich kleineren Fruchtkörpern. Grund hierfür ist das Fehlen runder Hülle-Zellen, die den jungen Fruchtkörper ernähren und in seiner Entwicklung unterstützen. LaeA spielt damit eine dynamische Rolle während der morphologischen und biochemischen Entwicklung des Pilzes, indem die Expression, Interaktion und die Modifikation der velvet Regulatoren kontrolliert werden. Im zweiten Teil der Arbeit wurde die VeA-Plattform für Protein-Protein Interaktionen weiter untersucht. VeA interagierende Proteine (Vips) identifiziert in einen „Yeast-two-hybrid" System führten zu einem trimeren Methyltransferase-Komplex, der Signaltransduktion mit epigenetischer Kontrolle verbindet. Der neuartige Komplex enthält das Plasmamembran-assoziierte Trimer VapA-VipC-VapB. Das Dimer VipC-VapB ist über das FYVE-ähnliche Zinkfinger Protein VapA an die Plasmamembran gebunden und ermöglicht dem nuklearen VelB-VeA-LaeA Komplex die Aktivierung der Transkription der sexuellen Entwicklung. Sobald die Abkopplung vom VapA stattgefunden hat, wird VipC-VapB zum Kern transportiert. VipC-VapB interagiert physikalisch mit VeA, vermindert dessen Transport zum Kern und die Stabilität. Folglich wird der Anteil des VelB-VeA-LaeA Komplexes im Kern reduziert. Die nukleare VapB Methyltransferase vermindert die Entstehung des fakultativen Chromatins indem es die Histon 3 Lysin 9 Methylierung (H3K9 me3) vermindert. Dies begünstigt die Aktivierung der frühen Regulatorgene *flbA* und *flbC*, die dann das asexuelle Programm im Licht vorantreiben. Der VapA-VipC-VapB Methyltransferase-Weg vereinigt die Kontrolle des Kernimportes und der Stabilität von Transkriptionsfaktoren mit der Modifikation von Histonen. Erst dieses komplexe Zusammenspiel unterschiedlicher Mechanismen erlaubt eine angemessene Antwort für die Differenzierung des Pilzes.

1. Introduction

1.1. Posttranslational modifications and gene expression

Posttranslational modifications (PTM) of proteins, which usually represent the covalent attachment of a chemical group to an amino acid residue in a protein, play decisive roles for the life of an organism (Prabakaran et al., 2012). There are many PTMs and some of them include the phosphorylation, acetylation, glycosylation, hydroxylation, palmitoylation, nitration, ubiquitylation, sumoylation and methylation, which have great influence on many cellular processes, including the protein degradation, enzyme activity, subcellular localization, cell division, protein-protein interactions and gene expression (Karve and Cheema, 2011). Multiple combinations of the PTMs lead to a great variety for the number of molecular states of the proteins, which then contributes to the complexity of the sophisticated cellular information flow. PTMs of the various proteins essentially influence the expression of genes, of which methylation is the most important (Yang and Bedford, 2013). In addition to its role in various biochemical reactions, methylation also plays a direct regulatory role for the control of eukaryotic gene expression due to its influence on histone proteins and chromatin state.

1.1.1. Methylation reactions

Attachment or substitution of a methyl group on biomolecules is one of the crucial chemical reactions that take place in cells. Methylation is an alkylation process that leads to delivery of a methyl ($-CH_3$) group to the target molecule via a covalent bond (Smith and March, 2001). This definition is often used in chemical, biochemical as well as soil sciences and generally accepted chemical description of methylation reaction is the replacement of a hydrogen atom with a methyl group (Figure 1A). Methylation reactions in biological systems are mediated by a class of enzymes called methyltransferases. These enzymes methylate a diversity of substrates, including heavy metals, small organic molecules (O-methyltransferases), lipids, carbohydrates, proteins (protein methyltransferases), nucleic acids DNA (DNA methyltransferases) and RNA (RNA methyltransferases). Usually, methylation reactions require a cofactor, S-Adenosyl-L-Methionine (SAM) also called AdoMet (Figure 1B). SAM is generated from ATP and the amino acid methionine by the enzyme methionine adenosyltransferase (Struck et al., 2012).
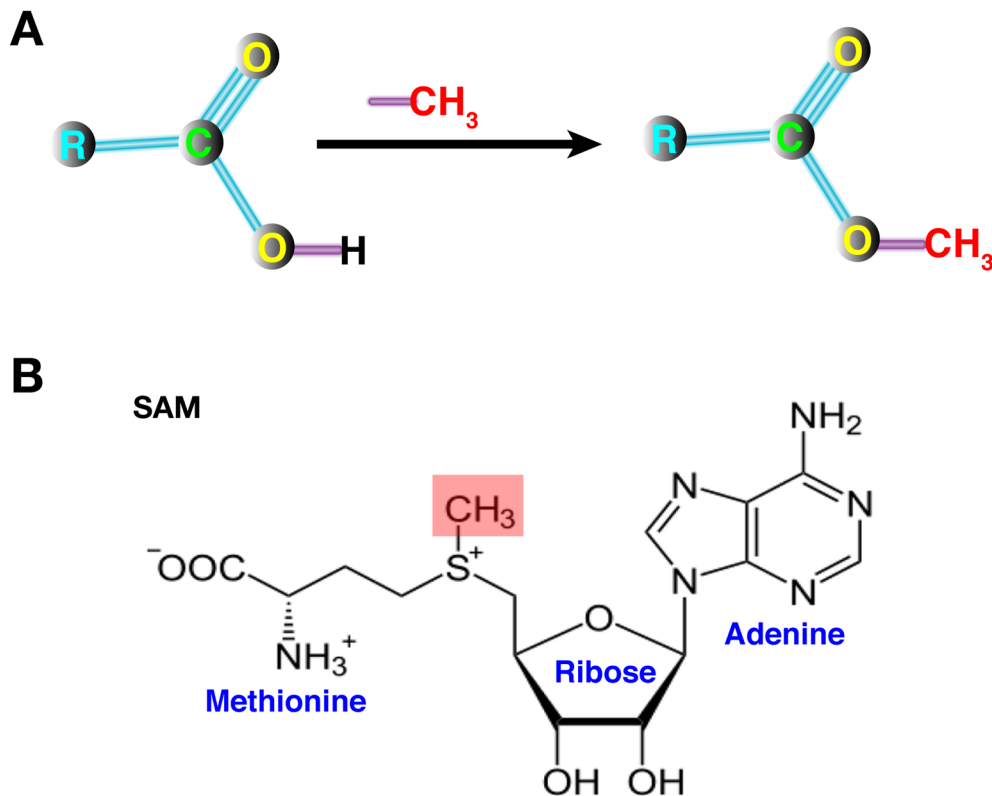
Figure 1. Simplified depiction of methylation reaction and chemical structure of S-Adenosyl L-methionine (SAM or AdoMet) molecule. **A.** Substitution of a hydrogen by a methyl molecule. **B.** Structure of SAM molecule. The reactive methyl group is shaded in red.

Attachment of a methyl group to the sulphur atom of methionine makes SAM chemically reactive, allowing the transfer of this methyl group to an acceptor substrate molecule via transmethylation reaction. It is one of the most common posttranslational modifications in proteins (Karve and Cheema, 2011).

Methylation of histone proteins and DNA has profound effect on the gene expression in eukaryotic organisms. Both modifications do not change the information stored in DNA but do change the level of gene expression (phenotype), which is commonly known as "*Epigenetics*".

1.1.1.1. Methylation of DNA

DNA methylation generally occurs at Cytosine-phosphate-Guanine (CpG) dinucleotide, causing the formation of 5-methylcytosine (5-mC). Cytosine is not the only DNA residue that can be methylated but the adenine is also methylated. The adenine methylation takes place in prokaryotes and is involved in postreplication

repair mechanisms. DNA methylation is a part of restriction modification system of many prokaryotes where DNA is frequently methylated in the adenine of a GATC consensus (G mATC) sequence by the Dam adenine methyltransferase (Low and Casadesus, 2008). Exogenous unmethylated foreign DNAs of viruses or other sources are cleaved and degraded by the sequence specific restriction enzymes, thereby protecting the bacteria from invading agents such as viruses. Therefore, DNA methylation is comparable to the immune defense system of higher organisms.

DNA methylation, which occurs at cytosine nucleotide in eukaryotes, is widespread in mammals and plant kingdom but limited in insects and fungi. For example, the filamentous fungus *Neurospora crassa* possesses DNA methylation but yeasts *Saccharomyces cerevisiae* and *Schizosaccharomyces pombe* as well as *Aspergillus nidulans* have almost completely lost the DNA methylation capability (Selker et al., 2003, Lee et al., 2008).

Methylation of DNA is involved in many processes, including genomic imprinting, supression of retroviral repetitive elements, cancer and X-chromosome inactivation. In mammalian genomes, almost 90% of the CpG dinucleotides are methylated, which has led to the deamination of 5-mC to thymine during evolution. Consequently, the unmethylated CpG dinucleotides are often clustered, also called "*CpG islands*", which are found in the promoter regions of many genes. Spontaneous hypermethylation of CpG islands in the promoters of oncogene supressor genes results in silencing of these genes, which therefore triggers cancer (Smith and Meissner, 2013).

1.1.1.2. Protein methylation

Methylation of proteins mostly takes place on either nitrogen atoms or oxygen atoms, but rarely on carbon atoms. Methylation of nitrogen atoms is preferred on the positively charged side chains of the proteins. The ε-amino ($-NH_2$), imidazole ring or guanidino groups of lysine, histidine and arginine, respectively, are the targets of the nitrogen methylation reactions (Fischle, 2012). The most common type of protein methylation occurs at the positively charged amino ($-NH_2$) group of lysine or arginine of histone proteins, strongly influences the expression of the eukaryotic genomes (Badeaux and Shi, 2013). The expressional state of eukaryotic genomes is controlled by the chromatin that is made from DNA and positively charged histone proteins.

1.1.2. Eukaryotic chromatin

The eukaryotic organisms have very large genomes, which are tightly packed into relatively small space of nucleus. This packaging of very extended DNA into such small volume requires the histones that are abundant nuclear proteins. There are five main class of histones present in eukaryotes; first four group includes H2A, H2B, H3, H4 that form the core histone and the fifth group contains the H1/H5 that act as linkers between the cores. Each two pairs of four core histones form the octameric nucleosome units. Histones possess positively charged side chains made of mostly lysine and arginine amino acids that facilitate the wrapping of the 147 bp negatively charged DNA around the histone core approximately 1.65 times (Luger et al., 1997, Struhl and Segal, 2013). This structure is called as nucleosome that represents the beads-on-a-string (10 nm fiber) form of chromatin. Binding of the linker histone H1 between the nucleosomes stabilizes the interaction of DNA with the histone cores and allows the establishment of higher order helical chromatin structure also called 30 nm fiber. However, the order of the nucleosomes in this structure is not completely resolved (Robinson et al., 2006). Further condensation of these fibers leads to rigid chromosomes representing the most compact form of metaphase chromosomes. The function of chromatin is not the only solely to package and fit the DNA into a tiny volume of nucleus, but also protect the DNA against shearing and damage (Chi et al., 2010). Furthermore, chromatin plays a vital role for gene expression and DNA replication. In an interphase nucleus, the chromatin is in the form of beads-on-a-string, which allows access of transcription and replication machineries. Interphase chromatin contains some segments that are actively transcribed called "*euchromatin*" (Figure 2A). When observed under microscope, euchromatin regions appear lighter in color. However, there are more tightly packaged segments called "*heterochromatin*". Replication of the heterochromatin takes place slowly during S-phase of the cell cyle (Grewal and Elgin, 2007). The genes found in heterochromatin are hardly expressed or not expressed at all. Heterochromatin can be divided into two parts, constitutive and facultative heterochromatin. Constitutive heterochromatin is constantly packed and covers the repetitive elements of the genome such as centromeres, telomeres and transposable elements, which serves as a constant block against recombination of these elements, therefore protects the stability of the genome. In contrast, facultative heterochromatin is more flexible and can be converted into euchromatin. Thus, the genes lying inside the facultative heterochromatin can be turned on or off depending

on environmental signals and developmental stages. This interconversion between the facultative heterochromatin and euchromatin is controlled by a combination of PTMs on histone proteins. These patterns of PTMs on histone proteins are also called histone codes that are recognized by the regulatory proteins (Figure 2B).

1.1.2.1. Histone codes

N-terminus of histone tails, which extends out of the nucleosome in the chromatin, undergoes many posttranslational modifications that serve as a signal for gene expression or silencing. Although the function of some modifications is known, the role of many histone PTMs is still elusive. PTMs of the histones constitute a complex language (Chi et al., 2010). This language is formed by the writer complexes and interpreted by the reader complexes. The composition of the writer and reader complexes is also very complicated (Fischle, 2012). There are five major types of known PTMs of histone tails, (I) phosphorylation, (II) acetylation, (III) sumoylation, (IV) ubiquitination, and (V) methylation (Figure 2B).

(I) Phosphorylation is historically the oldest known PTM of the histone proteins (Gutierrez and Hnilica, 1967). As many other proteins involved in cellular processes, phosphorylation of histones also takes place on serine or threonine residues. Phosphorylation of histone 3 serine 10 (H3S10) is the most intensively studied modification, which leads to activation of gene expression (Sassone-Corsi et al., 1999). However, hyperphosphorylation of H3 and H1 triggers the condensation of the chromosomes during mitosis (Shen et al., 1995).

(II) Acetylation is one of the most compherensively studied PTM catalyzed by histone acetyltransferases (HAT). Acetylation has mostly a positive influence on gene expression (Hebbes et al., 1988, Brownell et al., 1996). As it decreases the positive charge on the lysine residue and therefore reduces the affinity between the histone octamers and DNA.

(III) Modification of histone 4 by attachment of the small ubiquitin like modifier (SUMO) is an example of sumoylation influences gene expression at chromatin level. H4 sumoylation recruits histone

deacetylases (HDAC) that remove acetyl groups and repress the gene expression (Shiio and Eisenman, 2003). In *Saccharomyces cerevisiae*, lysine sumoylation of H4, H2A and H2B prevents positively acting acetylation and maintain the silencing of the genes (Nathan et al., 2006).
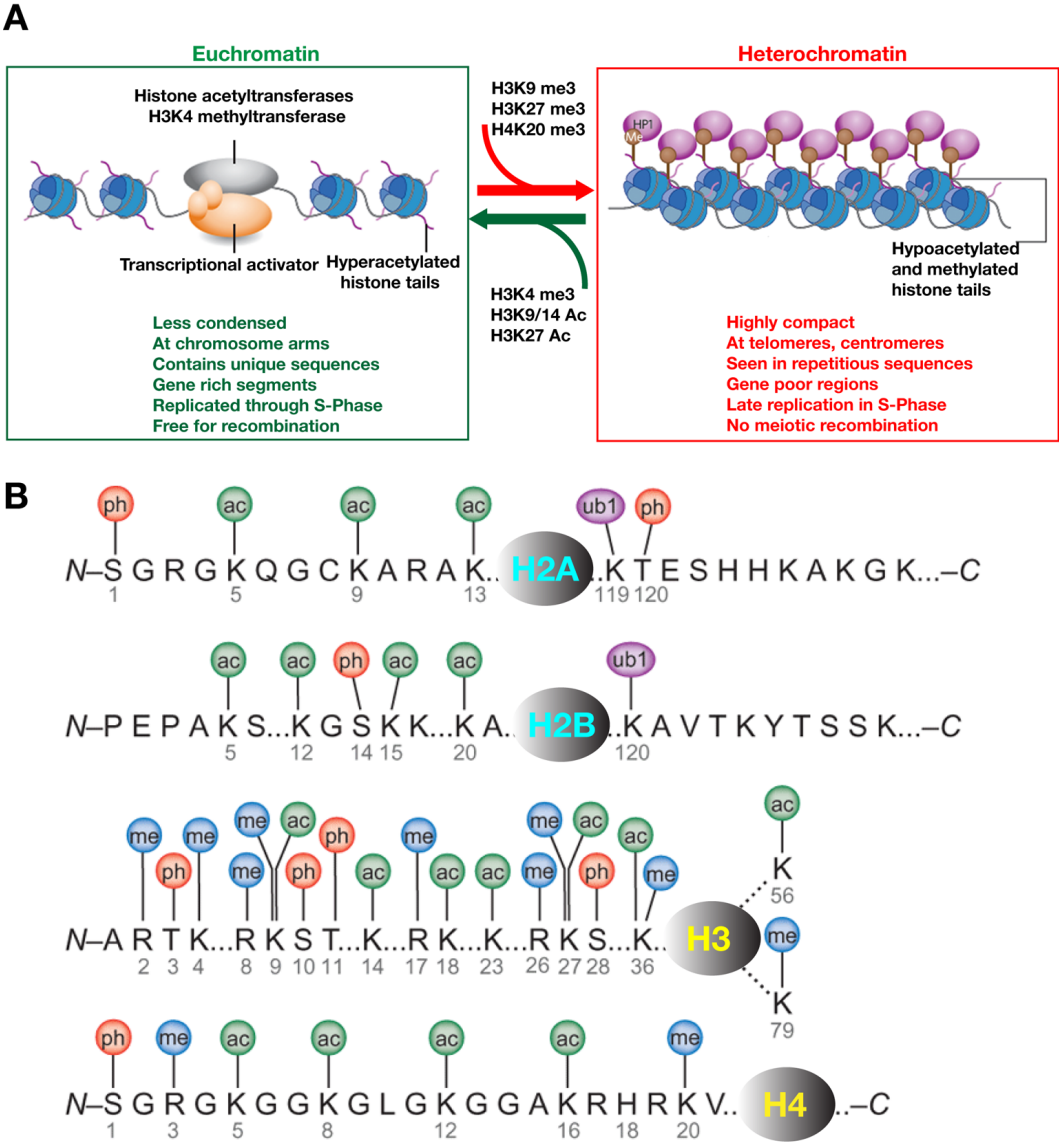
Figure 2. Eukaryotic chromatin and common posttranslational modifications on histone residues. A. Two states of eukaryotic chromatin, eu- and heterochromatin adapted from (Grewal and Elgin, 2007). **B.** PTM modifications of human nucleosomal histones modified from (Bhaumik et al., 2007). Modifications are phosphorylation (ph), acetylation (ac), methylation (me) and ubiquitination (ub1). N- and C- represent the amino and carboxy terminals of histone proteins. Numbers indicate the positions of amino acid residues. Most modifications appear at the N- terminus.

(IV)   Ubiquitination is one of the poorly understood modifications. However, it is tought that histone ubiquitinations support the ubiquitin pool in the nucleus and provide ubiquitin for ubiquitination reactions (Bond et al., 1988).

(V)   Methylation together with acetylation represents the most widely studied modifications (Bhaumik et al., 2007). Therefore, this modification will be analyzed in detail.

1.1.2.2. Modification of histones by histone methyltransferases

Amongst the all known histone modifications, methylation is the most complicated one and this modification can take place on many different residues. A residue can be mono-, di- or tri-methylated. Methylation of histones is catalyzed by the <u>h</u>istone <u>m</u>ethyl <u>t</u>ransferases (HMT) that are generally classified into two groups (I) lysine N-methyltransferases and (II) arginine N-methyltransferases. Both HMTs use SAM as a cofactor for their reactions. These enzymes can transfer one, two, or three methyl groups to a lysine or arginine residue, which frequently occurs at the histone H3 and H4. There are two types of lysine-specific HMTs; one of them is <u>Su</u>(var)3-9 <u>E</u>nhancer of zeste, <u>T</u>rithorax (SET) domain histone methyltransferase, which was originally discovered in fruit fly *Drosophila melanogaster* (Reuter et al., 1990) and the second one is non-SET domain HMT (Min et al., 2003). Arginine specific HMTs (PRMTs) modify their substrates in two different ways as mono- or dimethylation. Dimethylation appears either asymmetric or symmetric manner (Yang and Bedford, 2013).

1.1.2.3. Histone modifications (H3K4, H3K36 and H3K79) associated with active transcription

There are three types of common histone modifications that are linked with the actively transcribed genes. Those PTMs are methylations of H3K4, H3K36, and H3K79. These modifications are found in conjugation with the hyperacetylated form of H3K9 (Strauss and Reyes-Dominguez, 2010). The first two modifications (H3K4, H3K36) are catalyzed by the SET domain proteins, and the third one (H3K79) is mediated by a non-SET domain HMT.

SET domains consist of approximately 130 amino acids conserved catalytic domain where two motifs RFINHXCXPN and ELFXFDY (X any amino acid) are necessary for the function of the enzyme. Cysteins preceeding the SET domain form a zinc cluster that stabilizes the structure. Catalytic center of the SET domain possesses several β-sheet structures and small variations in those domains provide the target specificity for various substrates. SET1 proteins, which form a massive protein complex called "*COMPASS*" complex that is required for Histone 3 lysine 4 trimethylation (H3K4 me3), are conserved from yeast to human (Roguev et al., 2001, Krogan et al., 2002, Nagy et al., 2002). However, H3K36 me3 is mediated by the SET2 methyltransferase (Strahl et al., 2002).

Non-SET domain Dot1 HMT methylates the H3K79, which is important for transcriptional regulation, cycle progression, and DNA damage response. Different than SET domain proteins, C-terminal domain of Dot1 possesses a positive charge, permitting the protein interact with DNA (Feng et al., 2002, Min et al., 2003, Nguyen and Zhang, 2011).

1.1.2.4. Histone modifications (H3K9, H3K27 and H4K20) associated with gene silencing

H3K9 di- and trimethylation is a well-defined modification and signal for heterochromatin formation. Therefore, the presence of the H3K9 me2/3 is characteristic indication for the silencing of the genes in the vicinity of this histone mark. In fission yeast *S. pombe*, H3K9 methylation is initiated by the RNA-induced transcriptional silencing (RITS) complex, that later recruits H3K9 HMT Clr4 (Lejeune et al., 2010). Methylation of H3K9 attracts the heterochromatin protein 1 (Swi6 in yeast, HP1 in human) that binds to H3K9 me3 mark via its chromodomain. Accumulation of heterochromatin protein in H3K9 me3 sites results in gene silencing. Heterochromatin protein is almost exclusively present at the centromeres as well as telomeres of eukaryotic chromosomes except for yeast where silent information regulatory (Sir) proteins play similar roles (Kueng et al., 2013).

H3K27 me3 is catalyzed by the conserved polycomb repressive complex 2 (PRC2) (Tuncher et al., 2004). Once H3K27 is methylated, another subunit of the complex, PRC1 protein binds to histone N-terminal and catalyzes H2AK119 ubiquitination, which further induces chromatin condensation and gene repression

(Cao et al., 2002). Attachment of the methyl group to H4K20 is carried out by the Suv4-20 HMT and H4K20 me3 is frequently found in heterochromatin positions (Schotta et al., 2004).

1.2. The Fungal kingdom

Fungal organisms often possess haploid genomes suitable for genetic manipulations. This feature makes them excellent systems to study histone modifications and epigenetics. The fungi are not only used as model systems to study the eukaryotic development, cell biology and genetics, but also they are an integral part of our ecosystem. The fungal kingdom contains one of the highly heterogeneous groups of eukaryotic organisms with roughly estimated 1.5 million members (Hawksworth and Rossman, 1997). Recent estimates based on high-throughput sequencing of a soil community suggest as many as 5.1 million fungal species (O'Brien et al., 2005, Blackwell, 2011). However, only 90.000-100.000 species, a small fraction, have been described in scientific literature.

The presence of a cell wall composed of chitin is unique to fungi and insects when compared to those of plants and some of the protists, which have the cellulose polymers. Heterogenicity and plasticity of the fungal organisms, including the unicellular yeast, multicellular molds and macroscopic mushrooms make them widely distributed in all temperate regions of earth (Raspor and Zupan, 2006).

Some fungal species as mushrooms and truffels are consumed as direct food source. They are also used in food industry as leavening agent in bakeries, and in fermentation of various alcoholic beverages as well as soya souce. Application of biotechnological methods to fungi provides an immense source of industrially important enzymes, and chemical compounds. Saprophytic behavior of most fungi plays an essential role in decomposition and recycling of organic materials in the ecosystem, therefore provides significant contribution to the nutrient recycling and continuation of the life on our planet (Blackwell, 2011). The majority of the plant species has symbiotic interactions with the special arbuscular mycorrhizal fungi, which supports the survival of the plants and forests. Fungi also attract attention as pathogens of animals, human beings and plants. More than 10% of the world´s crop harvest is either spoiled or contaminated by the fungi, corresponding to an amount that can feed ~600 million people (Normile, 2010). Therefore, understanding the physiology, development, genetics, metabolism, and behavior of fungi is essentially

important in order to prevent the losses caused by fungi and simultaneously to increase the yield of beneficial matters produced by fungi.

1.2.1. The filamentous fungus *Aspergillus nidulans* as a model system for development and secondary metabolism

The filamentous fungus *Aspergillus nidulans*, which belongs to the ascomycetous fungi, is a tractable eukaryotic model system to study the cell biology, genetics, biochemistry as well as secondary metabolism. Moderate size of the genome (30 million bp) with eight haploid chromosomes and the presence of sexual cycle provide a unique opportunity for the use of this fungus in genetic studies (Galagan et al., 2005, Bayram and Braus, 2012). The influence of gene deletions or mutations can be easily observed as a phenotype due to the haploid nature of the genome. As many other fungi, *A. nidulans* grows by forming polar hyphae where similar cellular units are reiterated. The tip as well as branch points of the filamentous hyphae show increased cellular activity. Highly specialized cells include the ubiquitous airborne asexual spores that are often dispersed into the air for propagation. Especially, sexual spore formation can require complicated fruiting bodies consisting of additional specialized cells which form various tissues (Braus et al., 2002, Pöggeler et al., 2006, Sohn and Yoon, 2002).

A variety of signals control the above-mentioned developmental processes of fungi. One of the cues regulating the development of *A. nidulans* is the light signal. As all organisms living on the earth, *A. nidulans* also uses the light signal as a messenger to be aware of the environmental conditions. It is a soil dwelling fungus, therefore, being on or under the surface makes drastic differences in terms of abiotic and biotic factors (Rodriguez-Romero et al., 2010). For example, being on the surface means that the fungus is exposed to light, high concentration of oxygen, osmotic stress, high reactive oxygen species (ROS), and temperature shifts. However, growth under the soil provides low levels of oxygen, humidity, low ROS levels and less temperature fluctuations. Light induces asexual sporulation (conidiation) and represses sexual (fruiting body) formation. There are primarily two spectra of light, red (650-680 nm) and blue (400-450 nm) that affect the development. Although both types of light qualities induces asexual program, the influence of red light is stronger than the blue light. The light responses in *A. nidulans* are mainly mediated by a

diversity of light receptor proteins, including the red-light receptor phytochrome FphA, and blue-light receptors LreA and LreB and UVA-blue light receptor CryA (Blumenstein et al., 2005, Purschwitz et al., 2008b, Bayram et al., 2008a, Bayram et al., 2010). However, the phytochrome protein masks the influence of other light receptors on development. Deletion of the phytochrome encoding gene *fphA* results in an increase in the number of sexual fruiting bodies (cleistothecia) under red light conditions (Blumenstein et al., 2005). A mutant of cryptochrome-like *cryA* is blind to UVA light and therefore produces more cleistothecia under UVA light. Phytochrome FphA interacts with a variety of proteins, including the blue light receptors LreA/LreB as well as the light-dependent morphogenetic regulator VeA protein during control of development (Purschwitz et al., 2008).

1.2.2. Asexual propagation in *A. nidulans*

Formation of asexual conidiophores is initiated when the fungus completes its vegetative growth and becomes competent for reception of environmental signals (Figure 3). A specialized vegetative cell, also called "*foot cell*" buds from the vegetative hypha and elongates to form the stalk. Growing stalk swells, forming vesicle that gives rise to finger-like metulae and phialides. The phialides are the uttermost structures that produce mitotic asexual spores (conidia) that disseminate into the air to reach new habitats (Adams et al., 1998, Etxebeste et al., 2010, Park and Yu, 2012). Asexual development of the fungus is controlled by a cascade of transcription factors. BrlA is a C_2H_2 zinc finger transcription factor required for the foot cell and stalk formation. *brlA* mutant forms bristle-like long aerial hyphae instead of conidiophores (Park and Yu, 2012).

To initiate conidiation and to activate downstream regulatory proteins, upstream regulatory fluffy genes, *fluG, flbA, flbB, flbC, flbD*, and *flbE* that encode cell signaling elements and various transcription factors, are required (Adams et al., 1998, Wieser et al., 1994, Wieser and Adams, 1995, Kwon et al., 2010a, Kwon et al., 2010b). These genes are necessary for *brlA* gene activation. Diffusible extracellular factor, meroterpenoid dehydroaustinol and diorcinoal are necessary for initiation of asexual conidiation and *fluG* mutants cannot induce secretion of these chemicals (Rodriguez-Urra et al., 2012). FluG protein inhibits the vegetative growth and induces asexual differentiation by activating transcription of FlbA protein that is a regulator of G-protein signaling (RGS) (Yu et al., 1996).
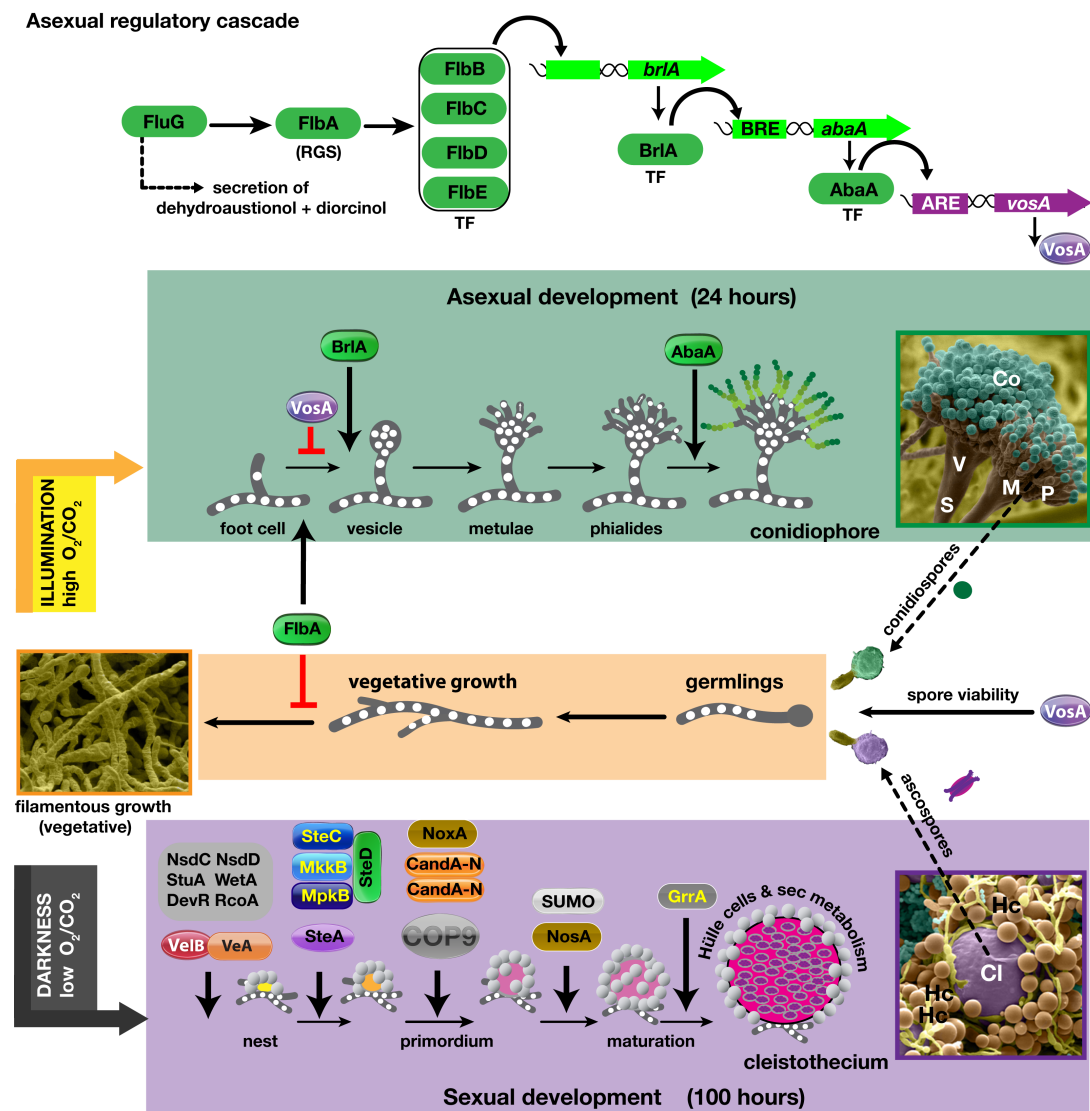
Figure 3. Life stages and light-dependent development of the filamentous fungus *A. nidulans.* The life cycle of *A. nidulans* was adapted from the pictures (Sarikaya Bayram et al., 2010, Bayram et al., 2012a). Germination of either asexual conidiospore or sexual ascospore leads to the vegetative hyphae that become competent for environmental signals 12-20 h postgermination. Upon environmental signals (e.g. light and high O_2/CO_2 ratio), the competent hyphae initiate the asexual program (detailed regulatory cascade is shown in upper panel) that ends up with the conidiophores carrying green-colored chains of conidia. Lack of light together with low O_2/CO_2 ratio triggers sexual differentiation, which results in closed sexual fruiting bodies (cleistothecia). Factors influencing both developmental programs are shown for each stage. V; vesicle, S; Stalk, M; metulae, P; phialides, Co; conidia, Cl; cleistothecium, Hc; Hülle cells, RGS; regulator of G-protein signaling, TF; transcription factor.

Activation of FlbA pathway inactivates the vegetative proliferation by counteracting a heterotrimeric G protein complex required for vegetative growth (Seo

et al., 2005). Simultaneously, FluG also activates the asexual pathway of transcription factors FlbB/FlbC/FlbD and FlbE. FlbC, which is a putative C_2H_2 zinc finger transcription factor, binds to the *cis* regulatory elements in *brlA* promoter. BrlA binds to B̲rlA r̲esponse e̲lement (BRE) at the promoters of the next transcription factors, including AbaA that is essential for proper seperation of conidia from the finger-like phialide structures (Sewall et al., 1990, Andrianopoulos and Timberlake, 1994, Adams et al., 1990). AbaA TF further activates the expression of genes necessary for spore color (*yA* gene encoding laccase), and maturation (*vosA*) by binding to A̲baA r̲esponse e̲lement (ARE). V̲iability o̲f s̲pores, *vosA*, which encodes one of the velvet family fungal specific protein, is responsible for trehalose accumulation and viability of asexual and sexual spores (Ni and Yu, 2007).

1.2.3. Sexual fruiting body formation in *A. nidulans*

Sexual events that are initiated and maintained by the regulatory proteins encoded by the mating type loci in fungi (Ni et al., 2011). There are frequently two mating type loci that encode transcription factors for sexual development. Depending on the presence of one or both mating type genes in the genome of a fungus, fungi are called heterothallic (self-sterile) or homothallic (self-fertile), respectively. Heterothallic fungi need a mating partner with an opposite mating type gene in order to undergo sexual development. Homothallic *A. nidulans*, which possesses the both mating type genes, is able to mate itself and undergoes sexual differentiation. When the conditions are favorable for sexual development (e.g in the dark), first a specialized aggregate of hyphae "*nest*" is formed. In the nest, fusion of two fungal hyphae leads to heterokaryons that carry different identity of nuclei (dikaryotic). These dikaryotic ascogenous hyphae lead to the "*crozier*" structures where the topmost crozier cell traps two nuclei that fuse to form a zygote. The zygote undergoes meiosis and mitotis, which ends up with a sac-like structure, containing 8 meiotically formed binucleate ascospores (Sohn and Yoon, 2002). Meanwhile, surrounding mycelia are also subject to differentiation to build the multilayered cleistothecia envelope. Sexual development of the fungus *A. nidulans* leads to formation of the closed form of fruiting bodies named cleistothecia that contain meiotically formed ascospores. Each cleistothecium may contain up to 80.000 viable ascospores. These fruiting bodies are covered by the globose Hülle cells that play a role for protection and nursing of sexually formed cleistothecia (Figure 3).

Sexual development of the fungus is also regulated by a repertoir of regulators. According to Dyer and Gorman (Dyer and O'Gorman, 2012), at least 78 genes, which are linked with sexual reproduction, have been identified in *A. nidulans*. However, not all of those genes are completely required for fruiting body formation. Therefore, the genes essential for fruiting body will be further discussed.

Lipid derived fungal hormones: A unique class of fungal pheromones, precocious sexual inducer (*psi*) factors, which are oxylipins, derived from lipid acids, regulate the balance between sexual and asexual development. Defects in the genes (*ppoA*, *ppoB*, and *ppoC*) responsible for the synthesis of *psi* factors give rise to a drastic perturbation in balance between sexual and asexual developments (Tsitsigiannis et al., 2004, Tsitsigiannis et al., 2005).

Signal transduction pathway components: There are a number of G-protein coupled signal transduction pathways identified in *A. nidulans*. Either deletion of the genes encoding the PreA and PreB G-protein coupled receptor proteins (GPCR), or the genes encoding any of the heterotrimeric G protein (α; FadA, β; SfaD, γ; GpgA) result in acleistothecial phenotype. Furthermore, RGS FlbA protein (mentioned earlier in 1.2.2.) is also required for sexual development. Particularly, the yeast pheromone response pathway homologs in *A. nidulans* play vital roles in fruiting body formation (Vallim et al., 2000, Wei et al., 2003, Paoletti et al., 2007, Bayram et al., 2012a). A complete set of the mitogen activated protein (MAP) kinase cascade is present in *A. nidulans*. These elements are MAPKKK Ste11 homolog SteC, MAPKK Ste7 homolog MkkB, and MAPK Fus3 homolog MpkB that physically interacts with a homeodomain transcription factor SteA, a homolog of yeast Ste12p transcription factor (Bayram et al., 2012a). Yeast Ste50 adaptor protein homolog SteD in *A. nidulans* is also responsible for sexual development. However, any homolog of yeast scaffold protein Ste5 in *A. nidulans* genome has not been identified by either bioinformatics or biochemical approaches (Paoletti et al., 2007, Bayram et al., 2012a). Without any exception, strains carrying mutant versions of those genes cannot develop sexually exhibiting acleistothecial phenotype. However, the deletion strains are still able to produce primitive nests encompassed by Hülle cells. It has been shown that deletion strains are not able to form initial hyphal fusions that are necessary for the first committed step of sexual development.

Transcription factors: There are several putative transcription factors that are crucial for cleistothecia formation. First group of the transcription factors is the <u>n</u>ever in <u>s</u>exual <u>d</u>evelopment (*nsd*) genes that were identified as a result of UV mutagenesis screen. Two of the *nsd* group genes *nsdC* and *nsdD* encode putative zinc finger domain transcription factors and their deletions lead to loss of cleistothecia during sexual development (Han et al., 2001, Kim et al., 2009). *Sordaria macrospora* Pro1 homolog of *A. nidulans* encoded by *nosA* gene plays a vital role in maturation of cleistothecia (Vienken and Fischer, 2006). *nosA* deletants have often small (30 μm instead of 200 μm) sized immature cleistothecia which do not have any ascospores. In contrast to aforementioned transcription factors that are prerequisite for sexual propagation, two transcription factor encoding genes *stuA* and *wetA* are both necessary for sexual as well as asexual development. *stuA* and *wetA* encode putative <u>b</u>asic <u>h</u>elix-<u>l</u>oop-<u>h</u>elix (bHLH) type transcription factors and knock-out strains are completely acleistothecial and generates abnormal conidiophores (Busby et al., 1996, Wu and Miller, 1997). Similar to *stuA* and *wetA*, *devR*, which also encodes a bHLH transcription factor, functions as an activator of sexual development as well as asexual conidiation (Tuncher et al., 2004). *rcoA* gene encoding the Tup1 homolog of yeast Tup1-Ssn6 general repressor system in *A. nidulans* influences both developmental pathways (Todd et al., 2006).

Velvet complex: The trimeric velvet complex, comprising of the VelB-VeA-LaeA, is required for fruiting body formation. VelB and VeA proteins belong to the velvet superfamily proteins that are well-conserved in the fungal kingdom (Bayram and Braus, 2012). In *A. nidulans*, there are four velvet family proteins, VeA, VelB, VelC and VosA. The founding member of the family, VeA protein acts as a bridge between the VelB protein and LaeA methyltransferase that is the global regulator of secondary metabolism (Bok and Keller, 2004). Deletion of both *veA* and *velB* genes result in loss of cleistothecia and brown pigmentation (Kim et al., 2002, Bayram et al., 2008b). Overexpression of *veA* gene promotes formation of numerous cleistothecia even in the light.

Cellular protein degradation machineries: Deficiencies of the genes controlling protein degradation machineries impair the fungal development. Deletion of the various subunits of COP9 signalosome (CsnD, CsnE) in *A. nidulans* causes an early block in fruiting body formation at primordia stage (Busch et al., 2003, Busch et

al., 2007). In addition to the blockage at primordia phase, COP9 mutants also exhibit a constitutive sexual development even under light conditions. The cullin-associated and neddylation-dissociated (CAND) mutants of *A. nidulans* are also unable to finalize the sexual development and blocked at early primordia stage (Helmstaedt et al., 2011). An important subclass of E3 ubiquitin ligases, Skp1-Cullin-F-box (SCF) complexes are also important for sexual development. It was shown that in the absence of yeast F-box protein Grr1 homolog, GrrA leads to the cleistothecia devoid of ascospores, suggesting that GrrA is involved in meiosis during ascosporogenesis (Krappmann et al., 2006). The defects in *A. nidulans* SUMO pathway also result in tiny cleistothecia that are empty of ascospores (Harting et al., 2013).

Other metabolic regulators: One of the physiological signal associated with differentiation is the cellular oxidation stage. *noxA* gene encodes a NADPH oxidase that generates reactive oxygen species. Lack of *noxA* results in a developmental block at the initial stage of sexual development. However, *noxA* mutants produce masses of Hülle cells (Lara-Ortiz et al., 2003). The cross pathway control genes *cpcA* and *cpcB* function in sensing of amino acid levels and regulate sexual development under limiting amino acid conditions (Hoffmann et al., 2001, Hoffmann et al., 2000). Deletion strains cannot proceed beyond the microcleistothecia stage and produce only Hülle cells.

1.3. Coordination of development and secondary metabolism

Natural products (amino acids, proteins, carbohydrates, lipids) of living organisms provide an essential fuel for the maintenance of the life on earth. Some natural products of fungi, plants and bacteria, also called secondary metabolites, are especially important for human health and pharmaceutical industry due to their potent influence on various physiological cellular processes (Keller et al., 2005, Brakhage, 2013). The fungal secondary metabolites are usually classified into four groups according to their biosynthetic origin or enzyme classes: (I) Polyketides, (II) Non-ribosomal peptides, (III) Terpenes and (IV) Indole alkaloids (Keller et al., 2005). The biological activities of secondary metabolites (SM) include mycotoxins, antibiotics, anti-tumor, -viral, -protozoan, -fungal and cytotoxic properties. In contrast to primary metabolism, secondary metabolites of fungi are not indispensable for the life of the fungus. However, they provide some advantages for the fungus to deter the competing organisms or predators, including bacteria, insects, molluscs, nematodes and

predatory amoebas (Caballero Ortiz et al., 2013, Doll et al., 2013). The genes encoding the secondary metabolites are often clustered in the subtelomeric segments of the fungal chromosomes (Bok et al., 2006). Therefore, they are easily co-regulated by the activating transcription factors that are mostly embedded in the cluster.

A. nidulans produces many secondary metabolites, the two important metabolites among them include the mycotoxin sterigmatocystin (ST) and antibiotic penicillin (PN). Sterigmatocystin is the penultimate precursor of aflatoxins that cause severe liver damage and hepatocellular carcinoma. Aflatoxins are produced by *A. flavus* as well as *A. parasiticus* species. The genes responsible for the biosynthesis of ST is clustered in a ~60 kbp subtelomeric region of the chromosome IV and are controlled by a cluster specific binuclear zinc finger transcription factor AflR (Brown et al., 1996, Fernandes et al., 1998). The ST as well as other gene clusters are regulated at the highest hierarchical level by the global regulator of secondary metabolism <u>l</u>oss of <u>afl</u>R <u>e</u>xpression <u>A</u> (LaeA) (see next page). Production of the secondary metabolites takes place at certain stages of development and defects in fruiting body formation often impairs secondary metabolite production (Bayram and Braus, 2012). The morphological development and secondary metabolism are coordinated by the regulatory protein complexes that either act as transcriptional activators or epigenetic regulators.

1.3.1. The trimeric VelB-VeA-LaeA complex at the interface between secondary metabolism and development

VeA and VelB are responsible for cleistothecia formation. However, they are not only necessary for sexual development but also for the production of ST and PN. Deletion mutants of *veA* and *velB* cannot express the ST gene cluster. In contrast, LaeA does not possess any morphogenetic consequences but exclusively control expression of secondary metabolite genes (Bok and Keller, 2004). The molecular mechanism underlying this phenomenon was revealed by a study where the authors showed that these proteins form a complex. The velvet complex, comprising the two velvet family proteins VelB-VeA and the methyltransferase LaeA control the development and production of secondary metabolites (Bayram et al., 2008b) (Figure 4). VeA protein, which is the founding member of the velvet family proteins, bridges the VelB protein to the global regulator of secondary metabolism. During illumination, the light-dependent regulatory protein VeA is mostly cytoplasmic (Figure 4). However,

incubation of the fungus in the dark leads to nuclear accumulation of the protein. In the course of nuclear import, VeA associates with VelB and co-import into the nucleus by the help of α-importin KapA. In the nucleus, VeA-VelB dimer further recruits the LaeA methyltransferase, which establishes the trimeric velvet complex that drives the expression of sexual as well as secondary metabolite genes.
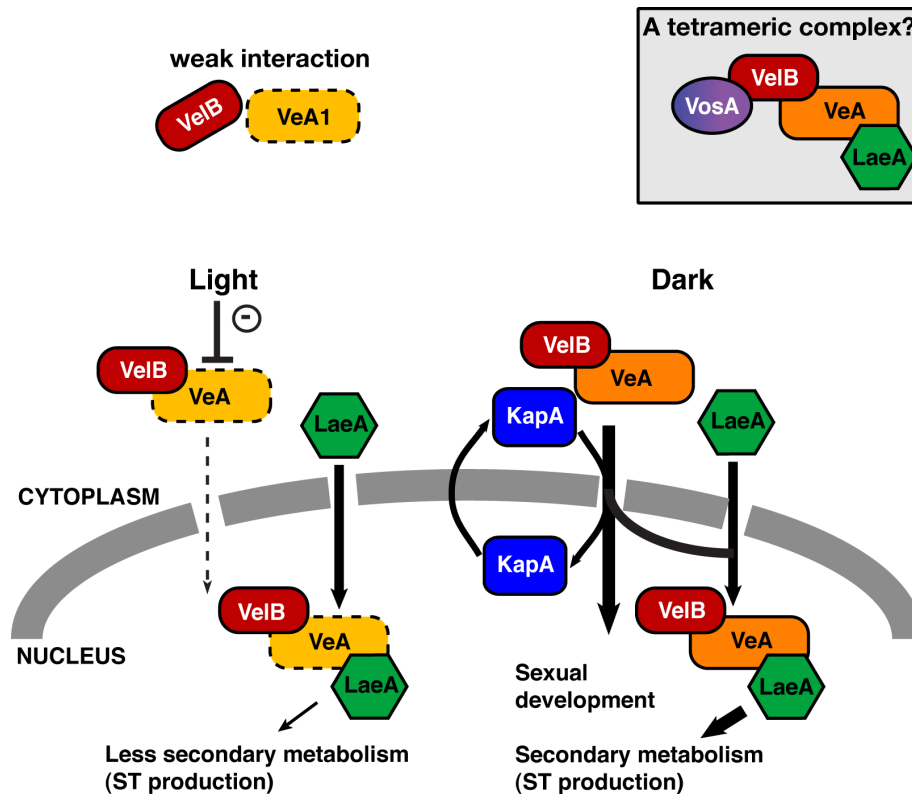
Figure 4. Control of development and secondary metabolism by the trimeric velvet complex. The model was adapted from (Bayram et al., 2008b). See the text for further details.

Many laboratory strains possess the *veA1* allele that encodes a truncated version of VeA. VeA1 protein lacks the first 36 amino acids at its N-terminus, due to a point mutation at start codon (Kim et al., 2002). Interaction of VeA1 with VelB is reduced, but it can interact with the LaeA (Bayram et al., 2008b). VeA1 protein exhibits more cytoplasmic distribution (Stinnett et al., 2007).

VeA protein also forms a complex with the red-light receptor FphA, which can be a functional connection between the light-dependent development and secondary metabolism (Purschwitz et al., 2008b). However, this interaction of VeA seems to be rather transient, because Bayram and co-workers could not identify any components of the light complex FphA-LreA-LreB as VeA interacting proteins

(Bayram et al., 2008b). Although detailed dissection of FphA-VeA interaction showed that histidine kinase domain of FphA physically interacts with VeA, but it does not phosphorylate the VeA protein (Purschwitz et al., 2009).

Pheromone MAPK pathway of *A. nidulans* in addition to its role in sexual fruiting body formation also plays crucial roles in secondary metabolism. AnSte50-AnSte11 (MAPKKK)-AnSte7 (MAPKK)-AnFus3 (MAPK) module is essential for ST production (Bayram et al., 2012a). Expression of both ST and PN genes are downregulated in the mutants of the MAPK pathway. Intriguingly, the *A. nidulans* pheromone module behaves different than yeast. The complete tetrameric module upon receiving the signals from plasma membrane migrates to the nuclear envelope where AnFus3 is released into the nucleus. AnFus3 interacts with VeA in the nucleus and phosphorylates the VeA protein in *vitro*. In the absence of AnFus3, interaction between VeA-VelB weakens, suggesting a sustaining role of AnFus3 for the velvet complex formation. Furthermore, this interaction provides evidence that VeA acts as a platform for the reception of different environmental signals including light, and pheromones. For this platform hypothesis, further evidence comes from a recent study, where a Laea like methyltransferase F (LlmF) interacts with VeA protein and prevents the nuclear import of VeA (Palmer et al., 2013). *llmF* mutants show increased VeA nuclear accumulation associated with elevated sexual development and ST production. Whereas overexpression of LlmF causes slightly decreased VeA nuclear import. However, exact molecular mechanism remains to be shown.

Bok and co-workers have recently shown a negative influence of VeA on the archetypal polyketide orsellinic acid (OA) gene cluster (Bok et al., 2013). Transcript levels of the OA gene cluster are elevated in *veAΔ* strains and therefore, *veA* mutants produce OA and its derivatives F9775B/A that possess anti-osteoporosis effect. The OA gene cluster is silenced under normal culture conditions and induced upon physical contact with the bacterium *Streptomyces rapamycinicus* (Schroeckh et al., 2009). COP9 mutants of *A. nidulans* also accumulate OA and the transcripts of the OA gene cluster are strongly upregulated in the mutants (Nahlik et al., 2010).

1.3.2. Roles of methylation and acetylation in epigenetic control of fungal development and secondary metabolism

The subtelomeric position of the SM gene clusters provides a unique mechanism to control many genes by the eukaryotic chromatin. Histone proteins that constitute the fungal chromatin are the substrate of various modifications as mentioned earlier (1.1.2.1). Especially, the methylation and acetylation of histones participate the local control of gene expression in the SM gene clusters. ST gene cluster is silenced by increased H3K9 me3 marks and heterochromatin protein HepA during the active growth of the organism. When the fungal growth stops, ST genes are activated by acetylation of histones and a decreased levels of H3K9 me3 (Strauss and Reyes-Dominguez, 2010). There are several other factors that regulate the modification of histones and expression of gene clusters.

LaeA methyltransferase: LaeA protein acts as a global regulator by influencing chromatin structure (Figure 5). Large scale microarray studies with *A. nidulans laeA* mutant showed that ST, PN as well as some other gene clusters are downregulated in the absence of LaeA (Bok et al., 2006). Similary, the 13 out of 22 gene clusters in *A. fumigatus* are expressed at very low levels in *laeAΔ* strain, suggesting that more than half of the secondary metabolite gene clusters depend on LaeA activity (Perrin et al., 2007). However, there are no solid data that LaeA directly regulates the modification of histones. Recently it has been shown that LaeA has an automethylation activity on methionine 207 that is not required for the *in vivo* function of LaeA on secondary metabolism (Patananan et al., 2013). In this study, the authors also could not show histone methyltransferase activity of LaeA. The evidence of LaeA involvement in epigenetic control comes from chromatin immunoprecipitation (ChIP) experiments that showed increased H3K9 me3 marks and heterochromatin occupancy in the *aflR* promoter of ST gene cluster in a *laeA* mutant (Reyes-Dominguez et al., 2010).

H3K9 methyltransferase and heterochromatin protein: Heterochromatin protein (HepA) of *A. nidulans* recognizes and binds to H3K9 me3 marks created by H3K9 methyltransferases to condense the given chromatin segment. Yeast Clr4 homolog, ClrD of *A. nidulans* represents the H3K9 methyltransferase containing pre-SET domain (Figure 5). Targeted deletions of the *clrD* as well as heterochromatin *hepA* gene do not cause any morphological changes (Reyes-Dominguez et al., 2010).

However, the transcripts of ST gene cluster increase in both *clrD* and *hepA* mutants whereas the expression of the genes outside of ST cluster remains unchanged.
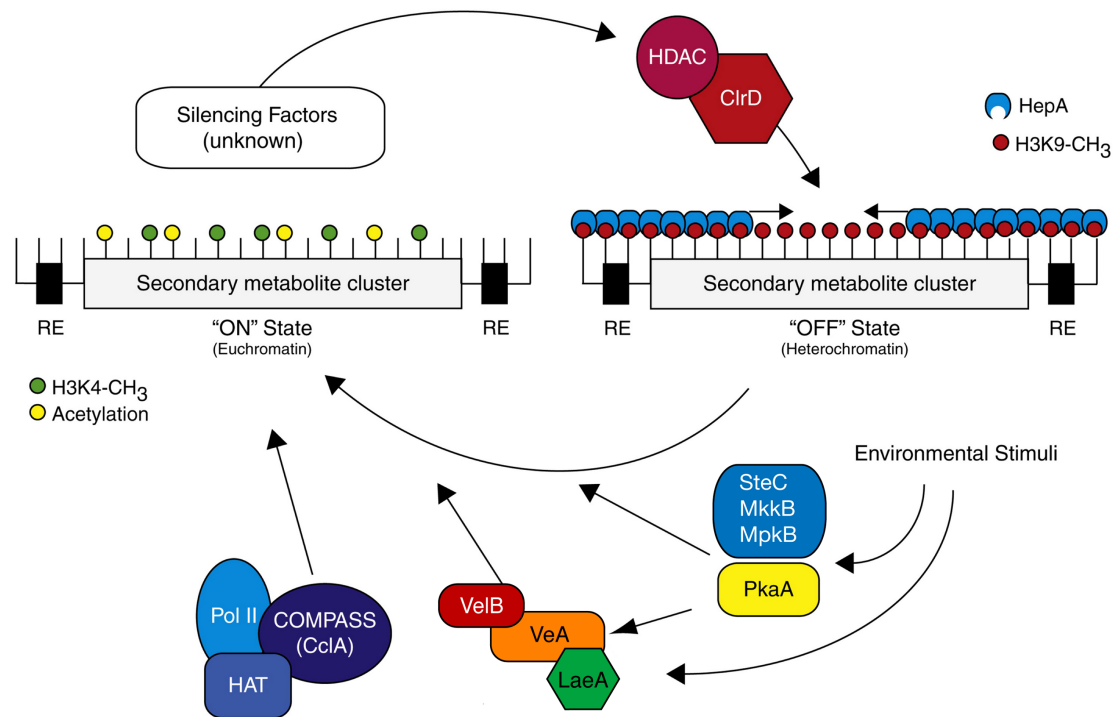
Figure 5. Epigenetic regulation of secondary metabolite gene clusters in *A. nidulans*. The model was modified from (Palmer and Keller, 2010). Repetitive elements (RE) often surround the secondary metabolite gene clusters. On-state of chromatin is associated with the activation marks, including methylation of H3K4 and acetylation of H3K9. COMPASS complex promotes the H3K4 marks and subsequent acetylation by HAT enzymes. Environmental signals are transduced via MAPK pathway (SteC-MkkB-MpkB) or protein kinase A (PkaA) (Ni et al., 2005, Shimizu et al., 2003). Histone deacetylases (HDACs) and H3K9 methyltransferase together with the heterochromatin protein HepA repress the SM gene expression in the off-state of chromatin.

H3K4 methyltransferase COMPASS complex: *A. nidulans* genome encodes all components of H3K4 methyltransferase complex, which is also named COMPASS complex. The COMPASS complex contains eight subunits made of SET domain proteins (see 1.1.2.3). Deletion of two subunits (*setA* and *cclA*) show identical phenotypes, which are characterized by pleitrophic phenotypes, including drastically impaired growth, brown pigmentation, and lack of sexual fruiting bodies (Bok et al., 2009, Harting et al., 2013). These phenotypes suggest that they are not only involved in secondary metabolism but also in primary metabolic processes causing such severe defects. *cclA* (H3K4 HMT) mutant produces antimicrobial monodictyphenone and

emodines that have anti-mutagenic, anti-cancer, immunosuppressive and anti-inflammation activities (Bok et al., 2009).

Histone acetyltransferases (HAT) and deacetylases (HDAC): As in other eukaryotic organisms, histones are acetylated at certain residues during gene activation in *A. nidulans*. In general, HAT enzymes have activating and HDAC enzymes have inhibitory role for secondary metabolite gene clusters. Because treatment of fungal cultures with HDAC inhibitor trichostatin leads to the overproduction of several metabolites and transcriptional activation of telomere proximal gene clusters (Shwab et al., 2007). However, telomere distal genes remain unaffected. In agreement with these results, deletion of the HDAC encoding gene *hdaA* triggers expression of ST and PN gene clusters. The expression of orsellinic acid gene cluster, which is silent under standard laboratory conditions, is induced after treatment of the cultures with HDAC inhibitor suberoylanilide hydroxamic acid (SAHA) and this induction is blocked by addition of HAT inhibitor anacardic acid (Nutzmann et al., 2011). SAGA-ADA histone acetlytransferase complex is required for the induction of OA gene cluster after treatment with bacteria *S. rapamycinicus*. Furthermore, SAGA-ADA complex does not only activate the OA gene cluster but also other clusters, including sterigmatocystin (ST), terrequione (TQ) and penicillin (PN).

1.4. Aim of this study

Development of the fungi requires different environmental signals, one of which is light. In the model organism *A. nidulans*, light triggers asexual and inhibits sexual development via various light receptors, including the red light receptor phytochrome FphA, and blue light receptors LreA, LreB, CryA. Light not only controls the development of the fungus but also the production of secondary metabolites. Coordination of the light-dependent fungal development and secondary metabolism is regulated by the velvet complex VelB-VeA-LaeA. Previous studies showed that TAP enrichment of the VeA and LaeA reciprocally recruited each other (Bayram et al., 2008b). However, enrichment of the VelB led to an additional interaction partner, third velvet family protein VosA, that is required for viability of asexual and sexual spores (Figure 4). This raised the question whether VosA is a part of the trimeric complex (a quaternary complex) or whether VelB is part of more than one complex. It

also provoked the question about additional roles of VelB in spore viability similar to VosA.

First aim of this study was to analyze whether VosA was the fourth component of the velvet complex. The two members of the velvet complex VeA and VelB possess strong developmental functions along with secondary metabolism. However, LaeA has only function in secondary metabolism. *laeA* gene had been characterized in *veA1* background, which is N-terminally truncated version of the *wild-type veA* allele (Bok and Keller, 2004). As a consequence, it was necessary to investigate the function of LaeA on development by creating *laeA* deletion in a *veA+* background, representing the *wild-type* allele. Pilot studies in our lab demonstrated that LaeA has an important role in the control of fungal development in addition to its major role in secondary metabolism. This sparked the intriguing question whether LaeA exerts this effect on development via its involvement in the velvet complex. Thus, the protein-protein interactions as well as protein levels were investigated in the *laeA* mutant.

TAP purified interaction partners of VeA represent stable protein-protein interactions within the cell. However, VeA presumably interacts with many other regulatory proteins in a transient manner as evidenced by recent studies (Bayram et al., 2012a, Palmer et al., 2013). Therefore, the second aim of this study was to reveal the transient interaction partners of VeA protein. A yeast two-hybrid screen using the VeA as a bait further led to the identification of velvet interacting proteins (Vips) and membrane bound VapA-VipC-VapB methyltransferase complex. This resulted in the discovery of a novel methyltransferase signal transduction pathway that is linked to epigenetics, transcriptional regulation and control of protein stability.

2. Materials and Methods

2.1. Strains, media and growth conditions

Strains used in this study are listed in Table 1. *Aspergillus nidulans* strains; TNO2A3 (*nkuA*Δ) (Nayak et al., 2006), AGB152 (Busch et al., 2003), AGB154 (Bayram et al., 2009), AGB551, AGB552 (Bayram et al., 2012a) served as *wild-type* transformation hosts for the deletion and epitope tagging as well as overexpression experiments. DH5α and MACH-1 (INVITROGEN) *Escherichia coli* strains were used for recombinant plasmid DNA preparations. The *wild-type* and transformant *A. nidulans* strains were grown in glucose minimal medium (GMM), containing either $NaNO_3$ or NH_4-L-tartrate as nitrogen source. For auxotroph strains, the GMM was supplied with appropriate amount of vitamins. For vegetative growth, strains were grown in liquid submerged cultures for 20-24 hours at 30 or 37 ºC. For developmental synchronization and induction of cultures, vegetatively grown mycelia (20-24 hours at 30 or 37 ºC) were filtered through the miracloth (CALBIOCHEM) and placed on solid GMM medium. For asexual induction, the shifted fungal mycelia were kept under continuous white fluorescent light (90 μW^2). The plates containing the mycelia were incubated in the dark for sexual propagation. For both asexual and sexual induction, strains were further incubated upto the given time points as indicated in figure legends. *E. coli* strains were grown in lysogeny broth (LB) medium in the presence of appropriate antibiotics at 37 ºC.

2.2. Nucleic acid methods

2.2.1. Transformations

Tranformation of *E. coli* and *A. nidulans* was performed as explained in detail (Hanahan et al., 1991, Punt and van den Hondel, 1992).

2.2.2. Construction of linear and circular recombinant DNA molecules

During processing and construction of linear and circular DNAs, standard recombinant DNA technology protocols were followed as given in detail (Sambrook et al., 1989). Plasmids and oligonucleotides (INVITROGEN) employed in the course of this study are listed in Table 2 and 3, respectively. PCR reactions (Saiki et al., 1986) were performed with various DNA polymerase combinations including *Pfu* (MBI

26

FERMENTAS), Platinum-*Taq* (INVITROGEN), *Phusion*™, Q5™ (NEW ENGLAND

BIOLABS), and *Taq* (FERMENTAS) polymerases.

Table 1. Fungal strains used in this study

Strain	Genotype	Reference
FGSCA4	*veA+*	FGSC*
FGSCA26	*veA1, biA1*	FGSC*
TNO2A3	*nkuAΔ, pyroA4, pyrG89, veA1*	(Nayak et al., 2006)
RNI14.1	*biA1*; *vosAΔ::argB$^+$*; *veA+*	(Ni and Yu, 2007)
RNI18.3	*pyroA4*; *velBΔ::AfpyrG$^+$, veA+*	(Ni and Yu, 2007)
DVAR1	*pabaA1, yA2; argBΔ::trpC*; *trpC801; veAΔ::argB*	(Kim et al., 2002)
H2DVIC	*vipCΔ::argB, anA1*	This study
AGB152	*pyroA4, pyrG89, veA+*	(Busch et al., 2003)
AGB154	*pabaA1, yA2, veA+*	(Bayram et al., 2009)
AGB389	*^{P}velB::velB::ctap::natR, veA+*	(Bayram et al., 2008b)
AGB448	*niiA-niiD/pyrG, pyroA4, pyrG89, veA+*	(Bayram et al., 2009)
AGB468	*laeAΔ::ptrA; nkuAΔ, pyroA4, pyrG89, veA1*	This study
AGB474	*vipC-phleo; vipCΔ::argB anA1, vipC*	This study
AGB475	*^{P}laeA::laeA::laeA^t-phleo; laeAΔ::ptrA; nkuAΔ, pyroA4, pyrG89, veA1*	This study
AGB480	*^{P}vipC::vipC::ctap::natR, vipCΔ::argB, anA1*	This study
AGB482	*^{P}vipC::vipC::sgfp::natR, vipCΔ::argB, anA1*	This study
AGB488	*^{P}niiA::vipC::niiA^t, A.f. pyrG; pyroA4, pyrG89, veA+*	This study
AGB493	*laeAΔ::ptrA, veA+*	This study
AGB494	*laeA-phleo; laeAΔ::ptrA, veA+*	This study
AGB506	*^{P}gpdA::mrfp::h2A / natR; pyroA4, pyrG89, veA+*	This study
AGB509	*^{P}vosA::vosA::ctap / natR, pyroA4, pyrG89, veA+*	This study
AGB510	*^{P}vosA::vosA::ctap / natR, veA+; laeAΔ::ptrA*	This study
AGB511	*^{P}velB::velB::ctap / natR, veA+; laeAΔ::ptrA*	This study
AGB512	*laeAΔ::ptrA, veA1*	This study
AGB513	*^{P}veA::veA::ctap / natR; laeAΔ::ptrA*	This study
AGB514	*^{P}mutA::sgfp, natR; pyroA4, pyrG89, veA+*	This study
AGB515	*^{P}mutA::sgfp, natR; laeAΔ::ptrA, veA+*	This study
AGB516	*^{P}niiA::n-yfp::velB/^{P}niiD::c-yfp::vosA, pyrG; ^{P}gpdA::mrfp::h2A / natR; pyroA4, pyrG89, veA+*	This study
AGB517	*^{P}niiA::c-yfp::velB/^{P}niiD::n-yfp::vosA, pyrG; ^{P}gpdA::mrfp::h2A / natR; pyroA4, pyrG89, veA+*	This study
AGB518	*laeA-phleo; laeAΔ::ptrA, veA1*	This study
AGB519	*^{P}niiA::laeA, phleoR; pyroA4, pyrG89, veA+*	This study
AGB521	*laeAΔ::ptrA; veAΔ::argB*	This study
AGB543	*^{P}niiA::n-yfp::velB/^{P}niiD::c-yfp::velB, pyrG; ^{P}gpdA::mrfp::h2A / natR; pyroA4, pyrG89, veA+*	This study
AGB544	*^{P}niiA::c-yfp::velB/^{P}niiD::n-yfp::vosA, laeAΔ::ptrA; nkuAΔ, pyroA4, pyrG89, veA1*	This study
AGB545	*^{P}niiA::nosA cDNA, phleoR, laeAΔ::ptrA, veA+*	This study
AGB546	*laeAΔ::ptrA; nkuAΔ, pyroA4, pyrG89, veA1; ^{P}niiA::n-eyfp::veA /^{P}niiD::c-eyfp::velB, pyrG*	This study
AGB551	*nkuAΔ::argB, pyrG89, pyroA4, veA+*	(Bayram et al., 2012a)
AGB552	*nkuAΔ::argB, pabaA1, yA2, veA+*	(Bayram et al., 2012a)
AGB741	*vipCΔ::ptrA, nkuAΔ::argB, pyrG89, pyroA4, veA+*	This study
AGB742	*^{P}veA::veA::gfp::pyrG; ^{P}gpdA::mrfp::h2A-pyroA; vapAΔ::ptrA, pyroA4, pyrG89, veA+*	This study
AGB743	*vapAΔ::ptrA, nkuAΔ::argB, pyrG89, pyroA4, veA+*	This study
AGB744	*vapAΔ::ptrA, nkuAΔ::argB, pabaA1, yA2, veA+*	This study
AGB745	*vapBΔ::ptrA, nkuAΔ::argB, pyrG89, pyroA4, veA+*	This study

Strain	Genotype	Reference
AGB746	*vapBΔ::ptrA, nkuAΔ::argB, pabaA1, yA2, veA+*	This study
AGB747	*vipCΔ::pabaA, vapAΔ::ptrA, veA+*	This study
AGB748	*vipCΔ::pabaA, vapBΔ::ptrA, veA+*	This study
AGB749	*veAΔ::argB, pyrG89*	This study
AGB750	*vapAΔ::ptrA, vapBΔ::ptrA, veA+*	This study
AGB751	*vipCΔ::ptrA, veAΔ::ptrA*	This study
AGB752	*^{p}vapA::ctap::natR, nkuAΔ::argB, pyrG89, pyroA4, veA+*	This study
AGB753	*^{p}vapA::sgfp::natR, nkuAΔ::argB, pyrG89, pyroA4, veA+*	This study
AGB754	*^{p}vapB::ctap::natR, nkuAΔ::argB, pabaA1, veA+*	This study
AGB755	*^{p}vapB::sgfp::natR, nkuAΔ::argB, pyrG89, pyroA4, veA+*	This study
AGB756	*^{p}gpdA::vapB::sgfp-phleo; ^{p}gpdA::mrfp::h2A / natR; pyroA4, pyrG89, veA+*	This study
AGB757	*^{p}gpdA::vapB::sgfp; vapB::ptrA, nkuAΔ::argB, pyrG89, pyroA4, biAΔ, veA+*	This study
AGB758	*^{p}vapA::vapA::sgfp::natR, nkuAΔ::argB, pyrG89, pyroA4, veA+*	This study
AGB759	*vapB-phleo; vapBΔ:: ptrA, nkuAΔ::argB, pabaA1, yA2, veA+*	This study
AGB760	*^{p}niiA::vapA::niiA^t, A.f. pyrG, pyroA4, pyrG89, veA+*	This study
AGB761	*^{p}niiA::vapB::niiA^t, A.f. pyrG, pyroA4, pyrG89, veA+*	This study
AGB762	*^{p}niiA::vapB::niiA^t, A.f. pyrG, vipCΔ::ptrA, pyroA4, pyrG89, veA+*	This study
AGB763	*^{p}niiA::vapB::niiA^t, A.f. pyrG, vapAΔ::ptrA, pyroA4, pyrG89, veA+*	This study
AGB764	*^{p}niiA::vipC::niiA^t, A.f. pyrG; vapAΔ::ptrA, pyroA4, pyrG89, veA+*	This study
AGB765	*^{p}niiA::vipC::niiA^t-^{p}niiD::vapA::niiA^t, A.f. pyrG, pyroA4, pyrG89, veA+*	This study
AGB766	*^{p}niiA::vapA::niiA^t-^{p}niiD::vapB::niiA^t, A.f. pyrG, pyroA4, pyrG89, veA+*	This study
AGB767	*^{p}niiA::vipC::niiA^t-^{p}niiD::vapB::niiA^t, A.f. pyrG, pyroA4, pyrG89, veA+*	This study
AGB768	*^{p}vipC::vipC::ctap:natR; vapAΔ::ptrA, nkuAΔ::argB, pyrG89, pyroA4, veA+*	This study
AGB769	*^{p}vipC::vipC::ctap:natR; vapBΔ::ptrA, nkuAΔ::argB, pyrG89, pyroA4, veA+*	This study
AGB770	*^{p}vipC::vipC::sgfp:natR; vapBΔ::ptrA, nkuAΔ::argB, pyrG89, pyroA4, veA+*	This study
AGB771	*^{p}vapA::vapA::sgfp::natR; vipCΔ::ptrA, pyrG89, pyroA4, veA+*	This study
AGB772	*^{p}vapA::vapA::sgfp::natR; nkuAΔ::argB, pyrG89, pyroA4, veA+*	This study
AGB773	*^{p}vipC::vipC::sgfp::natR; vapAΔ::ptrA, nkuAΔ::argB, pabaA1, yA2, veA+*	This study
AGB774	*^{p}gpdA::vapB::sgfp, A.f. pyrG; vapAΔ::ptrA, pyrG89, pyroA4, veA+*	This study
AGB775	*^{p}gpdA::vapB::sgfp, A.f. pyrG; vipCΔ::ptrA, pyrG89, pyroA4, veA+*	This study
AGB776	*^{p}vipC::vipC::sgfp::natR; vipCΔ::ptrA, pyrG89, pyroA4, veA+*	This study
AGB777	*^{p}niiA::n-yfp::veA/^{p}niiD::c-yfp::vipC, pyrG; ^{p}gpdA::mrfp::h2A-ptrA; pyroA4, pyrG89, veA+*	This study
AGB778	*^{p}niiA::n-yfp::vipC/^{p}niiD::c-yfp::vapA, pyrG; ^{p}gpdA::mrfp::h2A-natR; pyroA4, pyrG89, veA+*	This study
AGB779	*^{p}niiA::n-yfp::vipC/^{p}niiD::c-yfp::vapB, pyrG; ^{p}gpdA::mrfp::h2A-natR; pyroA4, pyrG89, veA+*	This study
AGB780	*^{p}niiA::n-yfp::vapB/^{p}niiD::c-yfp::vapA, pyrG; ^{p}gpdA::mrfp::h2A-natR; pyroA4, pyrG89, veA+*	This study
AGB781	*^{p}niiA::c-yfp::veA/^{p}niiD::n-yfp::vapA, pyrG; ^{p}gpdA::mrfp::h2A-natR; pyroA4, pyrG89, veA+*	This study

Strain	Genotype	Reference
AGB782	^{P}*niiA::c-yfp::veA*/^{P}*niiD::n-yfp::vapB, pyrG;* ^{P}*gpdA::mrfp::h2A-natR; pyroA4, pyrG89, veA+*	This study
AGB783	^{P}*veA::veA::gfp::pyrG;* ^{P}*gpdA::mrfp::h2A-pyroA; vapAΔ::ptrA, pyroA4, pyrG89, biAΔ, veA+*	This study
AGB784	^{P}*veA::veA::gfp::pyrG;* ^{P}*gpdA::mrfp::h2A-pyroA; vapBΔ::ptrA, pyroA4, pyrG89, biAΔ, veA+*	This study
AGB785	^{P}*veA::veA::gfp::pyrG;* ^{P}*gpdA::mrfp::h2A-pyroA; vipCΔ::ptrA, pyroA4, pyrG89, biAΔ, veA+*	This study
AGB786	^{P}*veA::veA::gfp::natR;* ^{P}*gpdA::mrfp::h2A-pyroA;* ^{P}*niiA::vapA::niiA^t, A.f. pyrG; pyroA4, pyrG89, veA+*	This study
AGB787	^{P}*veA::veA::gfp::natR;* ^{P}*gpdA::mrfp::h2A-pyroA;* ^{P}*niiA::vapB::niiA^t, A.f. pyrG; pyroA4, pyrG89, veA+*	This study
AGB788	^{P}*veA::veA::gfp::natR;* ^{P}*gpdA::mrfp::h2A-pyroA;* ^{P}*niiA::vipC::niiA^t, A.f. pyrG; pyroA4, pyrG89, veA+*	This study
AGB789	^{P}*veA::veA::3HA tag-pyroA, pyrG89, pyroA4, veA+*	This study
AGB790	^{P}*veA::veA::3HA tag-pyroA;* ^{P}*vipC::vipC::sgfp::natR, pyrG89, pyroA4, veA+*	This study
AGB791	^{P}*veA::veA::3HA tag-pyroA;* ^{P}*vapA::vapA::sgfp::natR, pyrG89, pyroA4, veA+*	This study
AGB792	^{P}*veA::veA::3HA tag-pyroA;* ^{P}*gpdA::vapB::sgfp;* ^{P}*gpdA::mrfp::h2A / natR; pyroA4, pyrG89, veA+*	This study
AGB793	^{P}*niiA::vapB1::niiA^t, A.f. pyrG, pyroA4, pyrG89, veA+*	This study
AGB794	^{P}*niiA::vipC1::niiA^t, A.f. pyrG, pyroA4, pyrG89, veA+*	This study
AGB795	^{P}*hepA::hepA::sgfp::natR; pyroA4, pyrG89, veA+*	This study
AGB796	^{P}*hepA::hepA::sgfp::natR;* ^{P}*niiA::vapB::niiA^t, A.f. pyrG, pyroA4, pyrG89, veA+*	This study
AGB797	^{P}*hepA::hepA::sgfp::natR;* ^{P}*niiA::vapB1::niiA^t, A.f. pyrG, pyroA4, pyrG89, veA+*	This study

* Fungal Genetics Stock Center, Kansas, USA

Table 2. Plasmids employed in this study

Plasmid	Description	Reference
pBluescript II SK	Cloning plasmid	FERMENTAS
pPTRII	Pyrithiamine resistance (*ptrA*) plasmid	TAKARA
pHybLex/ZeoTrp	Yeast two hybrid plasmid	S.K. Chae (PaiChai University, Korea)
pAN8-1	Phleomycin resistance cloning plasmid	(Punt and van den Hondel, 1992)
pME3157	^{P}*veA::veA::ctap, ptrA*, in pUC19	(Bayram et al., 2008c)
pME3160	*niiA*/*niiD* expression module with *pyrG* marker	(Bayram et al., 2008b)
pME3173	^{P}*gpdA::mrfp::h2A::trpC^t* (histone 2A) with *natR* marker	(Bayram et al., 2008b)
pME3189	^{P}*niiA::n-eyfp::veA* /^{P}*niiD::c-eyfp::velB, pyrG*	(Bayram et al., 2008c)
pME3296	^{P}*mutA::sgfp, natR*	(Bayram et al., 2009)
pME3634	^{P}*vipC::vipC::vipC^t* in the *Stu*I site of pAN8-1	This study
pME3635	*laeA* genomic locus in the *Stu*I site of pAN8-1	This study
pME3636	^{P}*vipC::vipC::ctap/natR* fusion in the *EcoR*V site of pBluescript II SK	This study
pME3637	^{P}*vipC::vipC::sgfp/natR* fusion in the *EcoR*V site of pBluescript II SK	This study
pME3645	^{P}*niiA::vipC* cDNA in *Pme*I site of pME3160	This study
pME3647	^{P}*niiA::vipC* cDNA in *Pme*I site of pME3166	This study

29

Plasmid	Description	Reference
pME3643	^{P}*niiA::n-yfp::veA* in *Pme*I- ^{P}*niiD::c-yfp::vipC* in *Swa*I site of pME3160 (VeA-VipC BIFC)	This study
pME3711	^{P}*veA::veA::ctap/natR*	This study
pME3712	^{P}*niiA::n-yfp::velB, pyrG* (BIFC recipient 1)	This study
pME3713	^{P}*niiA::c-yfp::velB, pyrG* (BIFC recipient 2)	This study
pME3714	^{P}*niiA::n-yfp::velB*/^{P}*niiD::c-yfp::vosA*, *pyrG* (VelB-VosA BIFC 1)	This study
pME3715	^{P}*niiA::c-yfp::velB*/^{P}*niiD::n-yfp::vosA*, *pyrG* (VelB-VosA BIFC 2)	This study
pME3716	^{P}*niiA::laeA, phleoR* (*laeA* overexpression)	This study
pME3717	^{P}*niiA::n-yfp::velB*/^{P}*niiD::c-yfp::velB*, *pyrG* (VelB-VelB BIFC)	This study
pME3718	^{P}*niiA-niiA*^{t} / ^{P}*niiD-niiD*^{t}, *phleoR*	This study
pME3719	^{P}*niiA::nosA, phleoR*	This study
pME3856	^{P}*gpdA::(Pme*I*)::trpC*^{t} in *Stu*I site of pAN8-1	(Bayram et al., 2012a)
pME3857	^{P}*gpdA::mrfp::h2A::trpC*^{t} (histone 2A) with phleomycin resistance marker	(Bayram et al., 2012a)
pME3858	^{P}*gpdA::mrfp::h2A::trpC*^{t} (histone 2A) with *pyrG* marker	(Bayram et al., 2012a)
pME4143	^{P}*gpdA::(Pme*I*)::trpC*^{t} promoter with *A.f. pyroA* marker	This study
pME4144	*A. nidulans* cloning plasmid for ectopic integrations with *A.f pyrG* marker	This study
pME4145	*vapB* (cDNA)*::sgfp* in *Pme*I site of pME4143	This study
pME4146	*vapB* (cDNA)*::sgfp* in *Pme*I site of pME3856	This study
pME4147	^{P}*vapB::vapB::vapB*^{t} *in Stu*I site of pAN8-1 (*vapB* complementation plasmid)	This study
pME4148	^{P}*niiA::vapA* cDNA in *Pme*I site of pME3160	This study
pME4149	^{P}*niiA::vapB* cDNA in *Pme*I site of pME3160	This study
pME4150	^{P}*niiA::vipC (Pme*I*)::niiA*^{t}- ^{P}*niiD::vapA (Swa*I*)::niiD*^{t} in pME3160	This study
pME4151	^{P}*niiA::vapA (Pme*I*)::niiA*^{t}- ^{P}*niiD::vapB (Swa*I*)::niiD*^{t} in pME3160	This study
pME4152	^{P}*niiA::vipC (Pme*I*)::niiA*^{t}- ^{P}*niiD::vapB (Swa*I*)::niiD*^{t} in pME3160	This study
pME4153	^{P}*niiA::vipC1* cDNA in *Pme*I site of pME3160	This study
pME4154	^{P}*niiA::vapB1* cDNA in *Pme*I site of pME3160	This study
pME4155	^{P}*niiA::n-yfp::vipC* in *Pme*I- ^{P}*niiD::c-yfp::vapA* in *Swa*I site of pME3160 (VipC-VapA BIFC)	This study
pME4156	^{P}*niiA::n-yfp::vipC* in *Pme*I- ^{P}*niiD::c-yfp::vapB* in *Swa*I site of pME3160 (VipC-VapB BIFC)	This study
pME4157	^{P}*niiA::n-yfp::vapB* in *Pme*I- ^{P}*niiD::c-yfp::vapA* in *Swa*I site of pME3160 (VapA-VapB BIFC)	This study
pME4158	^{P}*niiA::c-yfp::veA* in *Pme*I- ^{P}*niiD::n-yfp::vapA* in *Swa*I site of pME3160 (VeA-VapA BIFC)	This study
pME4159	^{P}*niiA::c-yfp::veA* in *Pme*I- ^{P}*niiD::n-yfp::vapB* in *Swa*I site of pME3160 (VeA-VapB BIFC)	This study
pME4160	^{P}*gpdA::vapB* (cDNA)*::sgfp* in *Pme*I site of pME4144	This study

Table 3. Oligonucleotides utilized for plasmid constructions and Northern hybridizations

Designation	Sequence in 5' > 3' direction	Size	Features
VosA-A	CGA AAT ACA CGG TCG GGG TTA CTC	24 mer	*vosA* 5 UTR
VosA-B	GCA TTA AAG GCA GAT ACG AGA TAG	24 mer	*vosA* nested 5 UTR
VosA-C	GAA ATT CTT TTT CCA TCT TCT CTT ACC ACC GCT ACC ACC CCG AGG AGT TCC GTT CGC TGA G	61 mer	*vosA ctap* connector
VosA-D	GAG CAG GCG CTC TAC ATG AGC ATG CCC TGC CCC TGA GGA TTC TCG TTT GTG GAA CAC CTG	60 mer	*vosA* 3 UTR *natR* connector
VosA-E	CCT TGA GAA CTC CAT GCG TGT CG	23 mer	*vosA* nested 3 UTR
VosA-F	GAT CCG CTG GAC TTG CTG GTG	21 mer	*vosA* 3 UTR
OZG29	CTA CTT GTA CAG TTC GTC CAT GCC GTG	27 mer	*sgfp* stop
OZG61	ATG TTT GAG ATG GGC CCG GTG GG	23 mer	*laeA* 5'
OZG62	TTA TCT TAA TGG TTT CCT AGC CTG GT	26 mer	*laeA* 3'
OZG63	ATG TAC GCT GTT GAG GAT AGG GC	23 mer	*velB* 5'
OZG64	TTA GTA TTC GTT ATC CAG ACC ATC G	25 mer	*velB* 3'
OZG73	ATG GTG AGC AAG GGC GAG GAG	21 mer	*n-yfp* start
OZG75	ATG GCC GAC AAG CAG AAG AAC	21 mer	*c-yfp* start
OZG77	GGA ATG CGC CCT ATC CTC AAC AGC GTA CAT GTG GTT CAT GAC CTT CTG TTT CAG	54 mer	*velB-c-yfp*
OZG167	TCA GGT TGA CTT CCC CGC GGA ATT CG	26 mer	*ctap* stop
OZG207	GGT GGT AGC GGT GGT ATG GTG AGC	24 mer	*sgfp start*
OZG304	TTT TGG GCC CAA GCT TGG TGA TCC TCG TCT TCG G	34 mer	*veA* 5' *Apa*I
OZG305	TTT TGG GCC CAA GCT TAT CCT CCA GGT TAC TGA CTC	36 mer	*veA* 3' *Apa*I
OZG320	ATG CCG GCA GCA CCG AGA AAG AAG	24 mer	*nosA* 5'
OZG321	TCA AAG AAG AAG GTA GTT CCA ACC G	25 mer	*nosA* 3'
OZG387	CGT GGC GAT GGA GCG CAT GAT ATA	24 mer	*n-yfp* 3'
OZG388	GTG GTT CAT GAC CTT CTG TTT CAG GTC	27 mer	*c-yfp* 3'
OZG397	CAA CTA CAA CAG CCA CAA CGT CTA TAT CAT GCG CTC CAT CGC CAC GAT GTA CGC TG	56 mer	*velB-n-yfp*
OZG436	CAA CGT CTA TAT CAT GCG CTC CAT CGC CAC GAT GAG TGC GGC GAA CTA TCC AG	53 mer	*vosA-n-yfp*
OZG437	GAA CGA CCT GAA ACA GAA GGT CAT GAA CCA CAT GAG TGC GGC GAA CTA TCC AG	53 mer	*vosA-c-yfp*
OZG438	TTT AAT CAC CGA GGA GTT CCG TTC GCT G	28 mer	*vosA* 3'
OZG694	CTG TCT GAG AGG AGG CAC TGA T	22 mer	*pyroA* 3'
OZG798	GCA AGT TGG CAA CTG AAA GAC AG	23 mer	*veA* 5 UTR
OZG799	CGG TTT ACA CGA TGT CAG TTG C	22 mer	*veA* nested 5 UTR
OZG800	ACC ACC GCT ACC ACC ACG CAT GGT GGC AGG CTT TGA G	37 mer	*veA sgfp* connector
OZG801	CAT GCC CTG CCC CTG AGT CAT AGT TCT TGG CGG GTT C	37 mer	*veA* 3 UTR *natR* connector
OZG802	GTC GTC ACA TCC ACA CGG AC	20 mer	*veA* nested 3 UTR
OZG803	CCC TCT TGA CTG AAT GCG AAG ACG	24 mer	*veA* 3 UTR
OZG804	GGT GGT AGC GGT GGT TAT CCC TAT GAT GTT CCT GAT TAT GCT GGC TAT CCG TAT GAC GTC CCG GAT TA	68 mer	*3xha* 5'
OZG805	TTA AGC AGG GGC ATA GTC GGG AAC GTC ATA AGG ATA GGA TCC GGC ATA ATC CGG GAC GTC ATA CGG	66 mer	*3xha* 3'
OZG811	GCC TCC TCT CAG ACA GGT CAT AGT TCT	37 mer	*veA* 3 UTR *pyroA*

Designation	Sequence in 5' > 3' direction	Size	Features
	TGG CGG GTT C		connector
OZG812	GGT GGT AGC GGT GGT TAT CCC	21 mer	*3xha* 5' short
OSB11	GCG GTT TGA AAC CTC CCA AG	20 mer	*vipC* 5 UTR
OSB12	GAA TTG ACT AGA GTA CAT TGC CTC	24 mer	*vipC* nested 5 UTR
OSB13	CTT TTT CCA TCT TCT CTT ACC ACC GCT ACC ACC CTC CGG CTT CTG CCC ATA AAC AAC	57 mer	*vipC ctap* connector
OSB14	CAG GCG CTC TAC ATG AGC ATG CCC TGC CCC TGA AGC TGG CTT ATT GTG GCT TCA GTC	57 mer	*vipC* 3 UTR *natR* connector
OSB15	GGT TTA GTA TAT CAC ACC CAA GG	23 mer	*vipC* nested 3 UTR
OSB16	GTT GAT CGC CGG AAG CTG TCT G	22 mer	*vipC* 3 UTR
OSB17	CGC CCT TGC TCA CCA TAC CAC CGC TAC CAC CCT CCG GCT TCT GCC CAT AAA CAA C	55 mer	*vipC sgfp* connector
OSB18	ATG GCG GAC ACG GAG CAC GG	20 mer	*vipC* ORF 5'
OSB19	CTA CTC CGG CTT CTG CCC ATA AAC	24 mer	*vipC* ORF 3'
OSB20	CCG TGC TCC GTG TCC GCC ATG TGG TTC ATG ACC TTC TGT TTC AGG TCG	48 mer	*vipC cyfp fusioner*
OSB22	GTA TGG AGT ACA GGA CCG GGT C	22 mer	*laeA* 5 UTR
OSB23	GTA TAA GTT CAG TAG TGT AGT TAG	24 mer	*laeA* nested 5 UTR
OSB24	CAT TTC GTT ACC AAT GGG ATC CCG TAA TCA ATT GGC GGG GAG ACG AGT TCC C	52 mer	*laeA* deletion 5' *ptrA* connector
OSB25	GAA AGA CAG TAT AAT ACA AAC AAA GAT GCA AGA GAG CAA AAG GCG ACC ACA TCC	54 mer	*laeA* deletion 3' *ptrA* connector
OSB26	CAG AAA TGG TCG GCA CTC GC	20 mer	*laeA* nested 3 UTR
OSB27	CGT TGT AGA ATG GCA TCC AAC C	22 mer	*laeA* 3 UTR
OSB32	CAA CGT CTA TAT CAT GCG CTC CAT CGC CAC GAT GGC GGA CAC GGA GCA CGG	51 mer	*vipC nyfp* fusioner
OSB33	CAG GCT TGG CCG TTT AAA GAC C	22 mer	*vapA* 5 UTR
OSB34	GTT AAT CAG ACC ATG ACC GTG GAC	24 mer	*vapA* nested 5 UTR
OSB35	CAT TTC GTT ACC AAT GGG ATC CCG TAA TCA ATT GGT TAA GGA CGG TGG GTC AGG	54 mer	*vapA* deletion 5' *ptrA* connector
OSB36	GAC AGT ATA ATA CAA ACA AAG ATG CAA GAT GAA GGG AGC GAG ACT CCA AAG TC	53 mer	*vapA* deletion 3' *ptrA* connector
OSB37	CCA GGG CCT GAT AAT TTA AAG AC	23 mer	*vapA* nested 3 UTR
OSB38	GTG AAT CCC CTA CTA ACC GCC ATC	24 mer	*vapA* 3 UTR
OSB42	TTTATGTCGACATCCCAGTCCG		*vapA* ORF 5
OSB44	GCC ACA ACG TCT ATA TCA TGC GCT CCA TCG CCA CGA TGT CGA CAT CCC AGT CCG ATG G	58 mer	*vapA nyfp* fusioner
OSB45	CGA ACG ACC TGA AAC AGA AGG TCA TGA ACC ACA TGT CGA CAT CCC AGT CCG ATG	54 mer	*vapA cyfp* fusioner
OSB46	GAA GGG AGA ATG TAG ACC AAA ATC	24 mer	*vapB* 5 UTR
OSB47	GAG AGT CTT GCA CAG ATC AAG GAC	24 mer	*vapB* nested 5 UTR
OSB48	CAT TTC GTT ACC AAT GGG ATC CCG TAA TCA ATT TTC GTC TCC ATG CTG CCG AGC	54 mer	*vapB* deletion 5' *ptrA* connector
OSB49	GAC AGT ATA ATA CAA ACA AAG ATG CAA GAG CTA TCC AGT GGT CAC GCG AAG AAG	54 mer	*vapB* deletion 3' *ptrA* connector
OSB50	GGG AAG CCC GAT ATG CCT TGT C	22 mer	*vapB* nested 3 UTR
OSB51	GAG TGT TAG AAC TCC CTC ACA GC	23 mer	*vapB* 3 UTR
OSB54	GCC CTT GCT CAC CAT ACC ACC GCT ACC ACC TTG AGC CCC AAG GTC CGC CTT TGC	54 mer	*vapB sgfp* connector
OSB55	CTT TTT CCA TCT TCT CTT ACC ACC GCT ACC ACC TTG AGC CCC AAG GTC CGC CTT TGC	57 mer	*vapB ctap* connector

Designation	Sequence in 5' > 3' direction	Size	Features
OSB56	GCG CTC TAC ATG AGC ATG CCC TGC CCC TGA TGA AGC CGA GTA TCC GAT TGA G	52 mer	*vapB natR* connector
OSB57	CAA CGT CTA TAT CAT GCG CTC CAT CGC CAC GAT GGG CCT TTC ATC CCT TCC GG	53 mer	*vapB nyfp* fusioner
OSB58	GAA CGA CCT GAA ACA GAA GGT CAT GAA CCA CAT GGG CCT TTC ATC CCT TCC GG	53 mer	*vapB cyfp* fusioner
OSB68	TCA TTG AGC CCC AAG GTC CGC CTT TG	26 mer	*vapB* ORF 3'
OSB70	CGC ATG GTT GAG GAA TAC AGG CTC GAG	27 mer	*vapB* ORF 5'
OSB72	CGT TAC CAA TGG GAT CCC GTA ATC AAT TTG CGA CCG ACA AAA TAG TAA AAT C	52 mer	*vipC* deletion 5' *ptrA* connector
OSB73	GAC AGT ATA ATA CAA ACA AAG ATG CAA GAA GCT GGC TTA TTG TGG CTT CAG TC	53 mer	*vipC* deletion 3' *ptrA* connector
OSB74	GCC CAA TCA CCA AGG AGC GGT GCC ATC CTG CGA CCG ACA AAA TAG TAA AAT C	52 mer	*vipC* deletion 5' *pabaA* connector
OSB75	CAT ATT TAT GCC TTC GCA CGC GAA ATG AGG AGC TGG CTT ATT GTG CTC AGT C	54 mer	*vipC* deletion 3' *pabaA* connector
OSB81	GGA TGG CAC CGC TCC TTG GTG ATT G	25 mer	*pabaA* ORF 5'
OSB82	CCT CAT TTC GCG TGC GAA GGC AT	23 mer	*pabaA* ORF 3'
OSB136	GAA CTC GTA AGC GGA ATG G	19 mer	*hepA* 5 UTR
OSB137	GCC CTT GCT CAC CAT ACC ACC GCT ACC ACC CGC ATC CGA GTC TTT AAA AAC TCT G	55 mer	*hepA sgfp* connector
OSB138	CAT GCC CTG CCC CTG ACA TTT TCC TGA TCT GTC TTT ATG CC	41 mer	*hepA* 3 UTR *natR* connector
OSB139	TAA CGG CAC GTT GAG CAC AC	20 mer	*hepA* 3 UTR
OSB140	GCC CAA TCA CCA AGG AGC GGT GCC ATC CTT CGT CTC CAT GCT GCC GAG C	49 mer	*vapB* deletion 5' *pabaA* connector
OSB141	CAT ATT TAT GCC TTC GCA CGC GAA ATG AGG GCT ATC AGT GGT CA CGC GAA G	52 mer	*vapB* deletion 3' *pabaA* connector
OSB144	AAA TCA GGA CTT GGG AGT CTC GCT C	25 mer	*vapA* ORF 3'
OSB145	TCC ATC TTC TCT TAC CAC CGC TAC CAC CGG ACT TTG GAG TCT CGC TCC C	49 mer	*vapA ctap* connector
OSB146	CCT TGC TCA CCA TAC CAC CGC TAC CAC CGG ACT TTG GAG TCT CGC TCC C	49 mer	*vapA sgfp* connector
OSB147	CGC TCT ACA TGA GCA TGC CCT GCC CCT GAT GAA GCA CAG GCT TGA TGG GC	50 mer	*vapA* 3 UTR *natR* connector
OSB328	CTG CCC AGA TGC CCG TAG CTG TGG CAA CAT CGA GGA CTT TCT GC	44 mer	*vapB* mutator 1
OSB329	CTA CGG GCA TCT GGG CAG TAG AAT TCG CAG ACC TTC ATC C	40 mer	*vapB* mutator 2
OSB330	TCG CCC AAA TCC CCG TAG CTG TGG CGA TAT CCA GTA CCC GCG CTG GG	47 mer	*vipC* mutator 1
OSB331	CTA CGG GGA TTT GGG CGA TTG ATT TCG CAG ATG AAC ACC CTG	42 mer	*vipC* mutator 1
tpsA 5'	CCA TCA CCA TAA AGC GAT CAG	21 mer	for Northern
tpsA 3'	CAG TTT CGA GAA GTT AAG CGC	21 mer	for Northern
orlA 5'	CAG CCG CAT CTC CAA CTT AG	20 mer	for Northern
orlA 3'	TGT TAG CAG CAA TTC ATC GCG	21 mer	for Northern
mutA 5'	ATG AAG ATC TTC CAC CGC TGC TG	21 mer	for Northern
mutA 3'	TAG GCG CTA AAA GAG CCA ACA T	22 mer	for Northern
nosA 5'	ATG CCG GCA GCA CCG AGA AAG AAG	24 mer	for Northern
nosA 3'	TCA AAG AAG AAG GTA GTT CCA ACC G	25 mer	for Northern
steA 5'	TTA TGT ACT CTC AGC ACG GTG CCC C	25 mer	for Northern
steA 3'	TTC TAT ATT TGC TGT TGC AGG AGT TG	26 mer	for Northern
nsdD 5'	ATG GGA TCA CTA GAG GCT GGA CAT AG	26 mer	for Northern
nsdD 3'	TTA ATG ACT CCT CGG TGA CAC CG	23 mer	for Northern
laeA 5'	GAA TTC ATG TTT GAG ATG GGC CCG GTG GG	29 mer	for Northern
laeA 3'	CTC GAG TTA TCT TAA TGG TTT CCT AGC CTG GT	32 mer	for Northern

Designation	Sequence in 5' > 3' direction	Size	Features
aflR 5'	ATG GAG CCC CCA GCG ATC AGC CAG	24 mer	for Northern
aflR 3'	TCA GGC GTG GCG GAG GAT GCT GAT C	25 mer	for Northern
ipnA 5'	ATG GGT TCA GTC AGC AAA GCC AAT G	25 mer	for Northern
ipnA 3'	CTA GGT CTG GCC GTT CTT GTT G	22 mer	for Northern
stcU 5'	ATG TCC TCC TCC GAT AAT TAC CG	23 mer	for Northern
stcU 3'	TTA TCT AAA GGC CCC CCC ATC AAC G	25 mer	for Northern
vipC 5'	ATG GCG GAC ACG GAG CAC GG	20 mer	for Northern
vipC 3'	CTA CTC CGG CTT CTG CCC ATA AAC	24 mer	for Northern
vapA 5'	ATG TCG ACA TCC CAG TCC G	19 mer	for Northern
vapA 3'	ATC AGG ACT TTG GAG TCT CGC TC	23 mer	for Northern
vapB 5'	ATG GTT GAG GAA TAC AGG CTC GAG	24 mer	for Northern
vapB 3'	TCA TTG AGC CCC AAG GTC CGC CTT TG	26 mer	for Northern
brlA 5'	ATG CGA AAT CAG TCC AGC CTG TCC G	25 mer	for Northern
brlA 3'	TCA TTC ATC CCA GCC GTC CAG GCT C	25 mer	for Northern
abaA 5'	ATG GCT ACT GAC TGG CAA CCC GAG	24 mer	for Northern
abaA 3'	CTA GAC AGC CTC AAC CGC AGT ATG	24 mer	for Northern
flbA 5'	ATG CCA ACT TCC ATA TCT ACC G	22 mer	for Northern
flbA 3'	TCA TGA ACG TTG TGA GCG ACT C	22 mer	for Northern
flbC 5'	ATG ACG ATG GTT ATT GAG AAC CAG AAC	27 mer	for Northern
flbC 3'	TTA CTC TTC GTC ATC GCC TGA AC	23 mer	for Northern
gpdA 5'	ATG GCA CCA ACA AAG AAA CAC CAG	24 mer	for Northern
gpdA 3'	CTA TTG GGC ATC AAC CTT GGA G	22 mer	for Northern
h2A 5'	TGC GGT CGT GTT AAG CGT TT	20 mer	for qRT-PCR
h2A 3'	CGG ATG GCA AGC TGT AGG TG	20 mer	for qRT-PCR
vapB 5'	GGA AGA AGG GAT CGA GGG ATG	21 mer	for qRT-PCR
vapB 3'	GCA TGG ATT CTT GGA GTG CG	20 mer	for qRT-PCR
laeA 5'	CAC AAC CAC TAC AGC TAC CAC	21 mer	for qRT-PCR
laeA 3'	GCA ACC GCG TAT CTG GTC G	19 mer	for qRT-PCR
veA 5'	CGA TCC AGA GCC TCT CAG AG	20 mer	for qRT-PCR
veA 3'	GGT CAT CAT GAC CGA ACG AC	20 mer	for qRT-PCR
velB 5'	CCT CCC ACA ATC GGA TAT TGC	21 mer	for qRT-PCR
velB 3'	GGG ATC TTG ATT CCT TGG TTC	21 mer	for qRT-PCR
aflR 5'	CCT TCG CTT CTT GAG GGT ATG G	22 mer	for qRT-PCR
aflR 3'	GCA GTA GGA GTG GCT TGT GGT G	22 mer	for qRT-PCR
stcE 5'	GCA TCT CGA TGT AGT GAT CG	20 mer	for qRT-PCR
stcE 3'	CTA GTC GCC TGG AAC AGT AG	20 mer	for qRT-PCR
stcQ 5'	GGT TGT AGC GTC TTT GCA ACG	21 mer	for qRT-PCR
stcQ 3'	GAA CAT CGT TGC AGA ACG TGG	21 mer	for qRT-PCR
stcU 5'	ACG CAT CAT CCT CAC AAG TTC C	22 mer	for qRT-PCR
stcU 3'	ACC GCA CAA AGG TGT CAA TCG	21 mer	for qRT-PCR
acvA 5'	GAC AAG GAC AGA CCG TGA TG	20 mer	for qRT-PCR
acvA 3'	GCA CAC CAT TAC TGC TAG AGG	21 mer	for qRT-PCR
ipnA 5'	GAG AGT AGC CCA GCA AAT CG	20 mer	for qRT-PCR
ipnA 3'	GGC ACG AAT CGC AAG GTC C	19 mer	for qRT-PCR
aatA 5'	CCA TTG ACT TCG CAA CTG GC	20 mer	for qRT-PCR
aatA 3'	CGT ACG AGT GTT GAG CAT GAC	21 mer	for qRT-PCR
tdiA 5'	CGA TGC CTG GAG TGC GAA TG	20 mer	for qRT-PCR
tdiA 3'	GCC GTT GCT GTC AAT GAA CG	20 mer	for qRT-PCR
tdiB 5'	CTC CTG AAG ATC AGG AGT CC	20 mer	for qRT-PCR
tdiB 3'	CTG TTC GAT CAG GTG GAC TG	20 mer	for qRT-PCR
orsA 5'	TGC TGG AGA CGG CAA CTA CAA C	22 mer	for qRT-PCR
orsA 3'	GAA GAG TCG GTG GTC AAA GTC G	22 mer	for qRT-PCR
orsC 5'	TCT CTT TCA GGC AAC GGA GTG T	22 mer	for qRT-PCR
orsC 3'	CGT GGG TTT GGA GGG ATG TAT T	22 mer	for qRT-PCR
orsE 5'	CGC CGC TGG TAT TCA GGT TAT T	22 mer	for qRT-PCR
orsE 3'	CGC TGG TGT AGG TGT CAG GTG T	22 mer	for qRT-PCR
AN7921 5'	CCT CTC TTA TGA AGC TCA CGA C	22 mer	for qRT-PCR
AN7921 3'	CGC TCA GAG GCC ATG CTT G	19 mer	for qRT-PCR
AN7903 5'	CAG CGT CAT TTG CTC CAG ATT G	22 mer	for qRT-PCR

Designation	Sequence in 5' > 3' direction	Size	Features
AN7903 3'	TTC TCA TAG TCG CAG GCA CAC A	22 mer	for qRT-PCR
VApaUP	AAG GGC CCG ATG GCT ACA CTT GCA G	25 mer	*veA*
VXhLW3	GCC TCG AGG ATG GAG CGG GAG TAG A	25 mer	*veA*

2.2.2.1. Yeast two-hybrid (YTH) screen for velvet interacting proteins (Vips)

pHybLex/ZeoTrp plasmid was used to construct *veA* bait vector for yeast two-hybrid analysis (kind gift from Prof. Dr. S.K. Chae at PaiChai University, Korea). Since full length VeA has a transcription activation activity, N-terminal 315 amino acid encoding part, which was amplified by PCR using forward VApaUP and reverse VXhLW3 oligos, was used as a bait. The PCR product containing the partial *veA* ORF was digested with *Apa*I and *Xho*I and cloned into *Apa*I-*Xho*I treated pHybLex/ZeoTrp, yielding pHybLex/ZTV3. This plasmid was transformed into yeast strain L40 (INVITROGEN), obtaining YHL/ZTV3 strain which was used as host strain for screening of *A. nidulans* cDNA library. *A. nidulans* cDNA library for yeast two-hybrid using HybriZAP-2.1 XR cDNA synthesis kit (STRATAGENE) was kindly provided by Dr. K.Y. Jahng (Chonbuk National University, Korea) as gift.

2.2.2.2. Generation of linear *laeA*Δ cassette and construction of *laeA* complementation and overexpression plasmids

In order to create *laeA* deletion construct 5' UTR region of *laeA* was amplified from the *wild-type* genomic DNA with primers OSB22/24 and 3' UTR region was amplified with OSB25/27. The two amplicons were fused to the *ptrA* marker (pyrithiamine resistance gene from pPTRII) with fusion PCR (Nayak et al., 2006) (nested oligos OSB23/26) yielding 4324 bp linear deletion construct which was used to transform TNO2A3, leading to *laeA*Δ/*veA1* AGB468 that was then crossed with AGB154. This crossing gave rise to prototrophic deletion strains *laeA*Δ/*veA1* (AGB512) and *laeA*Δ/*veA+* (AGB493), respectively. AGB493 and AGB509 strains were crossed in order to obtain *vosA::ctap*, *laeA*Δ/*veA+* combination (AGB510). The *velB::ctap*, *laeA*Δ/*veA+* hybrid (AGB511) was created by crossing AGB493 with AGB389 strain. The presence of *wild-type veA+* allele was verified by analytical PCR of the locus followed by *BstX*I digestion. *laeA* deletion as well as *vosA*- and *velB*-tap loci were confirmed by Southern blot. *ᵖmutA::sgfp* reporter plasmid, pME3296, was introduced into AGB152 (*wt*) and *laeA*Δ (AGB493) strains yielding AGB514 and

AGB515, respectively. For complementation of *laeA*Δ, the *laeA* genomic locus (3.7 kbp), containing 1.5 kbp promoter and 1 kbp terminator regions, was amplified from genomic DNA (OSB22/27) and cloned into the *Stu*I site of pAN8-1 (*phleo*^{R}) which yielded pME3635. Then pME3635 was introduced into *laeA*Δ strains, (*veA+*, AGB493) and (*veA1*, AGB512), resulting in AGB494 and AGB518, respectively. In order to overexpress *laeA* gene, *laeA* cDNA was amplified from cDNA library (OZG61/62) and inserted into the *Pme*I site (pME3718) under nitrogen source regulable *niiA* promoter, generating pME3716. This plasmid was eventually introduced into AGB152, which resulted in AGB519.

2.2.2.3. Generation of linear *vosA::ctap* gene replacement fragment

To replace the *vosA* locus with *vosA::ctap*, *vosA* ORF including 1 kbp of the *vosA* promoter (oligos VosA-A/C) and 1 kbp *vosA* terminator (VosA-D/F) were amplified from genomic DNA and the resulting amplicons were fused to the *ctap::natR* module via fusion PCR (VosA-B/E). Gene replacement cassette was introduced into AGB152, yielding AGB509. The substitution of the *vosA* locus by *vosA::ctap* was verified by Southern hybridization.

2.2.2.4. Generation of <u>b</u>imolecular <u>f</u>luorescence <u>c</u>omplementation (BIFC) vectors for *in vivo* protein interactions

velB cDNA was amplified (OZG397/64 for *n-yfp* , OZG63/64 for *c-yfp* fusion) from sexual cDNA library. Then *n-* (OZG73/387) and *c-yfp* (OZG75/388) amplicons were fused to *velB* cDNAs with oligos OZG397/64 (*n-yfp::velB*) and OZG63/64 (*c-yfp::velB*), respectively. *n-yfp::velB* and *c-yfp::velB* were cloned into the *Pme*I site of pME3160 yielding plasmids pME3712 and 3713, respectively. *vosA* cDNA was also amplified (OZG436/438 for *n-yfp*, OZG437/438 for *c-yfp* fusion) from sexual cDNA library. *vosA* cDNA amplicons (OZG436/438) and (OZG437/438) were fused to *n-yfp* (OZG73/387) and *c-yfp* (OZG75/388) via fusion PCR (Szewczyk et al., 2006). *c-yfp::vosA* and *n-yfp::vosA* fragments were inserted into *Swa*I site of pME3712 and 3713, respectively. Plasmids bearing *n-yfp::velB* / *c-yfp::vosA* and *c-yfp::velB* / *n-yfp::vosA* were named as pME3714 and pME3715, respectively. For the analysis of VelB-VelB dimer formation, *c-yfp::velB* fragment was cloned into the *Swa*I site of pME3712 generating pME3717. The BIFC plasmids, pME3714 (*n-yfp::velB*/*c-*

yfp::vosA), pME3715 (*c-yfp::velB/n-yfp::vosA*), and pME3717 (*n-yfp::velB/c-yfp::velB*) were introduced into the recipient strain AGB506 yielding AGB516 (*velB-vosA*), AGB517 (*vosA-velB*), and AGB543 (*velB-velB*) BIFC strains, respectively. pME3715 was transformed into *laeAΔ* (AGB468), resulting in AGB544 (*velB-vosA, laeAΔ*).

To create BIFC plasmids, comprising *vipC, vapA,* and *vapB* cDNAs were amplified from cDNA libraries with the following primers: OSB32/19 for *vipC n-yfp* fusion, OSB20/19 for *c-yfp* fusion of *vipC*, OSB44/144 for *n-yfp* fusion and OSB45/144 for *c-yfp* fusion of *vapA,* OSB57/68 for *n-yfp* fusion of *vapB,* OSB58/68 for *c-yfp* fusion of *vapB*. The amplified cDNAs were fused to *n-yfp* (OZG73/387), leading to *n-yfp::vipC* (OZG73/OSB19), *n-yfp::vapA* (OZG73/OSB144)*, n-yfp::vapB* (OZG73/OSB68)*.* Similarly, these cDNAs were fused to *c-yfp* (OZG75/388), resulting in *c-yfp::vipC* (OZG75/OSB19), *c-yfp::vapA* (OZG75/OSB144), *c-yfp::vapB* (OZG75/OSB68). Subsequently, these fusion fragments were cloned in *Pme*I and *Swa*I site of pME3160. Detailed overview of the BIFC plasmids are given in Table 2.

2.2.2.5. Epitope tagging of the *veA* locus

The *veA::ctap* fusion construct encompassing the promoter and terminator sequences was amplified from pME3157 with oligos OZG304/305. This amplicon was cloned in the blunted *Apa*I site of pNV1 (Seiler et al., 2006) generating pME3711. AGB513 strain that contains *veA::ctap* in *laeAΔ* strain was created by introducing pME3711 into AGB512. For tagging of *veA* with human influenza hemagglutinin (HA) epitope, *3xha* was amplified from a source plasmid with oligos OZG804/805 that was fused to *A. fumigatus pyroA* cassette with OZG812/694. *veA* promoter and ORF was amplified with OZG798/800 and terminator with 811/803. Finally, three linear fragments were fused to each other using OZG799/802 nested oligos, leading to 5.5 kbp *veA::3xha::pyroA* gene replacement fragment. For construction of *veA* to *sgfp* gene, OZG798/800 amplicon together with OZG801/803 (terminator) were fused to *sgfp::natR* cassette with nested oligos OZG799/802, yielding 5.7 kbp linear fragment. These fragments were transformed into the respective strains given in Table 1.

2.2.2.6. Generation of linear or circular DNA molecules for *vipC* deletion, *ctap* and *sgfp* epitope tagging

With the aim of constructing *vipC::ctap* and *vipC::sgfp* fragments, which are expressed under native promoter, *vipC* locus encompassing the promoter and coding region with primers OSB11/13 for *ctap* fusion and OSB11/17 for *gfp* fusion, and terminator region (OSB14/16) were amplified from genomic DNA. Resulted fragments were fused to either *ctap::natR* or *sgfp::natR* (nourseothricin resistance gene with epitope tags) cassettes with the primers OSB12/15, yielding *vipC::ctap::natR* (5.4 kbp) and *vipC::sgfp::natR* (5.6 kbp) linear fragments. Produced fragments were cloned in *EcoR*V site of pBluescript II SK (+) (FERMENTAS) providing pME3636 and pME3637 plasmids, respectively, which were then brought into *vipC*Δ (H2DVIC) strain, creating AGB480 and AGB482 strains, respectively.

In order to create *vipC* deletion construct, approximately 1.2 kbp 5' and 3' UTR regions were amplified with OSB11/72 and OSB16/73 from *wild-type* genomic DNA, respectively. These two DNA fragments were fused with *ptrA* marker by using nested primers OSB12/15, leading to 4.2 kbp deletion casette that was transformed into AGB551 recipient strain, generating AGB741. For generation of double deletions, *vipC* gene was deleted with *pabaA* cassette. 5' and 3' UTR flanking regions of *vipC* were amplified with OSB11/74 and OSB16/75, which were fused to *pabaA* marker (OSB81/82) with nested primers OSB12/15, leading to 4.5 kbp *vipC*Δ*::pabaA* deletion fragment that was subsequently used to create *vipC*Δ/*vapA*Δ and *vipC*Δ/*vapB*Δ double mutants by introducing into AGB744, and AGB746, yielding AGB747 (*vipC/vapA*) and AGB748 (*vipC/vapB*) strains, respectively. Deletion events were verified by Southern blot. For complementation of *vipC* deletion phenotype, a 3.7 kbp *vipC* locus comprising the promoter and terminator elements were amplified from genomic DNA with OSB11/16 primers and brought into *Stu*I site of *phleomycin* resistance carrying pAN8-1 plasmid. Generated pME3634 plasmid was transformed into *vipC*Δ strain, giving AGB474 strain. For analysis of the VipC interacting proteins, pME3636 was transformed into AGB743 and AGB745 resulting in AGB768 and AGB769, respectively.

2.2.2.7. Generation of *vapA* and *vapB* deletion constructs, complementations, and *ctap*, *sgfp* epitope tagging

To create *vapA* and *vapB* deletion constructs with *ptrA* marker, a 1.2 kbp part of 5' and 3' UTR regions were amplified from the *wild-type* DNA in following combinations: OSB33/35 (*vapA* 5UTR), OSB36/38 (*vapA* 3UTR) and OSB46/48 (*vapB* 5UTR), OSB49/51 (*vapB* 3UTR). OSB33/35, *ptrA* cassette, and OSB36/38 were fused by nested primers OSB34/37, forming a 4.2 kbp *vapA* knock-out cassette. Similarly, *vapB* deletion fragment was created with the primer pairs OSB47/50. Generated linear knock-out fragments were introduced into both AGB551 and AGB552, creating two *vapA* deletion strains with different markers AGB743 and AGB744, respectively. Likewise, AGB745 and AGB746 *vapB*Δ strains carrying two auxotrophic markers were formed. To generate double deletion of *vapA/vapB*, AGB743 and AGB746 strains were crossed, yielding AGB750 prototrophic offsprings that were confirmed by Southern blot hybridization.

    vapA and *vapB* genes were tagged with *ctap::natR* and *sgfp::natR* under their native promoter. *vapA* and *vapB* loci were amplified with the promoter, coding and terminator regions from the *wild-type* genomic DNA in following combinations: OSB33/145 (*vapA* promoter and ORF for *ctap*), OSB147/38 (*vapA* terminator) were fused to *ctap::natR* with OSB34/37. OSB33/146 (*vapA* promoter and ORF for *sgfp*), and OSB147/38 were fused to *sgfp::natR* in a similar strategy. Similarly, for *vapB* epitope tagging, OSB46/55 (*vapB* promoter and ORF for *ctap*), OSB46/54 (*vapB* promoter and ORF for *sgfp*), and OSB56/51 (*vapB* terminator) were fused to either *ctap::natR* or *sgfp::natR* cassettes with OSB47/50 primer pairs. Created endogenous fragments were transformed into AGB551, yielding AGB752 (*PvapA::ctap::natR*), AGB753 (*PvapA::sgfp::natR*), AGB754 (*PvapB::ctap::natR*), AGB755 (*PvapB::sgfp::natR*) strains. *vapA* deletion strain was complemented by a *PvapA::sgfp::natR* cassette (AGB758). For *vapB* complementation, the *vapB* locus with promoter and terminator sequences was amplified with OSB46/51 and cloned in *Stu*I site of pAN8-1 plasmid. The complementation plasmid pME4147 was ectopically transformed into a *vapB* deletion (AGB759).

    Alternatively, due to reduced functionality of *vapB::sgfp* under native promoter, functional *vapB::sgfp* were expressed under constitutively expressed glycolytic *gpdA* promoter. For this aim, *vapB* cDNA was amplified from sexual cDNA library of the *wild-type* strain (OSB70/54). The *vapB* cDNA was fused to *sgfp*

(OZG207/29) with OSB70/OZG29 primer pairs. The linear *vapB::sgfp* fragment was cloned under *gpdA* promoter in *Pme*I site of pME3856, which yielded to pME4146 (*PgpdA::vapB::sgfp*). The pME4146 was transformed into AGB506, providing AGB756. The same linear fragment was also cloned in *Pme*I site of pME4143, which led to pME4145 with *pyroA* marker. pME4145 was transformed into *vapB* deletion strain AGB745 yielding a complementation strain AGB757.

2.2.2.8. Tagging of heterochromatin protein encoding gene *hepA* with *sgfp*

For creation of *hepA::sgfp* fusion, promoter and ORF (OSB136/137), and terminator sequences (OSB138/139) were amplified. These two amplicons were fused to *sgfp::natR* cassette by (OSB136/139) yielding the *hepA::sgfp::natR* fusion that was introduced into the *wild-type*, *vapB*, and *vapB1* overexpression strains.

2.2.2.9. Construction of overproduction plasmids

In order to overexpress the corresponding genes, the following steps were performed: *vipC*, *vapA* and *vapB* cDNAs were amplified from cDNA library with OSB18/19, OSB42/144 and OSB70/68, respectively. Generated fragments were introduced into *Pme*I site of pME3160 under nitrogen source inducible *niiA* promoter, creating pME3645 (*vipC* OE), pME4148 for (*vapA* OE)*,* and pME4149 (*vapB* OE) plasmids. For co-overexpression experiments, the same amplicons were cloned in *Swa*I site of the corresponding plasmids under nitrogen source inducible *niiD* promoter. For the point mutations of SAM binding sites in VipC and VapB proteins, *vipC* was amplified with (N-terminus OSB18/330) and (C-terminus 331/OSB19). Fusion of the two fragments with OSB18/19 created *vipC1* allele. Likewise, *vapB* was amplified with (N-terminus OSB70/328), (C-terminus OSB329/68). Fusion of these two fragments with OSB70/68 resulted in *vapB1* allele with mutated SAM binding residues. Both *vipC1* (residues Glycine 107 and 109 to Alanine) and *vapB1* (residues Glycine 100 and 102 to Alanine) alleles were cloned in *Pme*I site of pME3160, yielding pME4153, and pME4154, respectively. *nosA* cDNA, which was amplified from sexual cDNA library (OZG320/321), was cloned into the *Pme*I site of pME3718 yielding pME3719. *nosA* OE construct (pME3719) was placed in AGB493, which led to AGB545. Integration of the plasmids into the genome was confirmed by diagnostic PCR.

Detailed list of the overexpression plasmids and their corresponding hosts are given in Table 1 and 2.

2.2.3. Hybridization techniques and analysis of nucleic acids

Northern (Brown and Mackey, 1997) and Southern (Southern, 1975) hybridization experiments were performed as given in detail (Bayram et al., 2008c). The Southern hybridization was performed with non-radioactive probes by using AlkPhos Direct™ detection-labeling system (GE HEALTHCARE) as described in the user manual. The Northern hybridizations were also carried out with non-radioactive digoxigenin (DIG) labeling kit (ROCHE). DIG labeled DNA or RNA probes of the corresponding ORFs were either amplified by DIG PCR kit (ROCHE) or transcribed *in vitro* using a transcription kit (ROCHE). DNA-RNA or RNA-RNA hybridizations were performed according to suppliers protocols. Band densities in the Northern blots were analyzed with IMAGEJ (NATIONAL INSTITUTES OF HEALTH) and normalized against rRNA. DNA and amino acid sequences were analyzed by using LASERGENE software (DNASTAR).

2.2.4. Quantitative real time PCR (qRT-PCR)

Total RNA was isolated by using RNeasy (QIAGEN) according to the manufacturer`s protocols. Following DNAase digestion, a 800 ng RNA was applied for cDNA synthesis by using the QuantiTect Reverse Transcription kit (QIAGEN). A Mastercycler® ep *realplex* (EPPENDORF) and the RealMaster SYBR Rox master mix (5 PRIME GMBH) were used for quantitative RT-PCRs with the samples, containing 50 ng template cDNA. All qRT-PCR experiments were carried out as duplicates. House keeping gene, Histone 2A levels were used as standard for relative quantification of Δct values (Livak and Schmittgen, 2001).

2.3. Fungal Physiology

2.3.1. Spore viability test

Viability of spores was examined as described (Ni and Yu, 2007). Two-day old conidia (10^5 per plate) of *wild-type* and the mutants were spread on solid GMM and incubated at 37 ^{o}C. After 2-10 days, the conidia were collected and counted in a hemocytometer. Approximately 200 conidia were inoculated on solid GMM and incubated for 2 days at 37 ^{o}C. Survival rates were calculated as a ratio of the number

of growing colonies to the number of spores inoculated. This test was performed in triplicate.

2.3.2. Trehalose assay

Trehalose was extracted from conidia and analyzed as described previously (d'Enfert and Fontaine, 1997, Ni and Yu, 2007). Two-day old conidia (2×10^8) were collected and washed with ddH_2O. Conidia were resuspended in 200 µl of ddH_2O and incubated at 95 °C for 20 min and the supernatant was collected by centrifugation. The supernatant was mixed with equal volume of 0.2 M sodium citrate (pH5.5) and samples were incubated at 37 °C for 8 h with or without 3 mU of trehalase (SIGMA), which hydrolyzes trehalose to glucose. The amount of glucose generated was assayed with a glucose assay kit (SIGMA). The amount of glucose by deducting trehalase untreated sample from trehalase-treated sample was converted into the trehalose amount (pg) per conidium (triplicate).

2.3.3. Stress tolerance test

Oxidative stress tolerance test was carried out as described previously (Han et al., 2004). Hydrogen peroxide sensitivity of conidia was tested by incubating 1 ml of conidial suspensions containing 10^5 conidia with varying concentrations (0.0, 0.25 or 0.5 M) of H_2O_2 for 30 min at RT. Each conidia suspension was then diluted with ddH2O, and the conidia were inoculated into solid MM. After incubation at 37 °C for 48 h, colony numbers were counted and calculated as a ratio to the untreated control. Sensitivity to oxidative stress was also tested by spotting 10 µl of serially diluted conidia (10 to 10^5) on solid MM with 0, 2.5, 5 M of H_2O_2 and incubated at 37 °C for 48 h.

UV tolerance test was carried out as described previously (Lima et al., 2005) with a slight modification. Two-day old conidia were collected in ddH_2O and plated out on solid MM (100 conidia per plate). The plates were then irradiated immediately with UV using a UV crosslinker and the plates were further incubated at 37 °C for 48 h. The colony numbers were counted and calculated as a ratio to the untreated control. UV sensitivity was also tested by spotting 10 µl of serially diluted conidia (10 to 10^5) on solid MM, which were then irradiated with UV and incubated at 37 °C for 48 h.

2.4. Protein methods

2.4.1. Immunoblottings

Primary and secondary antibodies used during this study were applied in following conditions and dilutions: polyclonal rabbit α-calmoduline binding peptide (CBP) (07-482, MILLIPORE), 1:1000 dilution in TBS with 5% skimmed milk, secondary antibody goat α-rabbit (sc-2006, SANTA CRUZ) 1:2000 in TBS 5% skimmed milk. Monoclonal α-GFP (GFP (B-2):Sc-9996, SANTA CRUZ) 1:1000 dilution in TBS, containing 5% skimmed milk, secondary antibody goat α-mouse (115-035-003, DIANOVA) 1:2000 in TBS 5% skimmed milk. Monoclonal α-HA (H 3663, SIGMA) 1:1000 dilution in TBS 5% skimmed milk, secondary antibody same as for α-GFP. Rabbit polyclonal α-SkpA and VeA (raised in GENESCRIPT) 1:2000 (5 μg) in TBS 5% skimmed milk with 0.1% Tween-20, same secondary antibody for α-CBP. Polyclonal α-Histone 3 (ab1791, ABCAM), H3K9/14 (pAb-005-050, DIAGENODE), 1:2500 in PBS 5% BSA, same secondary antibody for α-CBP, α-SkpA. H3K9me3 (MAb-153-050, DIAGENODE), H3K4me2 (MAb-151-050, DIAGENODE), 1:2500 in PBS 5% BSA, same secondary antibody as for α-GFP. Band intensities in the immunoblottings were analyzed with IMAGEJ (NATIONAL INSTITUTES OF HEALTH) and normalized against either SkpA or Histone 3 signals.

2.4.2. Protein extraction, nuclear enrichment, and dephosphorylation assay

Fungal mycelia were grounded in mechanical grinder MM400 (RETSCH) filled with liquid nitrogen. Protein extracts were prepared by resuspending the pulverized mycelia in protein extraction buffer (PEB) (100 mM Tris pH:7.5, 300 mM NaCl, 1 mM EDTA, 0.1% NP-40, 10% Glycerol, 1 mM DTT) containing protease inhibitor mix (ROCHE). Nuclei were isolated and prepared as described in detail (Palmer et al., 2008). Protein amounts of the crude and nuclear extracts were determined according to Bradford assay. For dephosphorylation assay, PEB without phosphatase inhibitors were used. Total protein extract (1 mg) was treated with 10 units of shrimp alkaline phosphatase (SAP, FERMENTAS) at 37 ºC for 30 min. SAP-treated extracts were used for immunoblottings.

2.4.3. <u>T</u>andem <u>A</u>ffinity <u>P</u>urification (TAP) protocol and LC-MS/MS Protein identification

Tap tag experiments and preparation of the protein crude extracts were perfomed as explained in detail (Bayram et al., 2008c). Protocols given elsewhere were followed for further data processing and analysis of the proteins (Bayram et al., 2012b).

2.4.4. <u>Co</u>-Immunoprecipitations (Co-IPs)

For *in vivo* interaction studies, GFP-Trap (CHROMOTEK) agarose was used. The fungal mycelia pulverized in liquid nitrogen was resuspended in PEB, containing protease inhibitor cocktail (ROCHE). 10 µl of GFP-Trap agarose was shortly resuspended and washed in 1 ml protein extraction buffer. From each strain, 8 mg total crude extract (1.5-2 ml) was incubated with a 10 µl prewashed GFP-Trap agarose for 4 hours at 4ºC on a rotator. The beads were washed with 1.5 ml protein buffer three times, which were finally boiled in a 40 µl 3x protein loading dye. A 5 µl of the mixture was run on 4-15% SDS polyacrylamide gel for detection.

2.5. Cell biology: Confocal spinning disc and fluorescence microscopy

Green fluorescent, enhanced yellow fluorescent, and monomeric red fluorescent protein (GFP, EYFP, mRFP) expressing strains were grown in a 450 µl liquid GMM media in borosilicate slide chambers (NUNC). The equal exposure time was used for the same set of strains used in the same experimental set-ups. Fluorescent proteins were observed with an inverted microscope, AXIOVERT OBERSVER. Z1 (ZEISS) connected with a QUANTEM:512SC (PHOTOMETRICS) digital camera in combination with a laser scanner unit CSU-X1 A1 from YOKOGOWA. Digital images were taken and processed with the SLIDEBOOK 5.0 software (INTELLIGENT IMAGING INNOVATIONS).

2.6. Metabolite analysis

2.6.1. <u>S</u>terigmatocystin (ST) and <u>T</u>hin <u>L</u>ayer <u>C</u>hromatography (TLC) analysis

Extraction of ST and running on TLC plates were performed as described in detail elsewhere previously (Bayram et al., 2009).

2.6.2. Metabolite fingerprinting

The culture supernatants of *wild-type* and overexpression strains were extracted by two phase partitioning and analyzed by Ultra Performance Liquid Chromatography coupled with a photo diode array detector and an orthogonal time-of-flight mass spectrometer (UPLC PDA TOF MS, WATERS CORPORATION) as described by Floerl et al., 2012. Data deconvolution of the raw mass spectral data was performed by the MarkerLynx Application Manager for MassLynx 4.1 software (WATERS CORPORATION). For further data processing, such as filtering, adduct identification, correction of raw masses, combination of data matrices, clustering, and visualization, the MarVis-Suite software (MarkerVisualization, http://marvis.gobics.de) consisting of the tools MarVis-Filter (Kaever et al., 2012) and MarVis-Cluster (Kaever et al., 2009) was used as described by (Floerl et al., 2012) with the following changes: For ranking and filtering an ANOVA test in combination with false discovery rate (FDR) control was performed to select 1197 high-quality marker candidates with an FDR < 10^{-6}. The identity of the markers OA, F-9776A and F-9776B was confirmed by comparison of the UV/VIS spectra with literature (Bok et al., 2009, Sanchez et al., 2010) and in case of OA by comparison with an authentic standard.

3. Results

3.1. LaeA control of velvet family regulatory proteins for light-dependent development and fungal cell-type specificity

3.1.1. Identification of an alternative light-regulated protein complex, VelB-VosA

Functionally tagged versions of all three proteins of the velvet complex VelB-VeA-LaeA are able to recruit the respective other subunits from a fungal protein extract. In addition, the phenotypes of the corresponding *velB* or *veA* deletion strains are similar: both mutants are unable to perform sexual development and are impaired in light control and secondary metabolism (Bayram et al., 2008c). However, only a tagged VelB, but neither VeA nor LaeA, is able to recruit another related protein, VosA (Bayram et al., 2008c). VosA was isolated as a high copy repressor of asexual development and is also required for spore maturation, trehalose biogenesis and long-term viability of asexual and sexual spores (Ni and Yu, 2007). We analyzed whether VelB has an additional yet unexplored function in fungal development.

We initially examined whether VosA is the fourth subunit of the velvet complex during the establishment of developmental competence. Developmental competence describes the phenomenon that *A. nidulans* spores require at least 20 hours of growth after germination to respond to external signals when placed on the surface of a medium (Axelrod et al., 1973). *A. nidulans* strain expressing a functional *vosA::ctap* fusion driven by its native promoter was cultivated in liquid medium and induced on the surface of solid medium for asexual or sexual development by incubation in light and dark, respectively. Purification of VosA::cTAP was performed from 12 hours post- induction cultures on surface of solid medium after developmental competence was achieved. Tagged VosA was only present in the dark and co-purified exclusively with the VelB protein, but neither with VeA nor LaeA (Figure 6A). VelB is not only a part of the VelB-VeA-LaeA velvet complex, but also a part of the second complex VelB-VosA when developmental competence is established.

Heterologous expression of VelB in *Escherichia coli* resulted primarily in dimers suggesting that VelB is able to form homodimers (data not shown) in addition to the VelB-VosA heterodimer. We employed a split-YFP system to determine the *in vivo* compartment where the subunits of the VelB-VosA heterodimer or of the VelB-

VelB homodimer interact. An mRFP histone fusion served as control to track the nuclei within the hyphae. The VosA-VelB YFP signal colocalized predominantly to the nuclear RFP signal, indicating that the VosA-VelB complex is formed in the nucleus (Figure 6B).
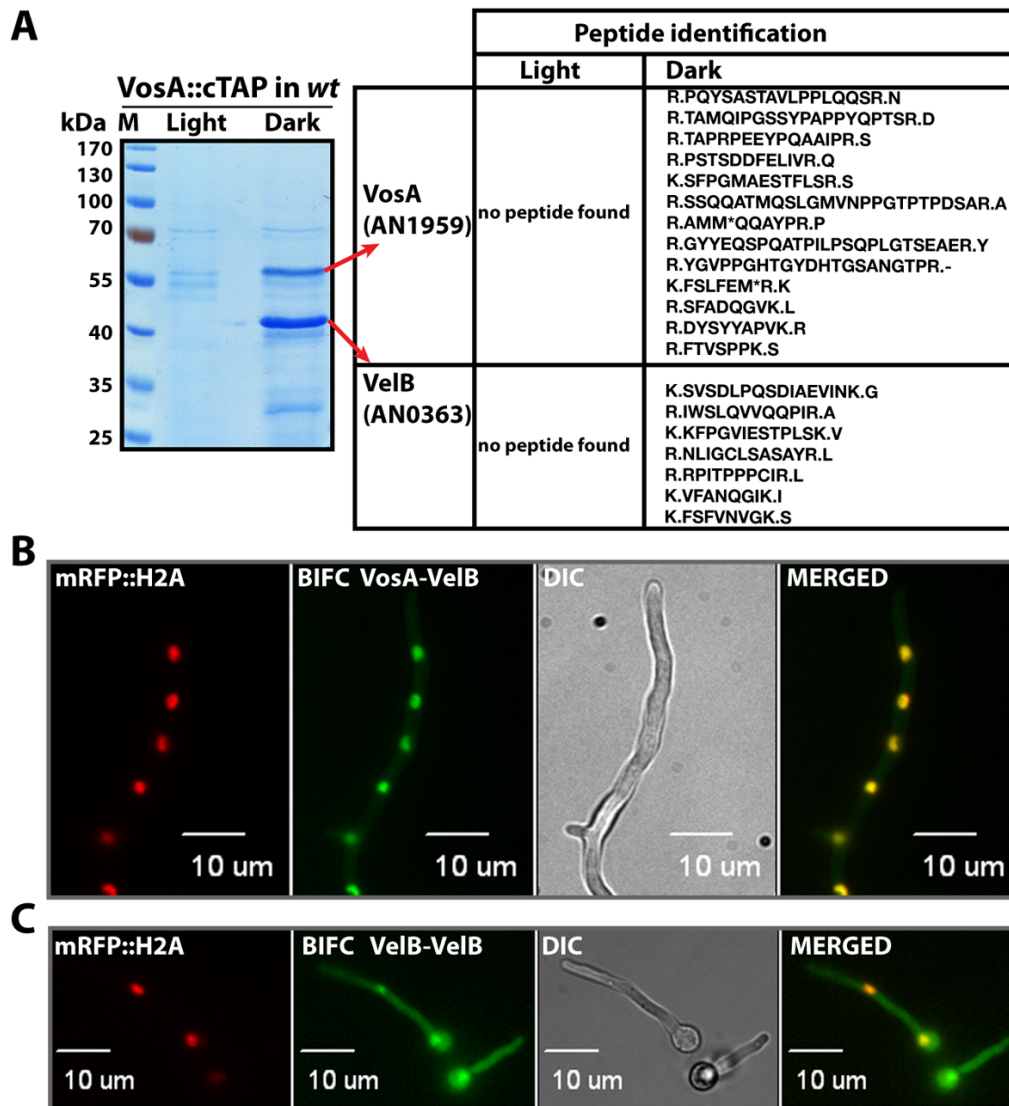
Figure 6. identification of the VosA-associated proteins by tandem affinity purification. A. SDS-polyacrylamide (10%) gel electrophoresis of TAP enrichment for VosA stained with brilliant blue G. Polypeptides identified from the bands of affinity purification from the light and dark grown cultures are shown. **B.** Bimolecular fluorescence complementation (BIFC) in vegetative hyphae with nuclear interaction of the VosA-VelB heterodimer. The N-terminal half of the <u>e</u>nhanced <u>y</u>ellow <u>f</u>luorescent <u>p</u>rotein (EYFP) fused to the N-terminus of the VosA protein (N-EYFP::VosA) interacts with the C-terminal half of EYFP fused to VelB (C-EYFP::VelB) *in vivo*. Histone 2A monomeric red fluorescent protein fusion (mRFP::H2A) visualizes the nuclei. **C.** BIFC of the VelB-VelB homodimer formation in the cytoplasm and nuclei. N-EYFP::VelB interacts with C-EYFP::VelB.

In contrast, we found the combined signal of N-YFP::VelB and C-YFP::VelB *in vivo* in the cytoplasm as well as in the nucleus (Figure 6C). These data suggest that

VelB is not only a component of the nuclear VelB-VeA-LaeA complex, but can also (i) form a VelB homodimer in the cytoplasm as well as in the nucleus, and (ii) be part of the nuclear VosA-VelB heterocomplex, which is hardly detectable in the cytoplasm.

3.1.2. The role of VelB in fungal spore maturation

VosA is not only a high-copy repressor of asexual development but also plays an essential role in the maturation and viability of spores primarily by coupling trehalose biogenesis and sporogenesis (Ni and Yu, 2007). We analyzed whether VelB plays a similar role, as it forms the nuclear VelB-VosA heterodimeric complex. The viability of spores, trehalose biosynthesis and tolerance against various stresses were compared between the *velB*Δ, *wild-type*, and *veA*Δ or *vosA*Δ strains (Figure 7A). The conidia of both *velB*Δ and *vosA*Δ strains displayed severe viability defects, whereas viability of the *veA*Δ conidia was similar to that of *wild-type*, indicating that VelB and VosA play a specific role in conferring spore viability. VelB is needed for the proper biogenesis of trehalose in conidia, because trehalose was undetectable in the *velB*Δ and *vosA*Δ conidia (Figure 7B). The mRNA levels of two genes (*tpsA* and *orlA*) associated with trehalose synthesis (Borgia et al., 1996, Fillinger et al., 2001) revealed that the *velB*Δ and *vosA*Δ strains both exhibited reduced *tpsA* and *orlA* transcript levels during the late phase of development and in conidia (Figure 7C). These results indicate that both VelB and VosA are necessary for trehalose biogenesis and viability of spores.

As trehalose plays an important protective role in response to various stresses, we tested whether the absence of *velB* would result in decreased tolerance of the spores against various stresses, and examined two-day old conidia of *wild-type*, *veA*Δ, *velB*Δ, and *vosA*Δ strains. Serially diluted spores were cultivated on solid medium containing various H_2O_2 concentrations. The *velB*Δ conidia were the most sensitive among those tested (Figure 7D). At 0.25 M H_2O_2, 90% of the *velB*Δ conidia were non-viable, whereas only about 40% of *wild-type* and the *veA*Δ conidia lost viability. After being treated with 0.5 M H_2O_2, most of the *velB*Δ and *vosA*Δ conidia were non-viable, whereas about 60% and 50% of *wild-type* and the *veA*Δ conidia, respectively, were viable (Figure 7D). These data were further confirmed by testing the tolerance against UV, where both the *vosA*Δ and *velB*Δ conidia were more sensitive than those of *wild-type*.
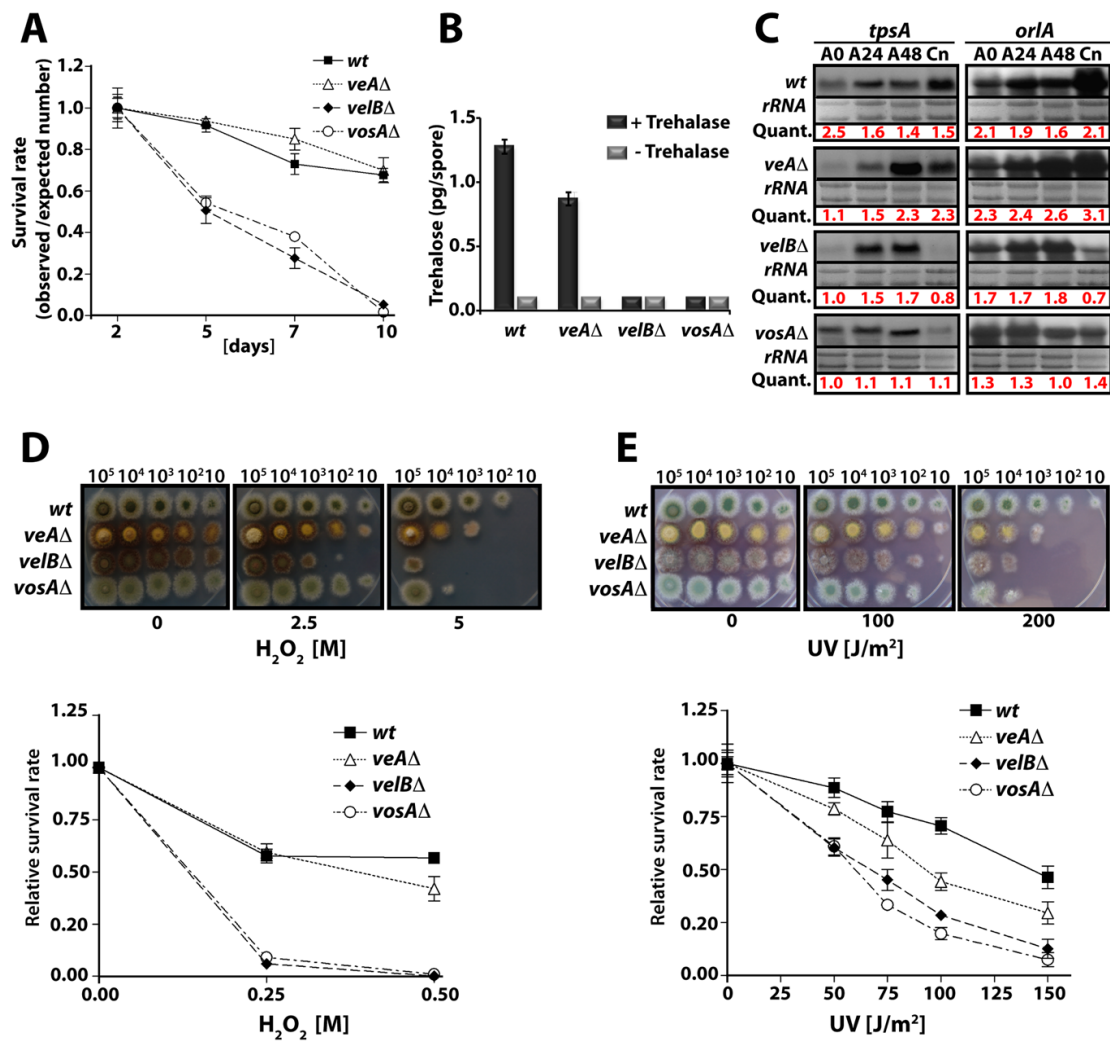
Figure 7. VelB function in spore viability and trehalose biogenesis. A. Viability of *wild-type* and velvet mutant strains conidia grown at 37 °C for 2, 5, 7, and 10 days. **B**. Amount of trehalose (pg) per conidium in the 2 day old conidia of *wild-type* and the velvet deletion mutants (measured in triplicate). Samples without the trehalase treatment served as controls. **C.** Levels of *tpsA* and *orlA* transcripts in *wild-type* and velvet mutant strains. Numbers indicate the time (hour) of incubation in post-asexual (A) developmental induction and (Cn) represents conidia. Equal loading of total RNA was evaluated by ethidium bromide staining of rRNA. Quantification of *tpsA* and *orlA* expression levels are indicated at the bottom of the blots. Quant: Quantification. **D.** Tolerance of the conidia of *wild-type* and velvet mutant strains against H_2O_2 (see text). **E.** Tolerance of the conidia of *wild-type* and velvet mutant strains against <u>u</u>ltra <u>v</u>iolet (UV) irradiation.

Being exposed to 100 J/m² UV only about 30% of the *velBΔ* and *vosAΔ* conidia were viable, whereas 80% of *wild-type* conidia could survive. The *veAΔ* conidia were also more sensitive compared to *wild-type* (Figure 7E). While the *velBΔ* and *vosAΔ* conidia were more sensitive to thermal stress than *wild-type*, the mutant and *wild-type* conidia were equally tolerant to high osmolarity (data not shown). These data indicate that both VelB and VosA are required for trehalose biogenesis in

spores, thereby conferring the viability and stress tolerance of spores. The VelB-VosA heterodimer might be the functional unit for these critical biological processes.

3.1.3. LaeA controls light-dependent formation of the VelB-VosA complex

The finding that both heteromeric complexes are located in the nucleus suggested that there might be a competition for VelB between the nuclear VelB-VeA-LaeA velvet complex and the nuclear VosA-VelB complex. VelB and VosA protein levels were monitored using functional TAP-fusions and the α−calmodulin antibody to address the developmental time window during which both subunits are expressed simultaneously and the VelB-VosA complex can be formed. In *wild-type* cells VelB and VosA were present abundantly during vegetative cultivation in submerged cultures but upon transfer to solid medium in the light both proteins became undetectable. In the dark both proteins were present at the beginning of sexual development (12 h sexual) and then undetectable during later stages of development (Left panels, Figure 8A, B). This suggests a potential role of the VosA-VelB complex during vegetative growth and at the beginning of sexual development in the dark when the velvet complex VelB-VeA-LaeA is also present. Simultaneous overexpression of VelB and VosA under an inducible promoter (*niiA*/*niiD*) resulted in a drastic repression of asexual development. The overexpression of VelB-VosA gave rise to 80% reduction in asexual sporulation, which further supports a common role of both proteins in development of the fungus (Figure 9).

We analyzed whether the VosA and VelB protein levels depend on the presence of VeA or LaeA. Expressional analysis of the two regulators in a *veA*Δ strain did not result in significant changes in the VelB or VosA protein levels in comparison to *wild-type* (data not shown). However, in a *laeA*Δ strain, both VosA and VelB were still present after 12 hours incubation in the light. Moreover they also appear during mid sexual stage (24, 48 h sex) (Right panels, Figure 8A, B). We performed VosA-TAP purification using a *laeA*Δ strain to determine whether the absence of LaeA also resulted in formation of the VelB-VosA complex in fungal extracts (Figure 8C).

TAP purification of VosA from cultures grown in either the light or the dark in the absence of LaeA demonstrated that the VosA-VelB association occured predominantly in the light, which was contrary to the *wild-type* situation where we only found the complex in dark grown cultures (Figure 6A). Formation of the VosA-

VelB nuclear complex in the light in a *laeA*Δ strain was further corroborated by BiFC assay (Figure 8D).
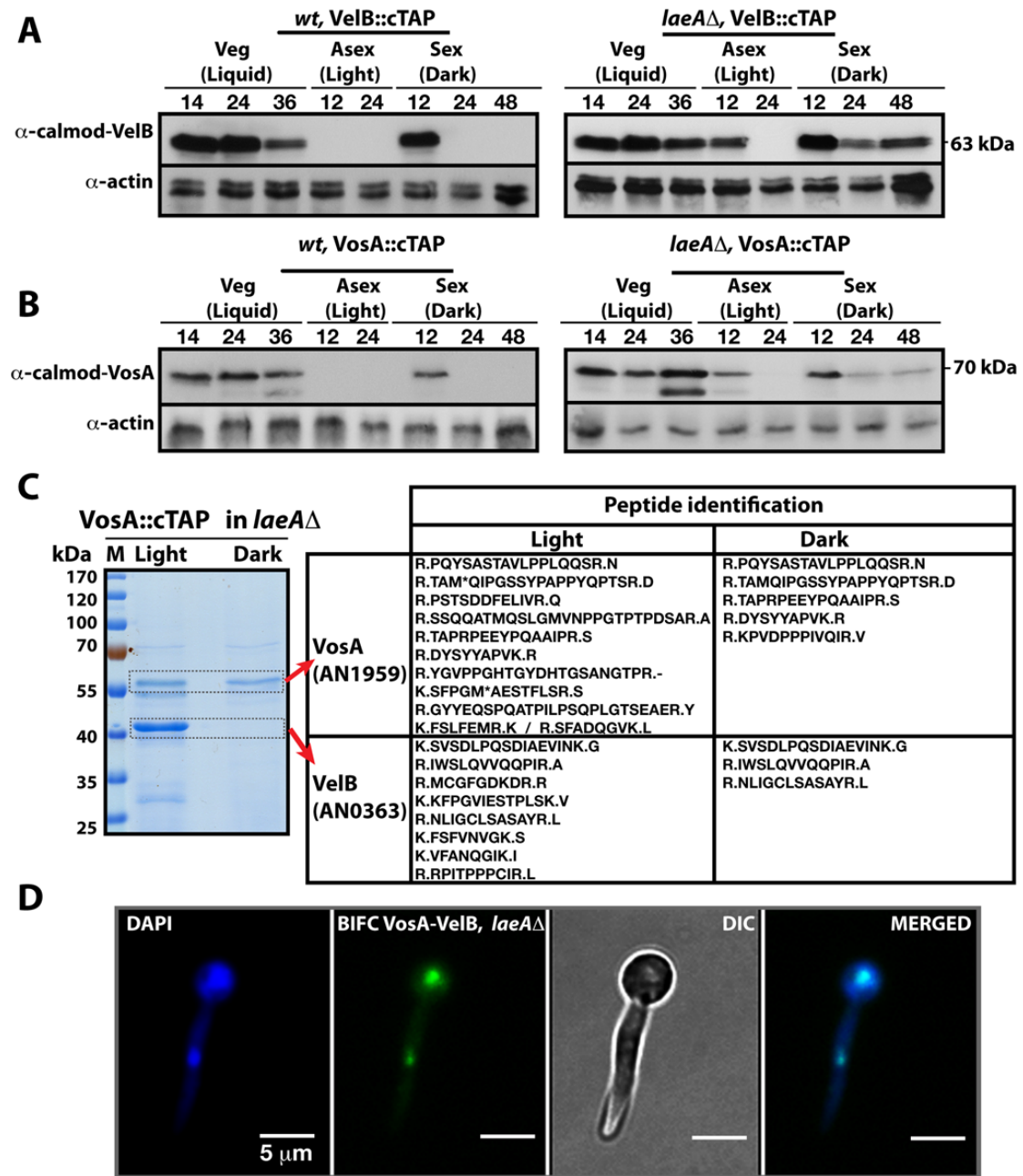
Figure 8. LaeA control of VosA and VelB protein levels and the VosA-VelB complex formation. A. VelB::cTAP and (**B**) VosA::cTAP fusion protein levels detected by α-calmodulin antibody during different developmental stages in *wild-type* (*wt*) and *laeA*Δ strains at 37 °C. α-actin served as internal control. Protein crude extracts (80 μg) were loaded in each lane. **C.** Brilliant blue G-stained 10% SDS-polyacrylamid gel of VosA::cTAP and identified polypeptides in *laeA*Δ strain grown in the light and dark are given. **D.** BIFC interaction of the nuclear VosA-VelB complex in *laeA*Δ strain. N-EYFP::VosA interacts with C-EYFP::VelB. Nuclei were counterstained with DAPI (blue).

velB::ctap and *vosA::ctap* mRNA levels in *wild-type* and *laeAΔ* did not correlate with the protein levels (Figure 10). Transcripts of the both genes were present during asexual conidiation and slightly upregulated in the absence of the *laeA* gene. These results suggest that there is a posttranslational control for the VosA-VelB proteins and LaeA plays a key role in light-dependent control of the VosA and VelB protein levels.
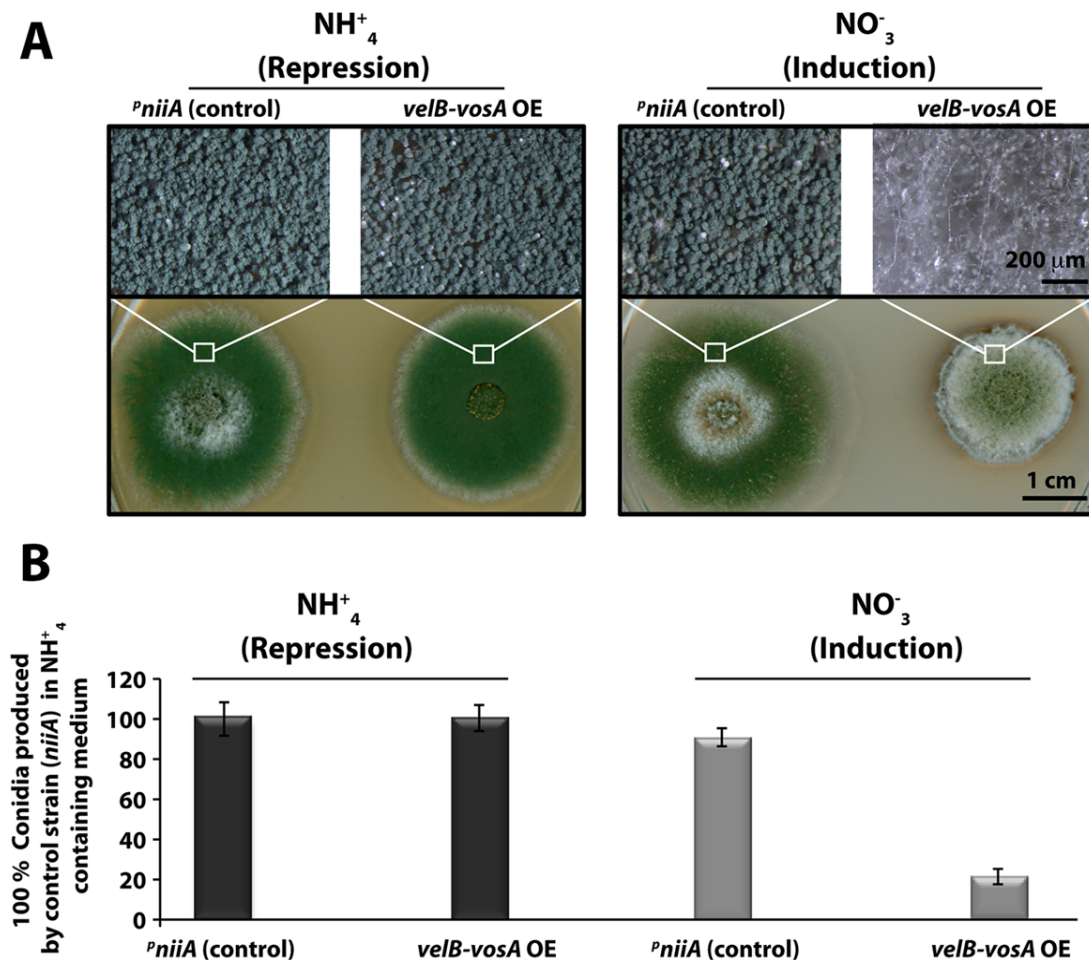
Figure 9. The VosA-VelB dimer and fungal development. Overexpression of *vosA-velB* under nitrate inducible bidirectional *niiA/niiD* promoter. **A.** Asexual development of control strain (empty *niiA/niiD* plasmid), and *vosA-velB* OE strain (*^{p}niiD::n-yfp::vosA-^{p}niiA::c-yfp::velB*) on either ammonium (repressive) or nitrate (inducing) containing plates as nitrogen source under light at 37 ^{o}C for 3 days. **B.** Quantification of asexual conidiation from plates (A). 5×10^3 conidia were point inoculated. From three independent plates, three sectors (10 mm^2) were counted and asexual conidiation of the control strain was used as 100% standard. Calculated standard deviations are indicated as vertical bars.
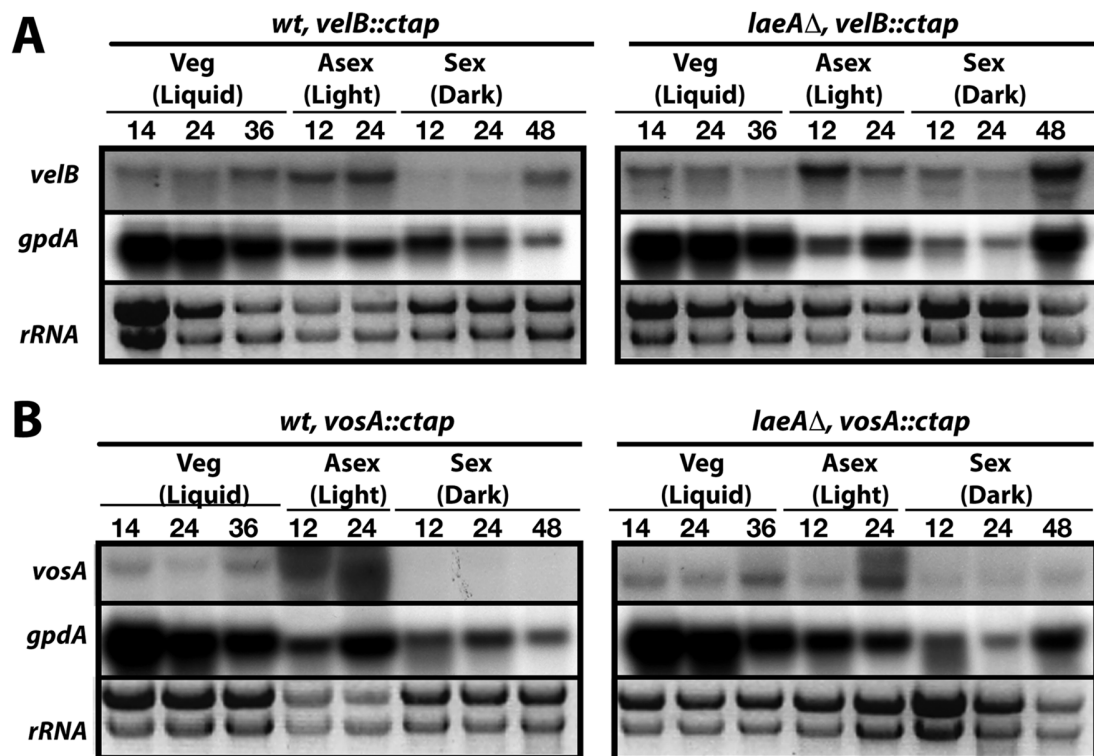
Figure 10. Transcript levels of *velB::ctap* and *vosA::ctap* during different developmental stages in *wild-type* and *laeA∆* strain. A. Expression of *velB::ctap* in the *wild-type* and *laeA∆* strain during vegetative growth (14, 24, and 36 hours), after post asexual induction under light (12, 24 hours), and sexual induction in the dark (12, 24, and 48 hours). **B.** Expression studies with *vosA::ctap* fusion at the same time points of development. *gpdA* gene expression and ethidium bromide stained rRNA were used as loading controls. 20 μg RNA was used for each lane.

3.1.4. LaeA controls VeA protein levels and inhibits a molecular size shift from 63 kDa to 72 kDa of VeA

We monitored the cellular levels of the VeA protein during development to explore whether the protein levels of all three members of the velvet family are controlled by LaeA. While it was previously reported that *veA* expression is upregulated in the *laeA∆* (Bayram et al., 2008c), the VeA protein levels have not been analyzed. α-VeA antibodies revealed that the cellular levels of the native 63 kDa VeA protein were comparable in *wild-type* and the *laeA∆* strain in crude cell extracts (Figure 11A, B).

A small subpopulation of a VeA isoform of a higher molecular weight (72 kDa) could be detected in *wild-type* cultures during vegetative growth or sexual development in the dark. During the light-mediated asexual development this isoform was hardly detectable.
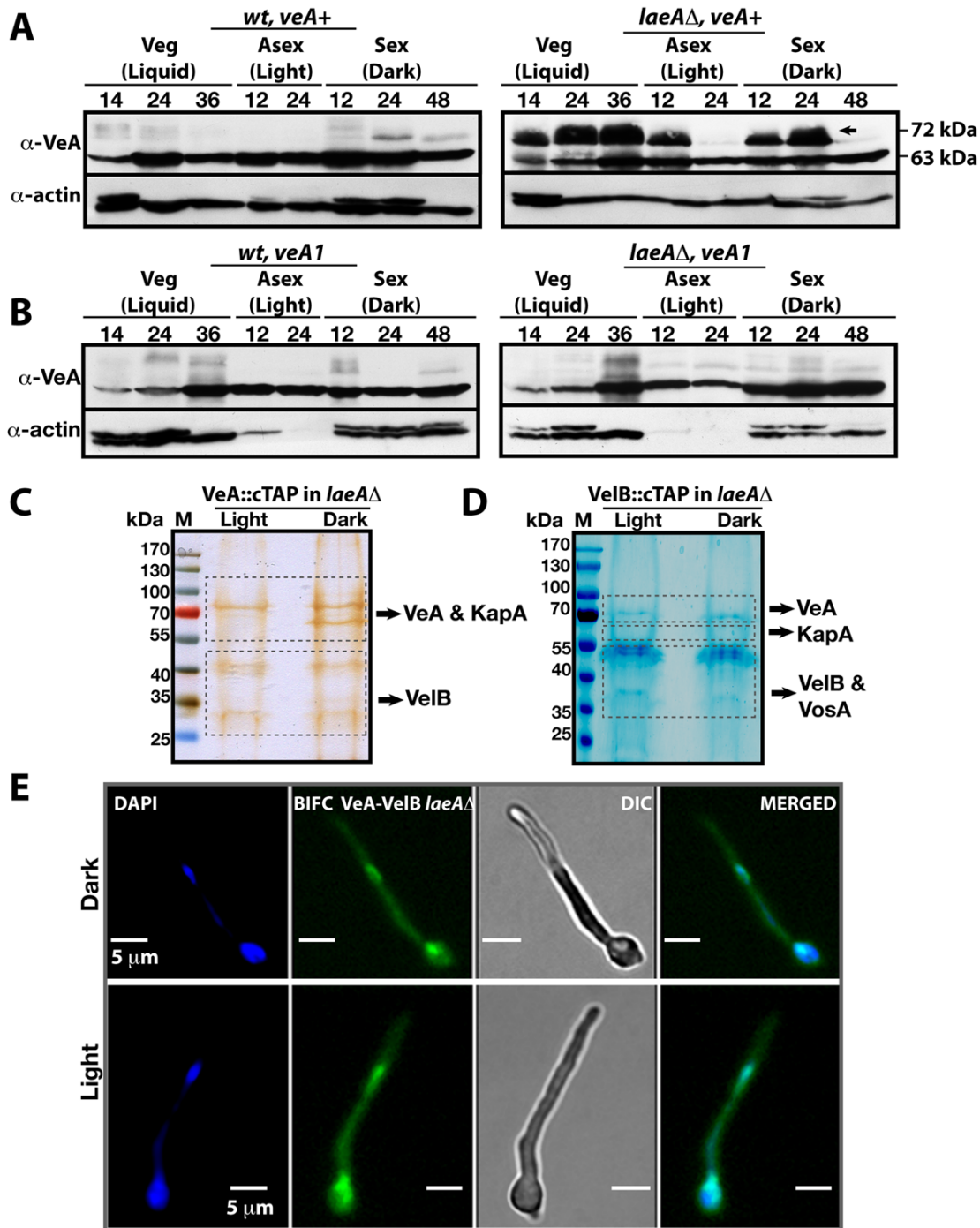
Figure 11. VeA-63 kDa and VeA-72 kDa protein levels in *wild-type* and in *laeAΔ* fungal strains.
A. The VeA protein levels in *wild-type* (*wt*) and *laeAΔ* strains during development (vegetative 14, 24, 36 h in submerged culture, asexual 12, 24 h on plates in the light, sexual 12, 24, and 48 h on plates in the dark at 37 °C) by using α-VeA antibodies; α-actin served as internal control. 80 μg total protein was loaded in each lane. **B.** The N-terminally truncated VeA1 protein levels in *wt* and *laeAΔ* strains. **C.** Silver stained 10% SDS- polyacrylamid gel of VeA::cTAP and identified proteins in *laeAΔ* strain grown in the light and dark. **D.** SDS-polyacrylamide (10%) gel electrophoresis of VelB::cTAP and associated proteins (in *laeAΔ veA+* strain) stained with brilliant blue G. **E.** BIFC interactions of N-EYFP::VeA and C-EYFP::VelB in *laeAΔ* fungal cells in light or dark. Nuclei were co-stained by DAPI.

This VeA-72 kDa isoform accumulated to higher levels than VeA-63 kDa in the *laeAΔ* strain in vegetative growth and early development with or without light. The total amount of the VeA protein in the absence of LaeA is therefore significantly higher in comparison to *wild-type*. This suggests that LaeA inhibits the overall protein levels of all three members of the velvet family members and specifically inhibits the formation of the 72 kDa VeA isoform.

VeA1 is a peculiar light-insensitive mutant variant of the VeA protein. The *veA1* mutant produces significantly reduced levels of sexual fruiting bodies and constantly high amounts of asexual spores in the dark as well as in the light (Kaefer, 1965). The *veA1* mutant phenotype develops by an unknown mechanism and depends on the truncation of the first 36 N-terminal amino acids in comparison to the full-length VeA (Kim et al., 2002). This shortened VeA1 mutant protein exhibits reduced protein interaction with VelB and decreased nuclear import of both proteins (Stinnett et al., 2007, Bayram et al., 2008c). In contrast to *wild-type*, the *veA1* mutant did not accumulate VeA-72 kDa (Figure 11B) suggesting that this LaeA dependent molecular shift correlates with light regulation and depends on an intact N-terminal part of VeA. In the presence of VeA1, actin levels decreased presumably due to the increased asexual conidiation (Light 12 and 24), (Figure 11B).

In the absence of LaeA we analyzed complex formation of VeA in the light, when the modified VeA-72 kDa, VosA and VelB proteins accumulated. A VeA::cTAP *laeAΔ* strain was shifted from vegetative liquid growth to solid medium in the light or in the dark for 12 hours to achieve developmental competence. We detected high levels of the VelB-VeA dimer associated with the α-importin KapA under both conditions (Figure 11C). The reciprocal experiment using VelB::cTAP recruited VeA and KapA, in addition to VosA. These proteins all co-purified with VelB in the dark as well as in the light (Figure 11C). However, VeA::cTAP in *wild-type* recruits these proteins only in the dark, but fails to recruit VosA and only small amounts of VelB in the light (Bayram et al., 2008c). BIFC localization studies revealed that the VeA-VelB interactions in the *laeAΔ* background can take place in nuclei of fungal hyphae both in the light and the dark (Figure 11E).

The data suggest that LaeA not only controls the amounts of VosA, VelB and VeA in the light, but also prevents the shift of VeA to the 72 kDa isoform, which presumably represents a post-translational modification. This LaeA controlled VeA

modification does not impair the transport of VeA-VelB into the nucleus assisted by the importin KapA. The finding that the importin KapA was only recruited together with VeA(-TAP)-VelB but not with VosA(-TAP)-VelB supports our earlier finding that VelB is preferentially transported into the nucleus together with VeA (Bayram et al., 2008c).

3.1.5. LaeA is required for light-mediated inhibition of sexual development

LaeA has been identified as a global regulator of secondary metabolism (Bok and Keller, 2004) in light-insensitive *veA1* laboratory strains (Kim et al., 2002). The *veA1* allele represents an artificial situation that could be misleading for the understanding of the molecular function of VeA. Therefore we analyzed the *laeA* deletion mutant in the *veA wild-type* background, which revealed distinct differences in colony morphology for *veA+* and *veA1*. The *laeAΔ veA+* colony is white, whereas *laeAΔ veA1* exhibits the typical green color of *wild-type* colonies, which is due to the pigmentation of the asexual spores (Figure 12A). All analyzed *laeAΔ* strains irrespective of the *veA* allele were unable to produce the mycotoxin ST underlining the well-known LaeA function as a global regulator of secondary metabolism (Figure 12B).

Microscopic examination revealed two major differences between the *laeAΔ veA+* strain and the other strains. *Wild-type* as well as *laeAΔ veA1* strain produced higher number of conidiophores bearing the asexual spores (conidia) than *laeAΔ veA+* strain in the light and dark. Quantification of the conidia indicated that conidia production in *laeAΔ* in the *veA+* background was significantly decreased in the light to approximately 20% of the *wild-type* and asexual development was unresponsive to illumination (Figure 12A). This suggests that there is a yet unexplored LaeA control for asexual spore formation, which only works in combination with an intact VeA N-terminus. In addition to a reduced number of conidia, the whitish appearance of *laeAΔ* colonies originated from significantly elevated levels of sexual structures both in the dark and light (Figure 12A). *Wild-type veA+* strain generated few cleistothecia (seen as black or white round structures) and many conidiophore heads (green structures) in the light, but more cleistothecia and less conidiophores in the dark.
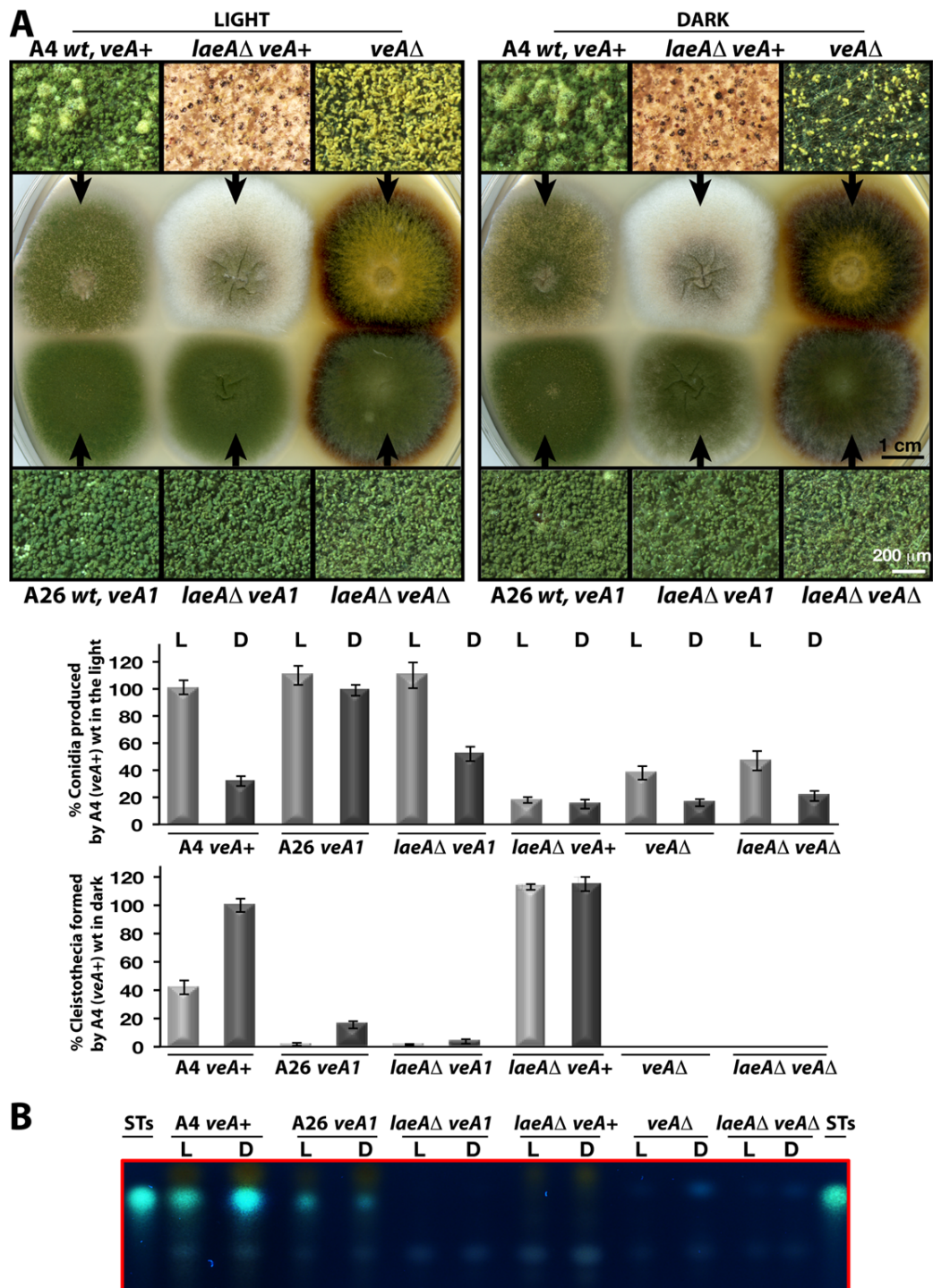
Figure 12. LaeA-VeA as regulators of development and secondary metabolism. **A.** Colony morphologies, quantifications of asexual spore (conidia, in light) and fruiting body (cleistothecia, in dark) formations of (A4) *veA+*, (A26) *veA1*, *laeAΔ/veA+*, *laeAΔ/veA1*, *veAΔ*, *laeAΔ/veAΔ* strains grown on the plates at 37 °C for 5 days in the light asexually or in the dark sexually. For the quantification of conidia or cleistothecia, the 5x10 mm^2 sectors from 5 independent plates were used and the standard deviations are indicated as vertical bars. *veA+* strains conidiation and cleistothecia levels were used as standard (100%). **B.** The secondary metabolite ST production levels of the strains from (A) examined by TLC. 5x10^3 conidia were point-inoculated at the center of the plates that were kept either in white light (90 μW^2) or in dark.

The *veA1* strain produced only few cleistothecia in the dark, therefore formed predominantly conidia under both light and dark conditions (Figure 12A). The unresponsiveness of the *laeAΔ* strain to the white light does not depend on specific light receptors. We determined photon fluence-rate response curves for the photoinhibition of fruiting body formation under near UV for CryA, blue-light spectra for LreA-LreB, and red-light spectra for FphA (Bayram et al., 2008a, Purschwitz et al., 2008b). *Wild-type* strain reduced cleistothecia formation with increasing photo dosage to below 20%. In contrast, the photoinhibition in the *laeA* mutant was lost under all irradiation conditions (UVA $_{366\,nm}$, blue $_{460\,nm}$, red $_{680\,nm}$) (Figure 13).
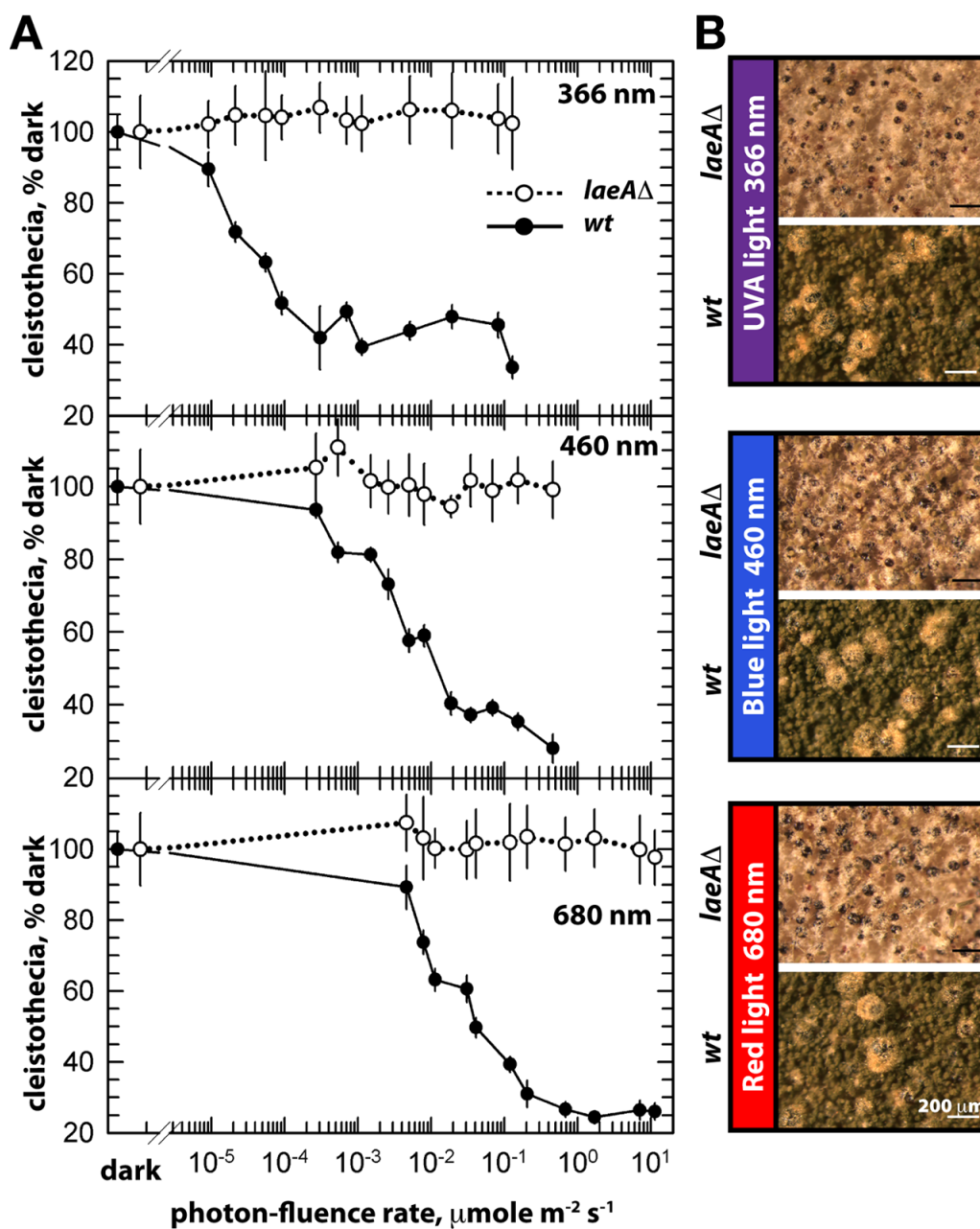
Figure 13. Photon fluence-rate response curves for the photoinhibition of cleistothecia formation in *wild-type* and *laeAΔ* strains. A. Petri plates point-inoculated with $5x10^3$ spores were irradiated with monochromatic light from overhead position at the given photon-fluence rates. *wt/veA+*; filled circle, *laeAΔ/veA+*; open circle. Standard errors are represented by vertical lines. **B.** Photographs of fruiting bodies (cleistothecia) of *wild-type* (*wt*) and *laeAΔ* strains under 366-, 460-, and 680_{nm} light illumination.

The lack of photoinhibition caused by a loss of LaeA was regardless of high or low light intensity, suggesting that *laeAΔ* strains are entirely blind and LaeA is required for light mediated inhibition of cleistothecia formation of all three known light qualities.

The functional relationship between *laeA* and *veA* was examined by creating the *laeAΔ veAΔ* double mutant. The double mutant exclusively manifested the *veAΔ* phenotype characterized by only asexual development. Thus, the *veA* mutation is epistatic to *laeAΔ* and sexual development of *laeA* mutants depends on VeA (Figure 12A). These results demonstrate that LaeA has an additional developmental role besides being a major regulator of secondary metabolism and is an essential part of the light-dependent control mechanism of fungal development.

Double mutant strains of *laeAΔ* with *fphAΔ*, *lreAΔ*, *lreBΔ* or *cryAΔ* representing photoreceptor genes always resulted in an epistatic *laeAΔ* phenotype (data not shown). The LaeA dependency of an intact VeA is essential to promote the asexual developmental program and to inhibit the sexual program of *A. nidulans* in the light. Truncation of the N-terminus part of VeA, which interacts with VelB, abolishes this LaeA mediated regulation. This suggests that LaeA controls the protein levels of the members of the regulatory velvet family but also the balance between VelB-VeA, VelB-VeA-LaeA or VosA-VelB complexes within the fungal cell.

3.1.6. LaeA is part of a cell-specific control for the formation of sex-specific Hülle cells

We compared in more detail the constitutively produced fruiting bodies of *laeAΔ veA+* and *wild-type*. This resulted in the discovery of two remarkable phenotypes. Both were verified by complementation of the *laeAΔ* strain by the *laeA wild-type* allele (Figure 14A). First, the *laeAΔ* mutant produced more fruiting bodies than *wild-type* but they were significantly smaller in size. Detailed inspection with scanning electron microscope (SEM) unveiled that the *wild-type* fruiting bodies of a

diameter of approximately 200 μm were reduced to 40 μm diameter cleistothecia in the *laeAΔ* strain (Figure 14A). In agreement with their small size, cleistothecia of *laeAΔ* contained only 20% of the ascospores compared to *wild-type* fruiting bodies.
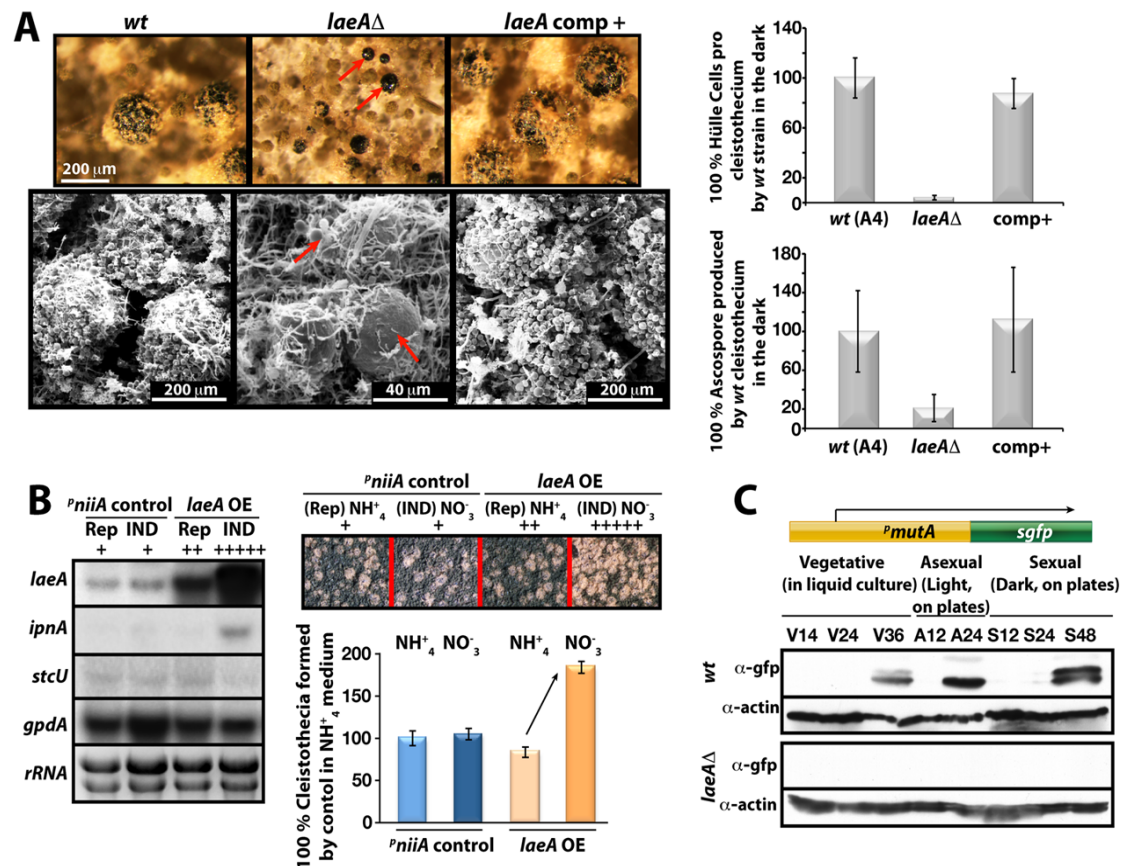
Figure 14. LaeA dependent Hülle cell formation. A. Stereo- (top) and scanning electron (SEM) micrographs of *wild-type* (*wt)*, *laeAΔ*, and *laeA* complemented strains and quantification of Hülle cells and ascospores per cleistothecium in the dark. Small cleistothecia produced by *laeAΔ* strain without Hülle cells are indicated by red arrows. Hülle cells and cleistothecia were counted from 10 different cleistothecia of *wt*, *laeAΔ* and *laeA* complemented strains photographed by SEM. Vertical bars represent standard deviations. Relative values (%) to the numbers of Hülle cells (100-120) or ascospores ($2x10^5$) per cleistothecium in *wild-type* are presented. **B.** Overproduction of LaeA in *veA+* strain increases sexual fruiting body formation in the dark. Growth of *wild-type* (*wt*) containing an empty *niiA* promoter plasmid (control), and *^{P}niiA::laeA* strains. Repressive (5 mM ammonium tartrate) and inducive (10 mM sodium nitrate) conditions were used to confer different levels of the *niiA* promoter activity. Fruiting body formation of *wild-type* is not affected by these nitrogen sources. The *laeA* transcript levels were monitored by Northern hybridization analyses in comparison to *ipnA, stcU. gpdA* levels and ethidium bromide stained rRNA were used as controls; 20 μg RNA were applied in each lane. Spores ($5x10^3$) were point-inoculated on solid medium and grown at 37 °C for 5 days on plates in the dark and cleistothecia were quantified as described (Bayram et al., 2009). **C.** Western blot analysis of Hülle cell specific activity. *^{P}mutA::sgfp* is specifically expressed in Hülle cells. *wt* and *laeAΔ* strains carrying the reporter were grown for indicated time points at 37 °C and Western blot with α-gfp, and α-actin as control were performed. 80 μg total protein was applied.

The small *laeA*Δ cleistothecia contained meiotically formed viable ascospores that germinated on appropriate medium, indicating that the fertility of ascospores was not affected (data not shown). *wild-type* cleistothecia are normally covered by spherical Hülle cells forming a tissue that is proposed to nurse the maturing fruiting bodies. In contrast to *wild-type* where cleistothecia were entirely surrounded by hundreds of Hülle cells, the cleistothecia in *laeA*Δ were in contact with only two to five Hülle cells per cleistothecium (Figure 14A).

We examined the influence of various degrees of LaeA overproduction on fungal development for a more comprehensive picture of the LaeA regulatory function in sexual development. We expressed *laeA* under the nitrate inducible *niiA* promoter (Muro-Pastor et al., 1999) in the *veA+* background (Figure 14B). Induction of *laeA* expression was verified by Northern blot hybridization. The *ipnA* and *stcU* genes were used as control because *ipnA* was previously shown to increase by high levels of LaeA (Bok and Keller, 2004) whereas *stcU*, a gene of the ST gene cluster, was not affected. Increasing degrees of LaeA expression did not disturb light inhibition of sexual development, which was functional as in *wild-type* (data not shown).

Only high levels of LaeA resulted in a significant developmental phenotype in the dark. This overexpression strain produced twice more cleistothecia than *wild-type*, when the *niiA* promoter was activated by cultivation on nitrate medium (Figure 14B). This further corroborates a developmental role of LaeA to control cleistothecia, which might be mediated by the Hülle cells.

Hülle cells were analyzed in more detail by monitoring the expression of cell specific genes in the *laeA*Δ strain. The α-mutanase encoded by *mutA* is particularly expressed in Hülle cells (Wei et al., 2001). A *mutA* promoter fusion to *sgfp* (<u>s</u>ynthetic <u>g</u>reen <u>f</u>luorescence <u>p</u>rotein) was constructed in *wild-type* and *laeA*Δ strains. Whereas *wild-type* showed a sGFP signal during late phases of vegetative growth and development, *laeA*Δ strain failed to generate detectable sGFP signal (Figure 14C). The GFP fluorescence of 100 Hülle cells for each strain was measured to analyze whether the single Hülle cell of the *laeA*Δ strain differs from the Hülle cell tissue of *wild-type*. Approximately 35 of the 100 *wild-type* Hülle cells showed a specific sGFP signal originating from the cytoplasm of the Hülle cells (not shown). In contrast, there was hardly any specific sGFP in the Hülle cells of *laeA*Δ strains except for a weak

autofluorescence. Transcript analysis of the *mutA* gene in *wild-type* and the *laeAΔ* strains further supported the failure of *laeA* mutants to express the Hülle cell specific *mutA* gene. Regardless of the *veA+* or *veA1* alleles, the *mutA* mRNA levels were drastically reduced in *laeAΔ* strains in comparison to *wild-type* (Figure 15).
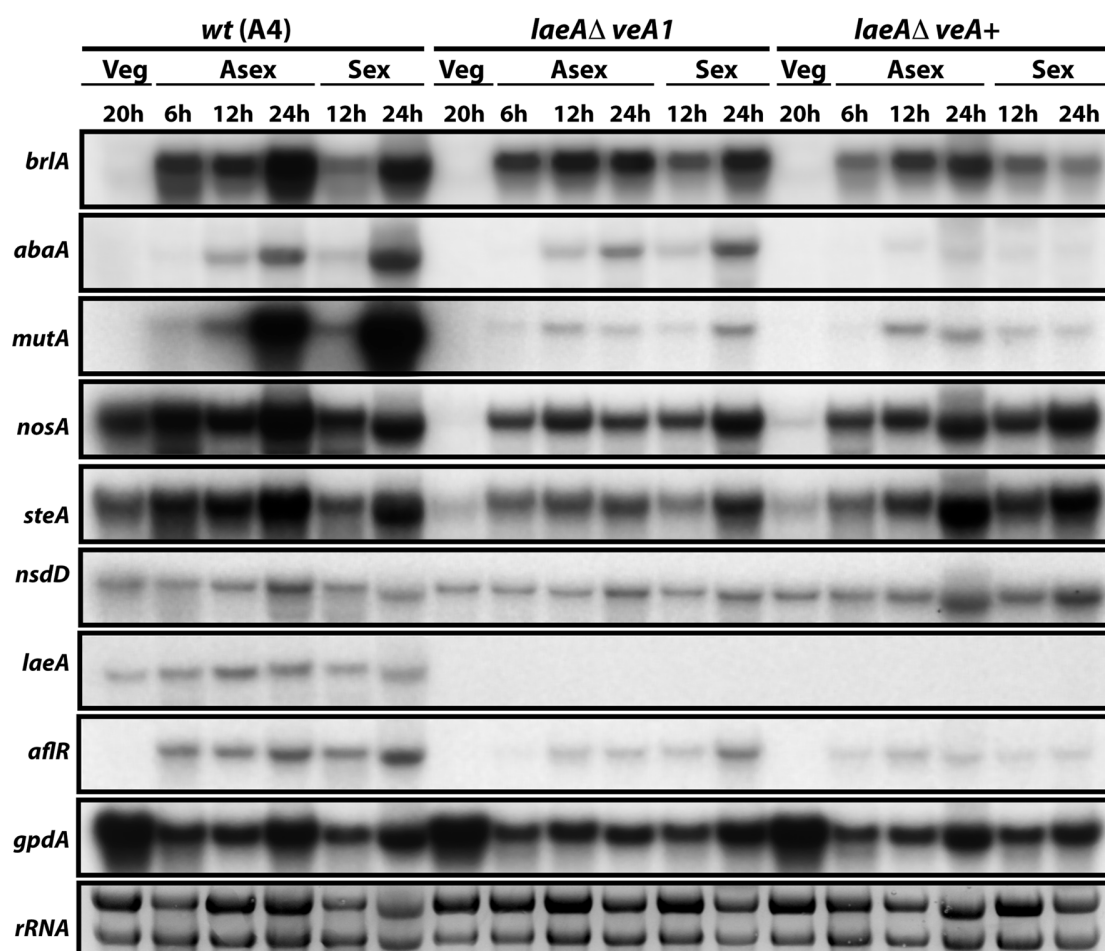
Figure 15. LaeA dependent gene expression. Northern hybridizations of developmental and secondary metabolism regulators in *wt* (*veA+*), *laeAΔ/veA1* (results in N-terminal truncation of the VeA protein), *laeAΔ/veA+* strains. Fungal strains were grown in submerged cultures vegetatively for 20 h, on plates asexually (in the light) for 6, 12, and 24 h and on plates sexually for 12 and 24 h (in the dark). Total RNA was isolated and transcript levels of genes encoding various regulators of development were monitored. The glycolytic gene *gpdA* levels served as internal expression control and ethidium bromide-stained ribosomal RNA (rRNA) was used as loading control. 20 μg total rRNA was used for each stage.

Our data suggest that LaeA affects VeA on gene expression and on protein levels potentially by inhibiting the modification of the VeA-63 kDa protein. The N-terminally truncated VeA1 protein is impaired in this control and also impaired in the interaction with VelB. Consistently, LaeA also controls the cellular levels of VelB and VosA as further members of the VeA regulatory protein family. This regulatory

network is involved in the promotion of asexual spore formation in the light (presumably by releasing the repressor function of VosA-VelB) as well as the light-dependent inhibition of sexual development. In addition, LaeA has functions which do not specifically require the VeA N-terminus but require some VeA activity. These include Hülle cell formation and/or controlling the Hülle-cell specific *mutA* gene activity (Figure 14) but also secondary metabolism control including *aflR* expression (Bok and Keller, 2004). These findings predict that there might be more regulatory developmental genes controlled by LaeA either in a VeA N-terminus dependent or independent way.

The screening of transcripts of various fungal developmental regulator genes (Figure 15) revealed that the asexual regulator *abaA* is one of the genes controlled by the LaeA when VeA N-terminus is intact. *abaA* encodes a transcription factor which is conserved from filamentous fungi to yeast (Andrianopoulos and Timberlake, 1994, Gavrias et al., 1996) and which is required for asexual spore formation. *abaA* expression levels were almost abolished during development of a *veA+ laeAΔ* strain. The effect seems to be specific because another key regulator of asexual development, *brlA* (Adams et al., 1998) was significantly less affected in its expression in the same mutant strains.

Various regulator genes of sexual development exhibited only subtle VeA dependent changes in gene expression during development. The two sexual regulatory genes *nosA* and *steA* (Vallim et al., 2000, Vienken and Fischer, 2006) were exceptions because they were transiently reduced in the *veA1 laeA* and the *veA+ laeA* deletion strains during vegetative growth (20h). This effect is therefore independent of the N-terminus of VeA and seems to be specific, because the mRNA for the GATA type transcription factor NsdD, which is essential for sexual development (Han et al., 2001), was not significantly changed in *wild-type* in comparison to both *laeA* mutant strains. Indeed, overexpression of *nosA* in *laeAΔ* moderately rescued the small cleistothecia phenotype (Figure 16).

Our data support that LaeA is required not only for differentiation of asexual spores but also for Hülle cells and their activity. It seems plausible that without LaeA and therefore without Hülle cells the cleistothecia are not nursed properly and can not reach their *wild-type* regular size. These results also indicate that formation of the Hülle cells is not an absolute prerequisite for fruiting body formation. Moreover, our

results further support that LaeA is involved in the control of regulatory genes in development and secondary metabolism and this control can be dependent or independent of the VeA N-terminus.
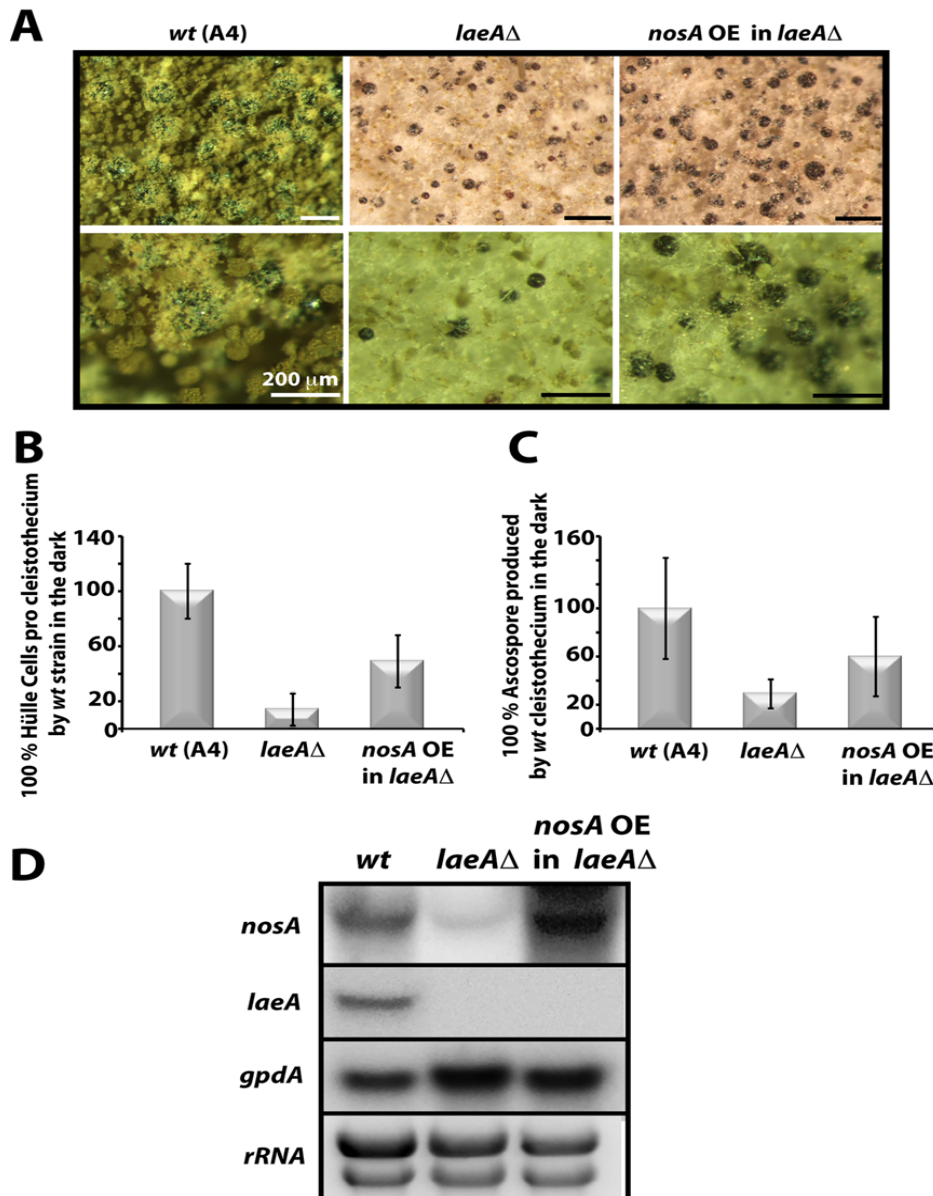
Figure 16. *nosA* overexpression in *laeA*Δ. A. Partial rescue of Hülle cell and ascospore formations by *nosA* overexpression. Stereomicroscopic pictures of *wild-type* (*wt*), *laeA*Δ, and *nosA* OE strains. **B.** Determination of the number of protective Hülle cells. Vertical bars represent standard deviations. The *wild-type* Hülle cell production serves as standard (100%). **C.** Quantification of the sexual ascospores. 10 independent cleistothecia were isolated and ascospores were counted. **D.** Verification of *nosA* overexpression and *laeA* expression in *wt*, *laeA*Δ, and *nosA* OE *laeA*Δ by Northern hybridization. *gpdA* expression and rRNA served as loading control. 20 μg RNA was loaded in each lane.

3.2. The membrane-bound VapA-VipC-VapB methyltransferase complex guides signal transduction for epigenetic and transcriptional control of fungal development

3.2.1. The velvet domain protein VeA interacts in the nucleus with the methyltransferase VipC to balance different developmental programs

The fungal-specific velvet domain is one of the interfaces of VeA for multiple protein interactions (Bayram et al., 2012a, Palmer et al., 2013, Bi et al., 2013). This includes the VeA bridging function between the second velvet domain protein VelB and the methyltransferase LaeA to form the velvet complex. This complex activates and coordinates sexual development and secondary metabolism (Bayram et al., 2008b). A YTH screen using VeA as bait led to the identification of several novel velvet interacting proteins (Vip) including VipC (Figure 17A). We analyzed the VeA-VipC interaction in more detail, because it represents a second cellular interaction of VeA with a putative methyltransferase. The VipC methyltransferase domain shows 52% similarity to LaeA. The VeA-VipC YTH interaction was verified by co-immunoprecipitation and BIFC (Figure 17B, C). BIFC revealed that VipC interacts with VeA in the nucleus, which is visualized by a monomeric red fluorescent protein fused to histone 2A (mRFP-H2A). The nuclear VeA-VipC interaction indicates a second nuclear role of VeA in addition to the function within the trimeric VelB-VeA-LaeA complex.

The cellular function of the second putative methyltransferase VipC was genetically addressed by generating a *vipC* deletion strain. The *vipC* mutant was compared to mutants of the trimeric velvet complex. A *wild-type* fungus forms more sexual fruiting bodies in dark than in light. A fungus lacking VipC produced elevated numbers of sexual fruiting bodies under light conditions whereas no change was observed in darkness, suggesting a function in light control. However, asexual development was decreased in light by 70-75% when compared to the *wild-type* (Figure 17D, E).

A *veA/vipC* double mutant was created to analyze the genetic interplay between *veA* and *vipC*. The *veA/vipC* deletant exhibited a predominant *veA* mutant phenotype, proposing that the *veA* gene is epistatic to *vipC*. This includes secondary metabolism control where the *veA* or the *veA/vipC* mutant lost the potential to

65

synthesize the mycotoxin ST, whereas the *vipC* mutant produced the toxin as *wild-type* (Figure 17F).
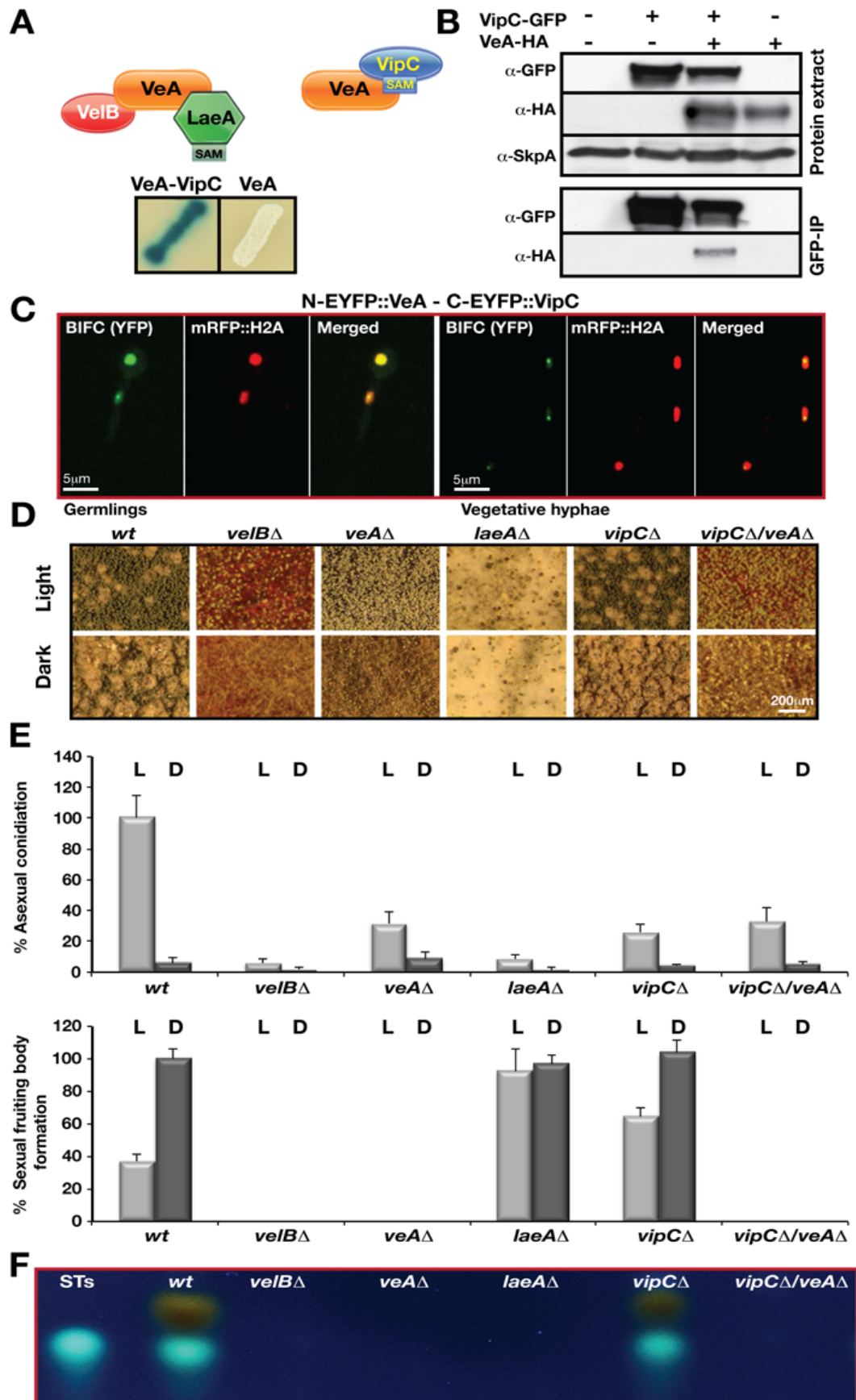
Figure 17. The putative methyltransferase VipC represents a <u>v</u>elvet <u>i</u>nteracting <u>p</u>rotein (Vip). A. Yeast two-hybrid (YTH) identification of VeA interacting protein VipC representing a second interaction with a putative methyltransferase. **B.** Co-immunoprecipitation (Co-IP) of VipC-VeA interaction. The VipC::GFP fusion copurifies VeA-HA from vegetative cells (grown for 24 h at 37 ºC). An antibody recognizing the SkpA subunit of the SCF complex was used as loading control. α-GFP and α-HA detects GFP and HA tagged proteins. **C.** Subcellular interactions of VeA-VipC in a bimolecular fluorescence complementation (BIFC) assay. Yellow fluorescent protein N-terminally fused to VeA (N-EYFP::VeA) interacts with C-EYFP::VipC in the nucleus of fungal cells. Nuclei are visualized (red) by monomeric red fluorescent protein (mRFP) fused to histone 2A. **D-E.** Comparison of *vipCΔ* and *wild-type* development. Stereomicroscopic images of a *wild-type* (*wt*), the velvet complex mutants *velBΔ*, *veAΔ* and *laeAΔ* together with *vipCΔ* and *vipCΔ/veAΔ* grown on glucose minimal media (GMM) for 5 days under constant light and dark. Three sectors from at least three independent plates were used for quantification. Conidia and fruiting bodies produced by *wild-type* in light or dark represent 100% production. The *vipCΔ* mutant strain showed derepressed sexual fruiting body formation and reduced asexual sporulation in comparison to *wild-type*. **F.** Thin layer chromatography (TLC) image showing the levels of mycotoxin ST produced by *wild-type* and mutant strains. Only *wild-type* or *vipCΔ* strains produce ST. STs: Sterigmatocystin standard.

These results show that the VeA protein can be part of two nuclear complexes, both of which include potential methyltransferases. Besides VelB-VeA-LaeA, VeA physically interacts with VipC. Whereas the trimeric velvet complex is an activator of the sexual pathway, the putative methyltransferase VipC is required for the light-dependent repression of sexual fruiting body formation but not for secondary metabolism control.

3.2.2. VipC is part of the trimeric plasma membrane-associated VapA-VipC-VapB complex which releases the VipC-VapB methyltransferase heterodimer to the nucleus

The VeA interacting methyltransferase VipC was analyzed for additional interaction partners. A functional VipC::TAP fusion repeatedly copurified two <u>V</u>ipC <u>a</u>ssociated <u>p</u>roteins named VapA and VapB (Figure 18A, B). Subunits of the trimeric velvet complex were not recruited which suggests that the VeA-VipC interaction is rather transient than stoichiometric. The sizes of the three proteins VipC, VapA and VapB are similar (330-350 amino acids) and interactions were verified by reciprocal tagging of VapA as well as VapB. Both tagged proteins were able to recruit the other two subunits, which supports the presence of a cellular trimeric VapA-VipC-VapB complex (Figure 18C, D). The VapA protein contains three FYVE-like (Fab1, YOTB, Vac1, EEA1) zinc finger (ZF) domains that are named after the four cysteine-rich proteins where they have been originally found (Gaullier et al., 1998). The first two of

the ZF motifs of fungal VapA homologs are highly conserved with some alterations in the last cysteine residue of the third motif in some fungi (Figure 19).
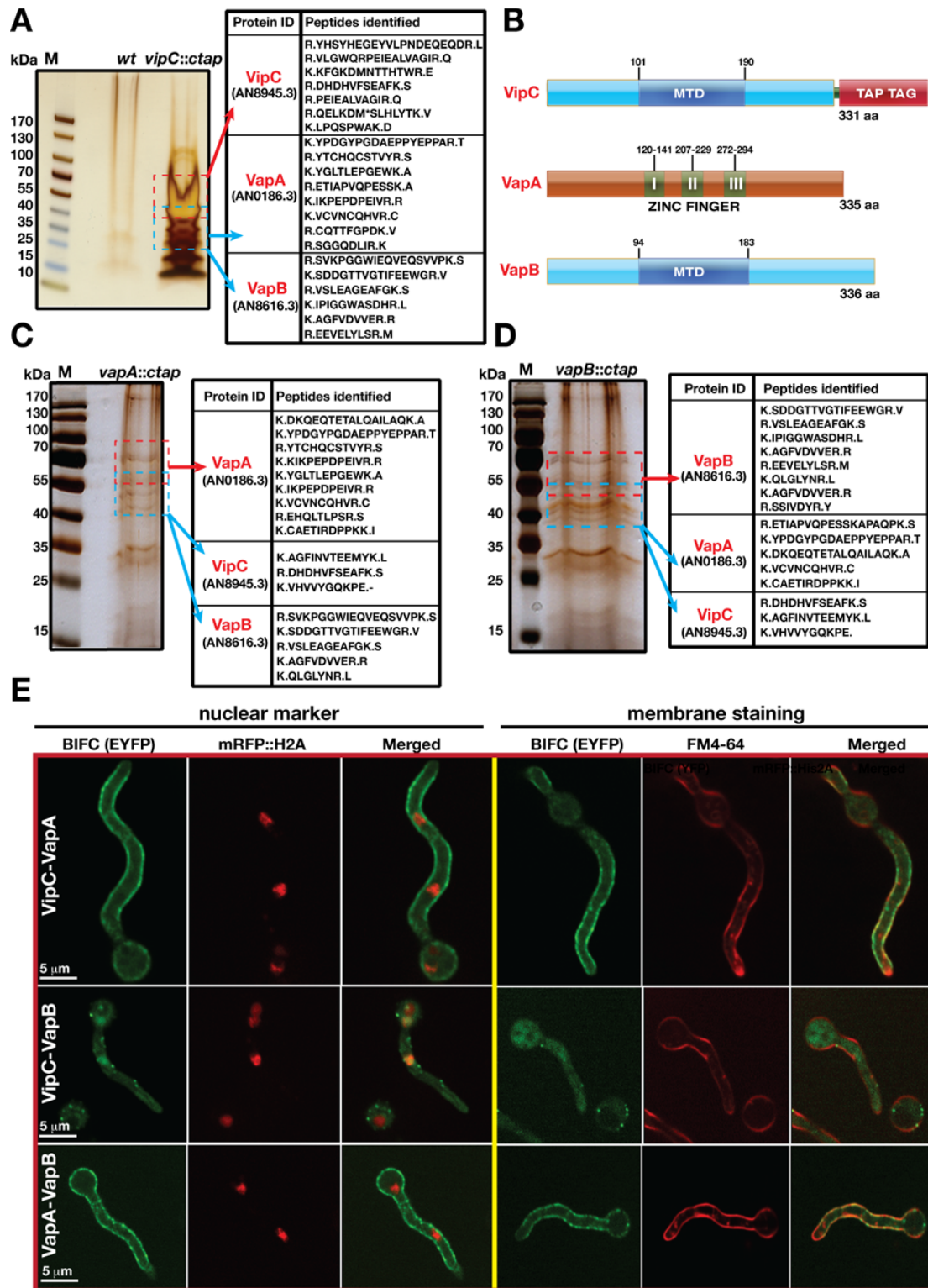
Figure 18. Trimeric plasma membrane-associated VapA-VipC-VapB methyltransferase heteromer to the nucleus. A. Tandem affinity purification (TAP) of VipC::TAP enriched proteins separated by 4-15% SDS-polyacrylamide gel electrophoresis and stained with silver reagent. Polypeptides identified in mass spectrometry from the TAP are given next to the SDS gel. Two <u>Vip</u>C <u>a</u>ssociated <u>p</u>roteins VapA (encoded by AN0186.3 locus), and VapB (AN8616.3) were identified. **B.** Scheme of domain architecture of VipC methyltransferase associated proteins. MTD: methyltransferase domain including SAM binding site. Numbers indicate domain positions. **C.** Silver stained 4-15% SDS-polyacrylamide gel of VapA::TAP enrichment and identified polypeptides. VapA recruits the methyltransferases VipC and VapB. **D.** TAP purification of VapB interacting proteins VipC and VapA. **E.** *In vivo* visualization of subcellular interactions of VipC-VapA, VipC-VapB or VapA-VapB heterodimers by BIFC method. VipC-VapA and VapA-VapB interact along the plasma membrane and the VipC-VapB methyltransferase heterodimer interacts at the membrane and in the nuclei (visualized by mRFP::Histone 2A fusion). FM4-64 dye stains the plasma membrane (red).

FYVE ZF domains are characterized by six to eight cysteine pairs. In contrast to canonical ZF domain transcription factors, FYVE type ZF domain proteins bind to membrane lipids and insert into cell membranes. They function in membrane trafficking and cell signaling (Gillooly et al., 2001, Hayakawa et al., 2007, Hayakawa et al., 2004). The BIFC method was applied to verify and localize the physical VapA-VipC interaction in the cell. N-EYFP::VipC methyltransferase fusion interacted with C-EYFP::VapA zinc finger protein fusion along the plasma membrane which was consistent with the typical FYVE zinc finger feature to attach to various membranes (Figure 18E). The third interaction partner VapB is different in its domain structure from VapA. It shares with VipC a SAM-dependent putative methyltransferase domain (Figure 18B) that includes three characteristic consecutive glycine (G) residues which are well-conserved in fungi (Figure 19) but also in plants and humans (Kozbial and Mushegian, 2005). BIFC assay resulted in a similar decoration of the plasma membrane for VapA-VapB as it was the case for VapA-VipC, supporting that the novel trimeric VapA-VipC-VapB complex is localized at the fungal cell membrane. The BIFC of the two putative methyltransferases VipC-VapB revealed two interacting subpopulations. In addition to membrane-associated VipC-VapB, a substantial part of the cellular VipC-VapB heteromers was localized in the nucleus of the fungal cells (Figure 18E), indicating that two heteromers VipC-VapB, which are tethered by the FYVE zinc finger VapA to a trimeric complex at the fungal cellular membrane, can be released from the membrane and migrate into the nucleus. Conservation of all components of the heterotrimeric VapA-VipC-VapB complex among the various members of the fungal kingdom hints to a general methyltransferase transduction pathway between membrane and nucleus across the fungal kingdom.
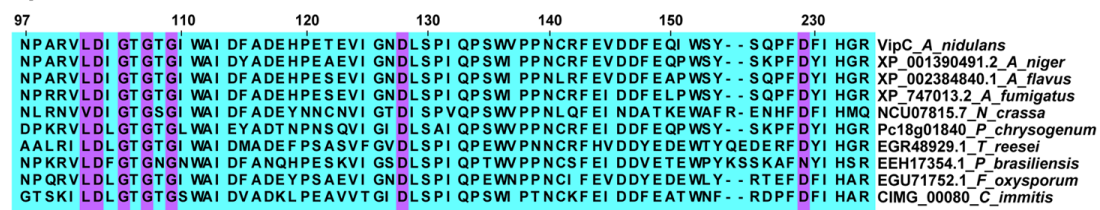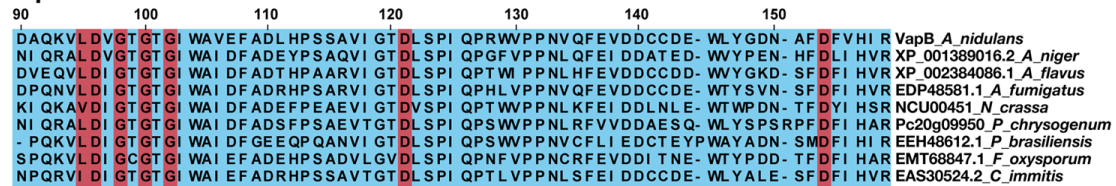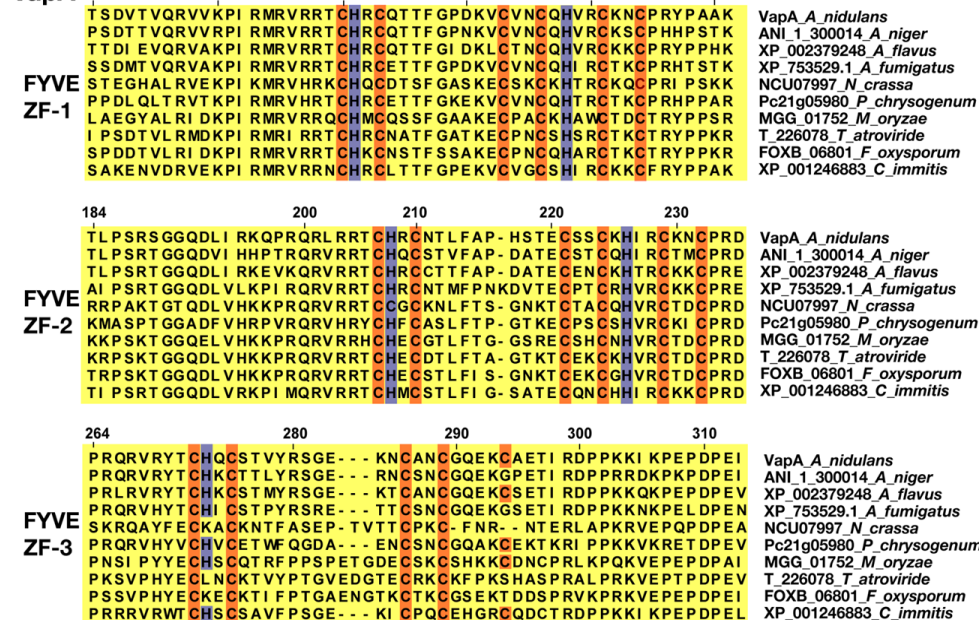
Figure 19. Conserved domains of the VapA-VipC-VapB complex proteins from various fungal groups. A Global ClustalW protein alignment of VipC, VapB and VapA homologs from at least nine different fungal organisms. The complex components are highly conserved in the filamentous fungi. Methyltransferase domains of VipC and VapB proteins are shown with bluish alignment chart. SAM binding sites were shaded in purple or red color. SAM binding domains are highly conserved on both alignments. Alignment of VapA FYVE-like zinc finger proteins from various fungal groups are demonstrated with yellow alignment block. Three putative zinc finger forming cysteins (C) and histidines (H) are shaded orange and blue. The last cysteine of the third motif is less conserved or due to improper annotations of the genomes. *A. nidulans*, *A. flavus, Magnaporthe oryzae*, and *Penicillium chrysogenum* have kept the last cysteine.

3.2.3. VapA is predominantly a membrane protein, whereas the VipC and VapB methyltransferases are enriched in the nucleus

The interaction studies revealed membrane associations for VapA-VipC-VapB and nuclear interaction for the methyltransferases VipC-VapB. Cellular localization of the subunits was monitored by functional GFP fusions that were expressed under the respective native promoters and that complemented deletion phenotypes described below. The expression of the VapB fusion protein was driven by the constitutive *gpdA* promoter due to the weak fluorescence signals. VipC protein did not decorate the entire membrane but was visible as small membrane-associated vesicles or dots (Figure 20A).

VipC was also present in the nucleus where it co-localized with the mRFP::H2A. The localization pattern of the second methyltransferase VapB was similar to VipC, which are both found at the plasma membrane and in the nuclei. The FYVE zinc finger VapA-GFP fusion decorated the entire plasma membrane along the fungal cell but was hardly found in the nucleus (Figure 20A). Membrane-associated VapA-GFP was in permanent motion and moved along the plasma membrane dynamically (data not shown). Nuclear enrichment corroborated these findings and showed high amounts of the VipC-VapB heteromeric methyltransferase but only trace levels of VapA were present within the nucleus (Figure 20B). These findings demonstrate that a trimeric complex, which is tethered by VapA to the membrane, releases VipC-VapB heterodimers to cross the cytoplasm and enter the nucleus. Interdependent localizations of the trimeric membrane complex subunits were investigated by examining the subcellular distribution of each fusion protein in respective deletion strains.

VapA localization in *vipC* or *vapB* mutants was as in *wild-type* (not shown). VapB did not have an influence on VipC membrane localization. The absence of VapA, however, led to the loss of VipC signals at the plasma membrane. Membrane localization of VapB was not only impaired in the *vapA* but also in the *vipC* mutants. This indicates that VipC plays a more important role in bridging the membrane-associated VapA to the methyltransferase VapB than *vice versa*. The VapB nuclear subpopulation increases in the *vapA* as well as *vipC* mutants in comparison to *wild-type.* VapB is primarily a nuclear protein without VapA (Figure 20B,C). Analysis of the protein levels in the deletion strains corresponded to the microscopic observations with one exception. The lack of VipC reduced the overall protein levels of VapB

significantly with still a substantial amount of VapB in the nucleus (Figure 20D), indicating that VipC protects VapB from degradation in the cytoplasm after the release from the trimeric membrane complex and before entering the nucleus.
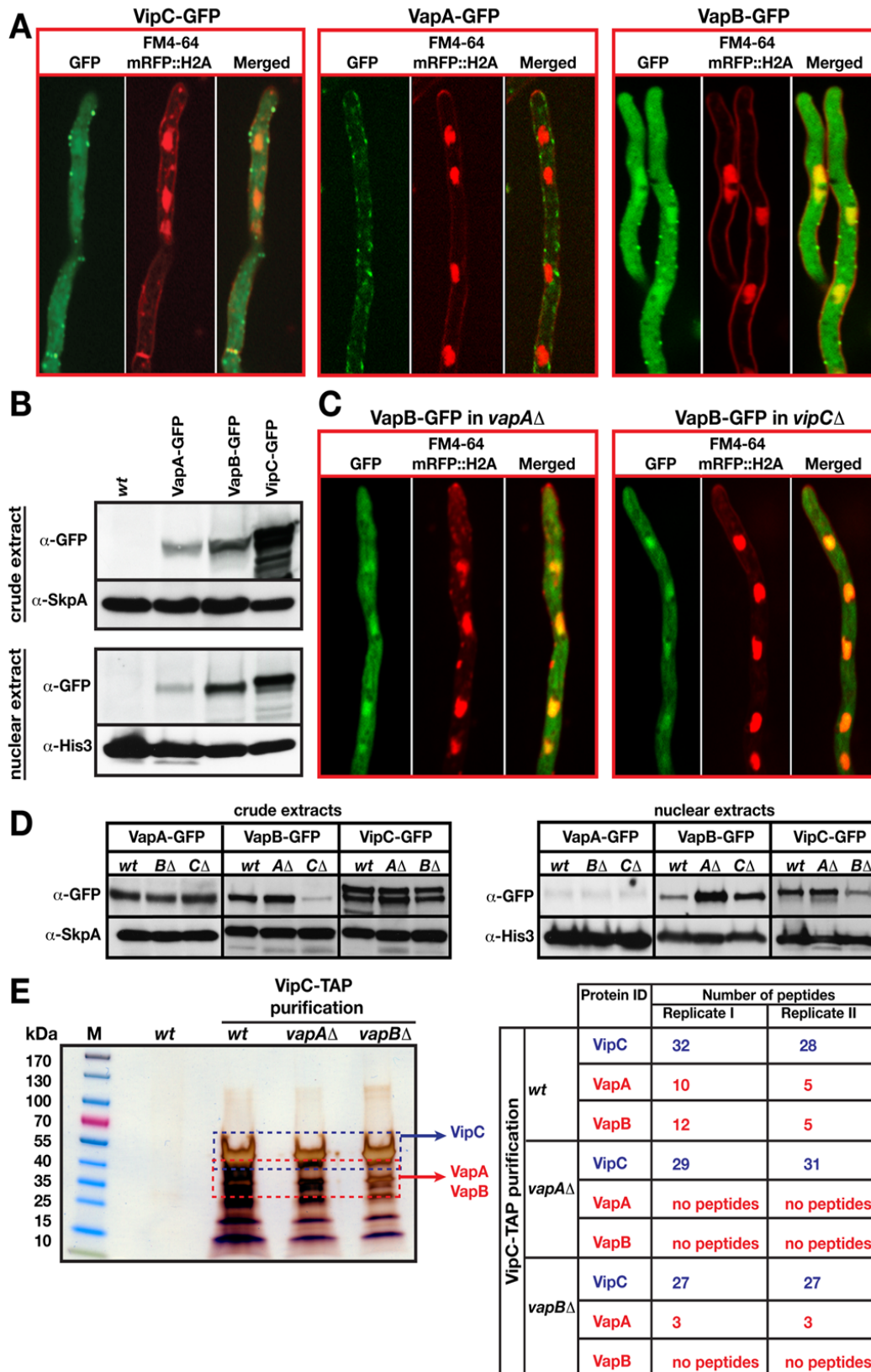
Figure 20. Subcellular distribution of the VapA-VipC-VapB complex subunits. A. Localization of subunits within the fungal cells. VipC and VapA::GFP fusions were expressed under native and VapB expression was driven by a constitutive *gpdA* promoter. Both methyltransferases are present at the plasma membrane and within the nuclei, whereas VapA is primarily present at the plasma membrane. Plasma membrane was visualized by red dye FM4-64 and nuclei by mRFP::histone2A. **B.** Functional VipC, VapA, and VapB GFP fusion protein levels in crude and nuclear extracts with significant nuclear VipC and VapB fractions. 50 µg crude and enriched nuclear extracts were used for immunoblottings. α-GFP, α-SkpA, and α-histone 3 were used for visualization. **C.** Localization of VapB in either *vapA* or *vipC* deletion strains. Membrane accumulation of the VapB protein is impaired in the absence of VapA and VipC. **D.** Subcellular levels of the complex components in the respective deletion strains. VapB is enriched in the nucleus in the absence of VapA. **E.** TAP of VipC from *vapA* and *vapB* mutants. 4-15 % SDS polyacrylamide gel electrophoresis of VipC TAP enrichments from vegetative cultures at 37 ºC for 24 h. VipC is unable to recruit VapB in the absence of VapA. Protein peptides identified from mass spectrometry are given next to the gel picture.

The effect of the different subunits on complex formation was further elucidated in the mutant strains. *In vivo* associations of VipC were analyzed by TAP enrichment in the absence of VapA or VapB. (Figure 20E). VipC-TAP recruited VapA and VapB in *wild-type* but the VipC-VapB interaction was abolished in the absence of VapA. BIFC studies of VipC-VapB methyltransferases also did not result in interaction signals in a *vapA* mutant (not shown). The VipC-VapA interaction was reduced in the *vapB* mutant. There is only a partial requirement of VapB for the binding of VipC through VapA to the membrane but VapA seems to be important to allow VipC-VapB heterodimer formation.

Taken together, these results underscore that VapA is required for membrane assembly and motion of a trimeric VapA-VipC-VapB complex. A yet unknown trigger results in the release of the heterodimer VipC-VapB from VapA. The VipC subunit presumably stabilizes VapB when the VipC-VapB methyltransferase migrates from the membrane into the nucleus.

3.2.4. Membrane-associated VapA prevents developmental control functions of the VipC-VapB methyltransferases

The methyltransferase VipC is released together with a second methyltransferase VapB from the membrane to the nucleus. VipC is important for the appropriate adjustment of asexual or sexual developmental programs in response to external cues as light. In addition, VipC interacts in the nucleus with the VeA protein. Protein levels and transcripts of all three subunits of the VapA-VipC-VapB complex were analyzed to monitor developmental responses as a consequence of different stimuli (Figure 21).
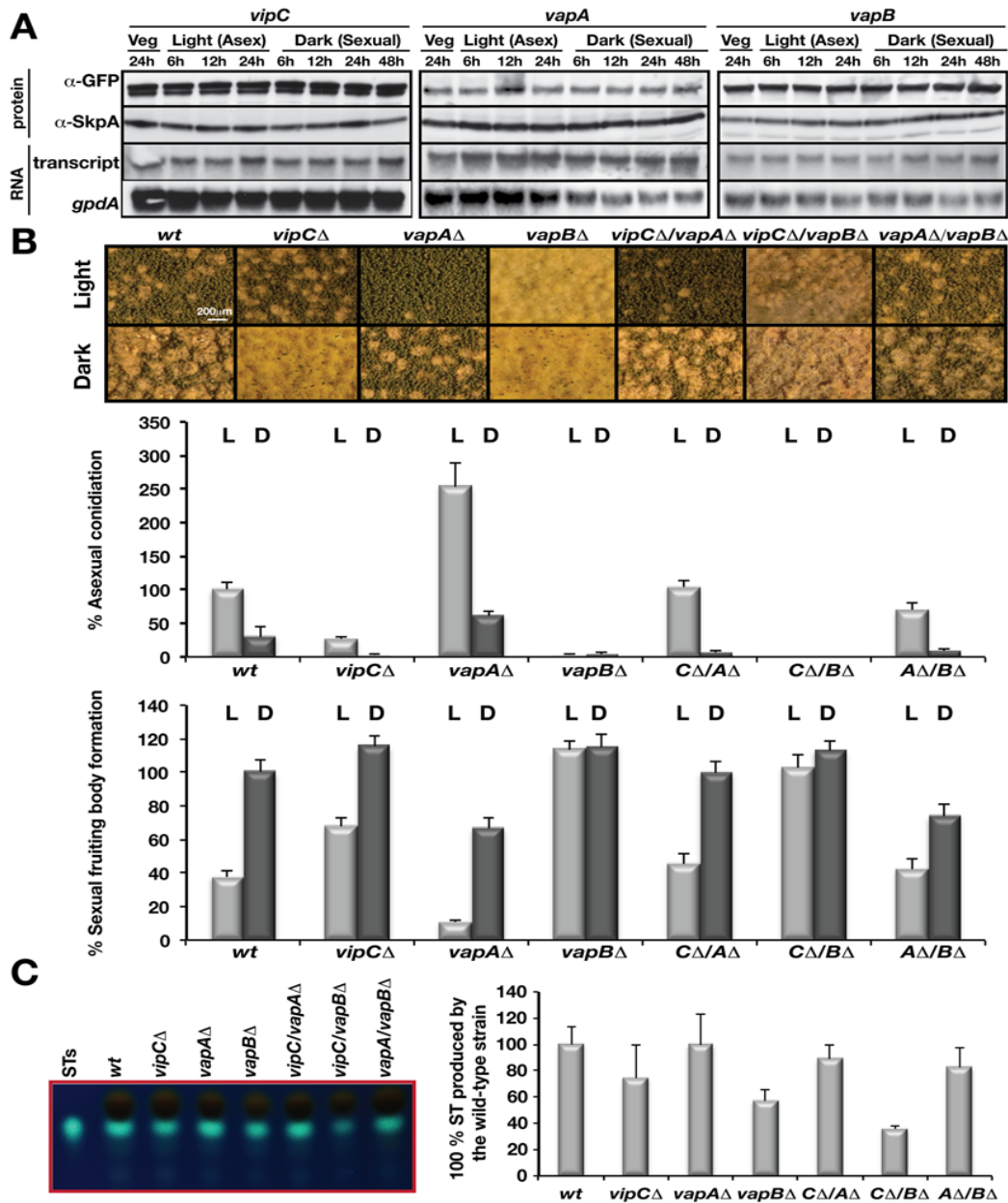
Figure 21. Expression and light-dependent development of genes for membrane-attached VapA-VipC-VapB or nuclear VipC-VapB. A. Protein and transcript levels of *vipC*, *vapA* and *vapB* RNA and derived proteins. Corresponding GFP gene fusions were expressed under native promoter. After 20 h vegetative growth in liquid shaking GMM media, the grown mycelia were transferred to solid GMM to induce differentiation. Plates were kept under constant light for 6 h, 12 h and 24 h to induce asexual or under constant dark for 6 h, 12 h, 24 h and 48 h to induce sexual development. At each time point, proteins and RNAs were isolated. Fusion proteins were detected with an α-GFP. Loading controls: α-SkpA for proteins, glycolytic gene *gpdA* (encoding glyceraldehyde-3-phosphate dehydrogenase) for RNA. **B.** Light-dependent fungal development. Stereomicroscopic images of the phenotypes for *wild-type* (*wt*), single mutants of *vipCΔ*, *vapAΔ*, *vapBΔ*, and double mutant combinations (*vipCΔ/vapAΔ*, *vipCΔ/vapBΔ*, *vapAΔ/vapBΔ*). Strains were grown on GMM for 5 days under constant light or dark conditions. Five sectors from at least five independent plates were used for quantification of conidiation and fruiting body formation. The number of conidia and fruiting bodies produced by *wild-type* represents 100%. Standard deviations were given as vertical bars. **C.** ST productions of the strains visualized on TLC plates. Sts: ST standard.

Submerged cultures result preferentially in vegetative filamentous growth, whereas illumination favors asexual spore and darkness sexual fruiting body formation, respectively (Figure 21A). Each member of the complex is constantly expressed under all tested conditions, suggesting that rather physical interactions and their consequences on activity, stability or localization than expression levels are important for the molecular control mechanism. The function of *vapA* or *vapB* genes for fungal development was further evaluated and compared to *vipC* by analyzing corresponding deletion strains during illumination or in darkness (Figure 21B).

Comparison of both mutant strains revealed that VapB is required even more than VipC to promote asexual and to repress sexual development in light. The *vapB* mutant was blind to light and hardly produced any asexual spores but formed constantly high amounts of sexual fruiting bodies in light or dark. Growth tests under different light spectra, including red (630 nm), blue (450 nm) and UVA (365 nm) always resulted in the same phenotype, which was unresponsive to light (data not shown). A double deletion of both methyltransferase genes *vipC* and *vapB* displayed predominantly the *vapB* phenotype. Whereas both methyltransferases VipC and VapB are required for asexual spore formation and light dependent reduction of sexual development, membrane bound VapA has a different and antagonizing function. The *vapA* mutant produced 2.5 times more asexual conidia than *wild-type*. In addition, this strain produced significantly less sexual fruiting bodies. Therefore, VapA is necessary to repress asexual but also to enhance sexual development. Double mutants of *vipC* and *vapB* with *vapA* exhibited an intermediate phenotype, showing that there is no epistacy among the genes for membrane binding and the methyltransferases. Since development is linked with secondary metabolite production, we analyzed the function of complex subunits for ST production. Except for some reduction in the *vipC/vapB*Δ double mutant, toxin levels did not change significantly (Figure 21C). This indicates only a minor contribution of the methyltransferases to secondary metabolism control.

Our data support a molecular mechanism where prior to an environmental trigger VapA keeps VipC and VapB in a trimeric complex at the plasma membrane to prevent their developmental functions. When VapA is triggered by a yet unknown environmental signal, the VipC-VapB heterodimer is released from the membrane and transported to the nucleus. There, VipC and VapB are essential for accurate development, including promotion of asexual and reduction of sexual development in

response to light. This might not only include the nuclear methyltransferase activity of the VipC-VapB heterodimer but also the alternative nuclear VipC-VeA interaction.

3.2.5. The interplay between trimeric VapA-VipC-VapB membrane complex and nuclear VipC-VapB directs transcription of global regulators for asexual development

The combined genetic and cell biological analyses support a molecular mechanism where membrane-associated VapA excludes VipC-VapB methyltransferases from the nucleus and therefore reduces their nuclear developmental functions. We analyzed whether nuclear VipC-VapB acts at the gene expression level to promote asexual and repress sexual development in light. A nuclear regulatory developmental function of VipC-VapB should be reflected by altered gene expression of prominent regulatory genes of asexual (Figure 22A) or sexual development in mutant strains (Figure 22B).

FlbA represents a negative regulator of heterotrimeric G-protein signaling which is required for light-dependent activation of asexual development. FlbA activates a regulatory cascade of the transcription factors FlbC, BrlA and AbaA to allow and promote the formation of asexual spores (Park and Yu, 2012). The absence of membrane-associated VapA correlates with higher levels of nuclear VipC or VapB protein (Figure 20D). This situation led to a strong increase in the expression of two downstream asexual developmental regulators, *brlA* and *abaA* in the dark and light. There was also a slight but less pronounced increase in the transcripts of two upstream factors FlbA and FlbC (Figure 22A). We also compared the expression of sexual regulatory genes in corresponding mutants and *wild-type*. These include *veA*, *velB* or *laeA* which are required for development of the sexual fruiting bodies. Additionally, *steA* and *nosA* encoding transcription factors for early sexual development and for fruiting body maturation were analyzed (Vallim et al., 2000, Vienken and Fischer, 2006). Transcripts of the sexual regulatory genes were not seriously affected in the examined mutants (Figure 22B).

Membrane-bound VapA is primarily required for inhibiting transcription of asexual regulatory genes and does not significantly affect sexual development. The location of VapA at the membrane suggests that this inhibition might be indirect. Whereas deletion of the *vipC* or *vapB* methyltransferases did not considerably affect regulators of sexual development, the impact of VipC-VapB on asexual development is notably different than VapA.
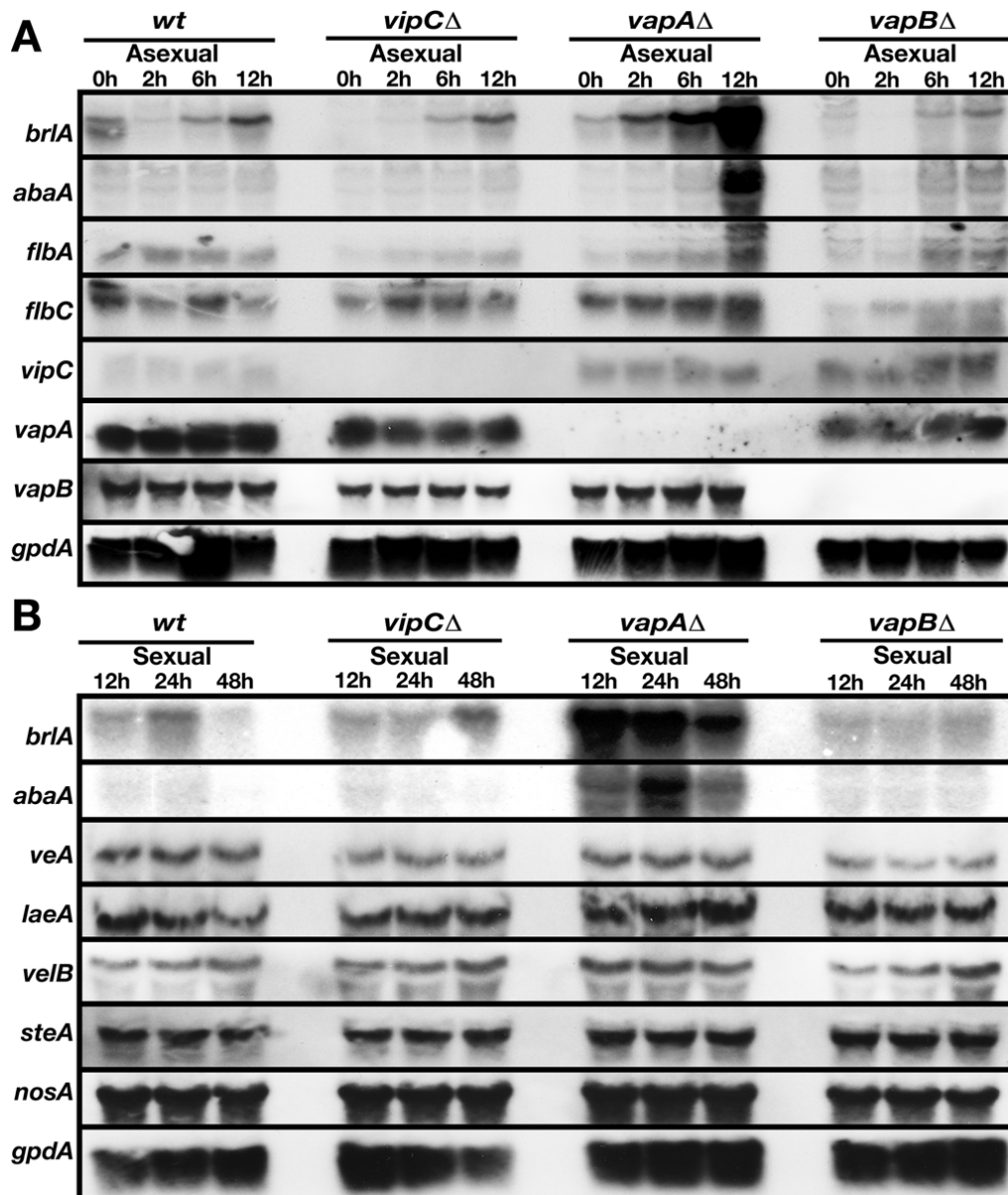
Figure 22. Control of major developmental regulatory genes by membrane-attached VapA-VipC-VapB and nuclear VipC-VapB. Cultures from *vipC*, *vapA* or *vapB* deletion strains were grown for 20 h in GMM liquid shaking media and taken onto solid GMM plates to propagate development. Total 20 μg RNA of indicated time points was loaded. The glycolytic gene *gpdA* served as expression control. **A.** Transcripts of genes for pivotal asexual transcription factors BrlA, AbaA, FlbC, and signaling protein FlbA during illumination with white fluorescent light (inducing asexual development in *wild-type*). *brlA* and *abaA* transcripts are only upregulated in the *vapA* mutant strain, whereas *flbA* or *flbC* are rather downregulated in *vapB* and *vapC* mutants. **B.** Transcripts of genes for developmental regulators during darkness (promoting sexual development and inhibiting asexual development in *wild-type*). Transcripts for asexual regulators *brlA* and *abaA* and major sexual regulators *steA, nosA, veA, laeA and velB* were monitored.

In contrast to a *vapA* deletion, the deletion of *vipC* and *vapB* did not increase transcription of *brlA* or *abaA* and rather led to a decrease in *flbA* and *flbC* transcripts of early asexual regulators. This suggests that VipC and VapB exhibit the opposite

function to VapA and are important for the activation of asexual conidiation. Transcripts of the VipC-VapA-VapB did not change in respective deletion strains significantly. These data express that the shuttling between membrane-bound trimeric VapA-VipC-VapB complex and nuclear VipC-VapB heteromers primarily act by controlling the induction of asexual development, which might be triggered by light. Light-dependent inhibition of sexual development might not be a direct impact of nuclear VipC-VapB activity on gene expression.

3.2.6. Increased cellular VipC-VapB methyltransferase protein levels do not only influence fungal development but also secondary metabolite production

The equilibrium between nuclear and membrane-bound VipC-VapB methyltransferase heteromers by VapA plays an important role for the induction of regulatory genes of asexual development. Light-dependent inhibition of sexual fruiting body formation might be an indirect effect of the release of VipC-VapB into the nucleus. Imbalances in the cellular levels of these complexes should influence development and allow further insights into the regulatory mechanism. This was addressed by overexpression of *vipC*, *vapA* or *vapB* genes (Figure 23).

Overexpression of each *vipC* or *vapB* methyltransferases severely affected development. Overproduction repressed almost any differentiation under light conditions and reduced vegetative growth, asexual conidiation and even sexual fruiting bodies. In contrast, increased *vapA* levels resulted in colonies similar to *wild-type* (Figure 24A, B). More detailed analyses revealed differences between VipC and VapB functions. High levels of VipC caused defects in nuclear distribution of germlings. These strains accumulated many nuclei in the swollen spores (Figure 23B). *vapB* overproduction induced a retardation and reduction in fruiting body formation, which is the opposite effect of the *vapB* deletion in sexual development. High VapB levels also disturbed secondary metabolism leading to secretion of a brown pigment into the medium and reduced asexual conidiation.

The interactions and subcellular locations of VapA, VipC and VapB are interdependent. Without VapA, a VipC-GFP protein is unable to bind to the plasma membrane and to interact with the other methyltransferase VapB. *vipC* or *vapB* overexpression in a *vapA* deletion or a deletion of the other methyltransferase gene did not cause significant developmental impacts. Similarly, overexpression of two

genes had no developmental effect with the exception of concurrent overexpression of both methyltransferases VipC-VapB, which caused further enhanced phenotype on development. Strains with high levels of VipC-VapB resembled a *veA* deletion strain that could not produce any fruiting bodies (Figure 24A, B).
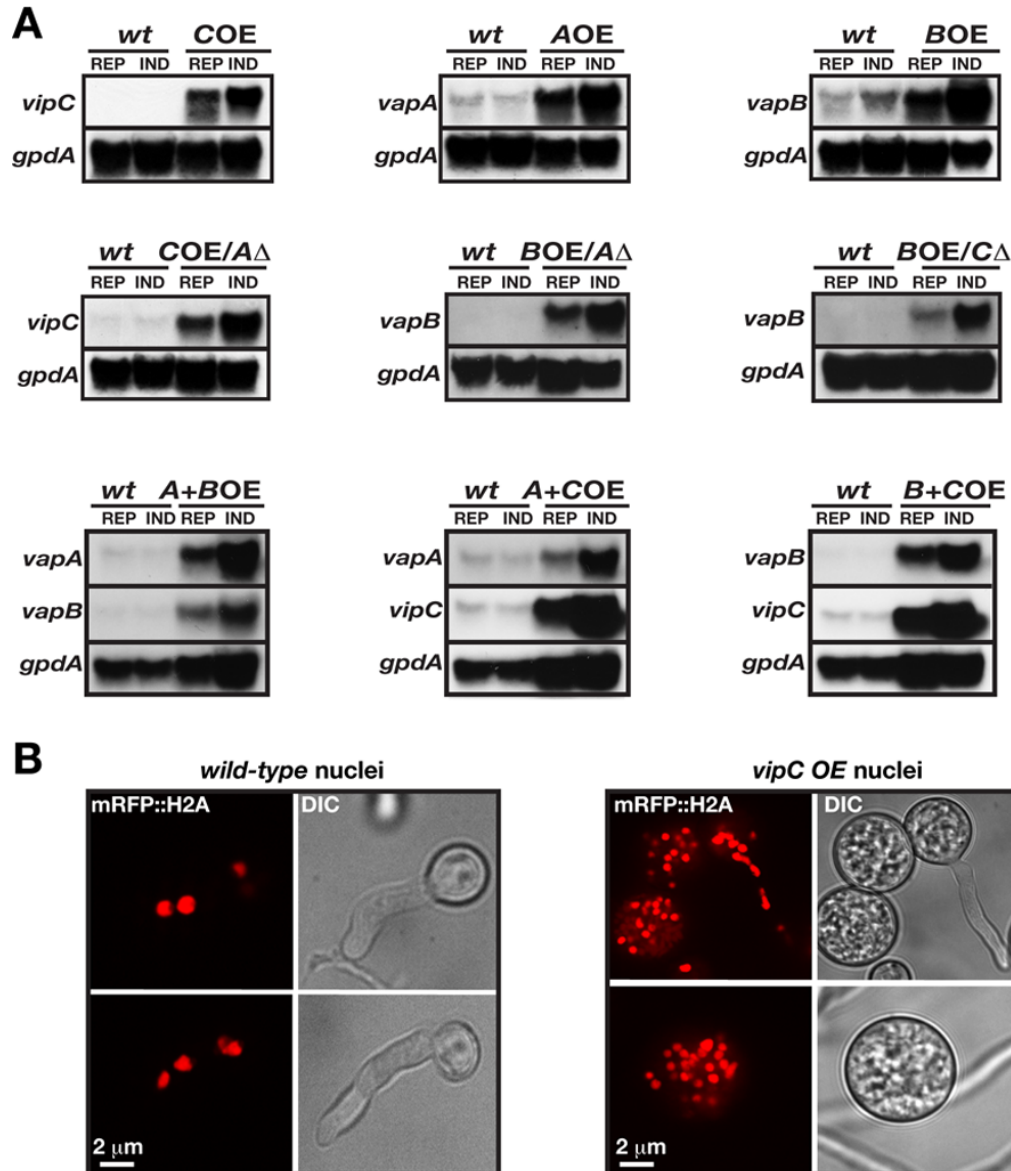
Figure 23. Northern hybridization validation of increased transcripts of the corresponding genes in overexpression strains. A. The genes were strongly overexpressed under nitrogen source inducible the *niiA/niiD* promoters. Each lane contains 20 μg RNA. DIG labeled ORF of the corresponding genes were used as Northern probes. The *gpdA* expression was used as expressional control. A; VapA, B; VapB, C; VipC. *A+B* OE; VapA + VapB overexpression, *A+C* OE; VapA + VipC overexpression, *B+C* OE; VapB + VipC overexpression. **B.** Nuclear distributions of the *wild-type* and *vipC* OE strains during germination of spores. The nuclei were made visible by a mRFP::Histone 2A fusion protein. Respective strains were germinated at 30 ºC for 8-9 h. REP; Repression, IND; Induction.

A *veA* mutant is impaired in development and secondary metabolism (Kim et al., 2002, Kato et al., 2003) and VeA interacts with VipC (Figure 17A). Whereas the

vapB deletion strain was not altered in secondary metabolism, *vapB* overexpression resulted in brown pigmentation.
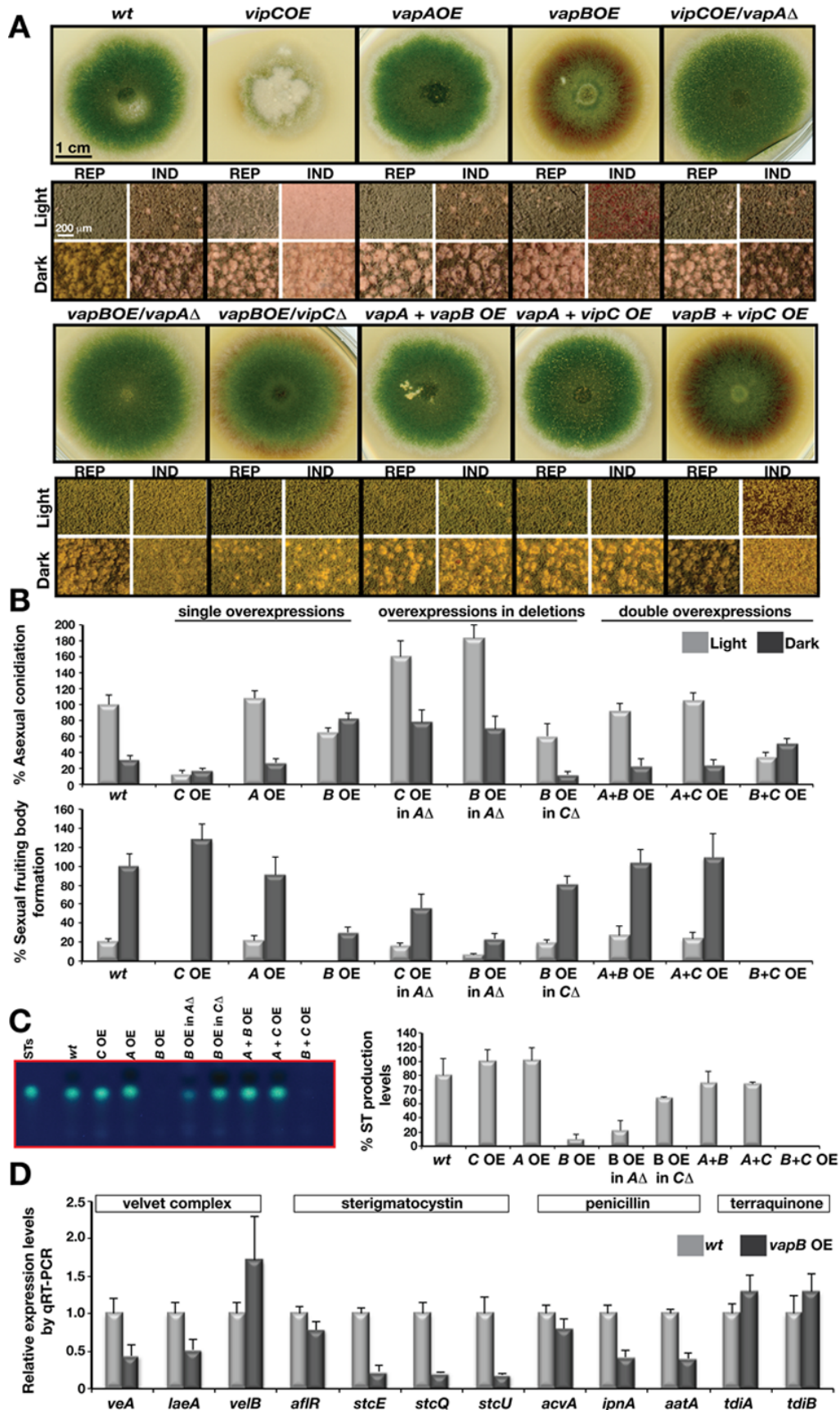
Figure 24. **Overproduction of VipC-VapA-VapB and their developmental and secondary metabolism consequences. A.** Growth of strains where *vipC*, *vapA*, and *vapB* cDNAs were overexpressed (OE) under nitrogen source inducible bidirectional *niiA* or *niiD* promoters in *wild-type* (*wt*) or indicated deletion strains. Development was induced on solid media after 5 days of incubation under continuous white fluorescent light at 37 °C. Stereomicroscopic images of the cultures grown on inducing or repressing media under light and dark are shown as enlarged squares. **B.** Quantification of asexual conidia and sexual fruiting body formations. Overexpression of both methyltransferase encoding genes *vipC* and *vapB* resulted in defects in growth, conidiation and sexual development. Co-overexpression of membrane binding VapA neutralizes the influence of high levels of VipC and VapB. Conidia and fruiting bodies produced by the control strain expressing the empty plasmid serve as 100%. **C.** A TLC plate of ST production of the indicated overexpression strains. Overproduction of *vapB* reduces ST production but *vapB* needs *vipC* for this function. ST levels were quantified in comparison to *wild-type* control as 100%. **D.** qRT-PCR expression levels in *vapB* overexpression strain of *veA*, *laeA* and *velB* genes encoding subunits for the velvet complex, and structural genes for the secondary metabolite gene clusters of ST, PN and TQ, respectively.

We investigated whether there are additional effects on secondary metabolism in overexpression strains by measuring production of the mycotoxin ST. Toxin production was only abolished in the presence of high levels of VapB or combined overexpression of VipC-VapB, whereas high levels of VapA could suppress this phenotype (Figure 24C). We used this readout system to examine whether VapB and VipC methyltransferase activities are necessary for the observed effects. Therefore, the SAM binding motif was impaired by generating mutant alleles, *vipC1* and *vapB1*. Both alleles carry a substitution of gly (G) to ala (A) in the SAM binding motif. Overexpression of *vipC1* and *vapB1* abolished any effect on development and secondary metabolism that was observed by overexpression of the *wild-type* alleles (Figure 25).

The phenotypes derived from *vapB* overexpression correspond to a *veA* deletion. We examined the impact of *vapB* overexpression on transcription of the subunits of the nuclear VelB-VeA-LaeA complex (Figure 24D). *vapB* overexpression caused almost 50% reduction in *laeA* or *veA* transcript levels but increased *velB* transcripts two-fold. We further investigated expression of the ST gene cluster that is controlled by the transcription factor AflR and consists of 25 genes (Brown et al., 1996, Fernandes et al., 1998). *vapB* overexpression only slightly decreased expression of the regulatory *aflR* gene, but drastically reduced transcription of the three structural genes *stcE*, *stcU* and *stcQ* that represent different locations in the cluster. An impact on secondary metabolism was further corroborated by the analysis of additional clusters. *vapB* overexpression also affected genes of additional clusters as PN and TQ

(Figure 24D). Contrastingly, overexpression of *vapB* caused an opposite effect on the cryptic orsellinic acid gene cluster (Figure 26).
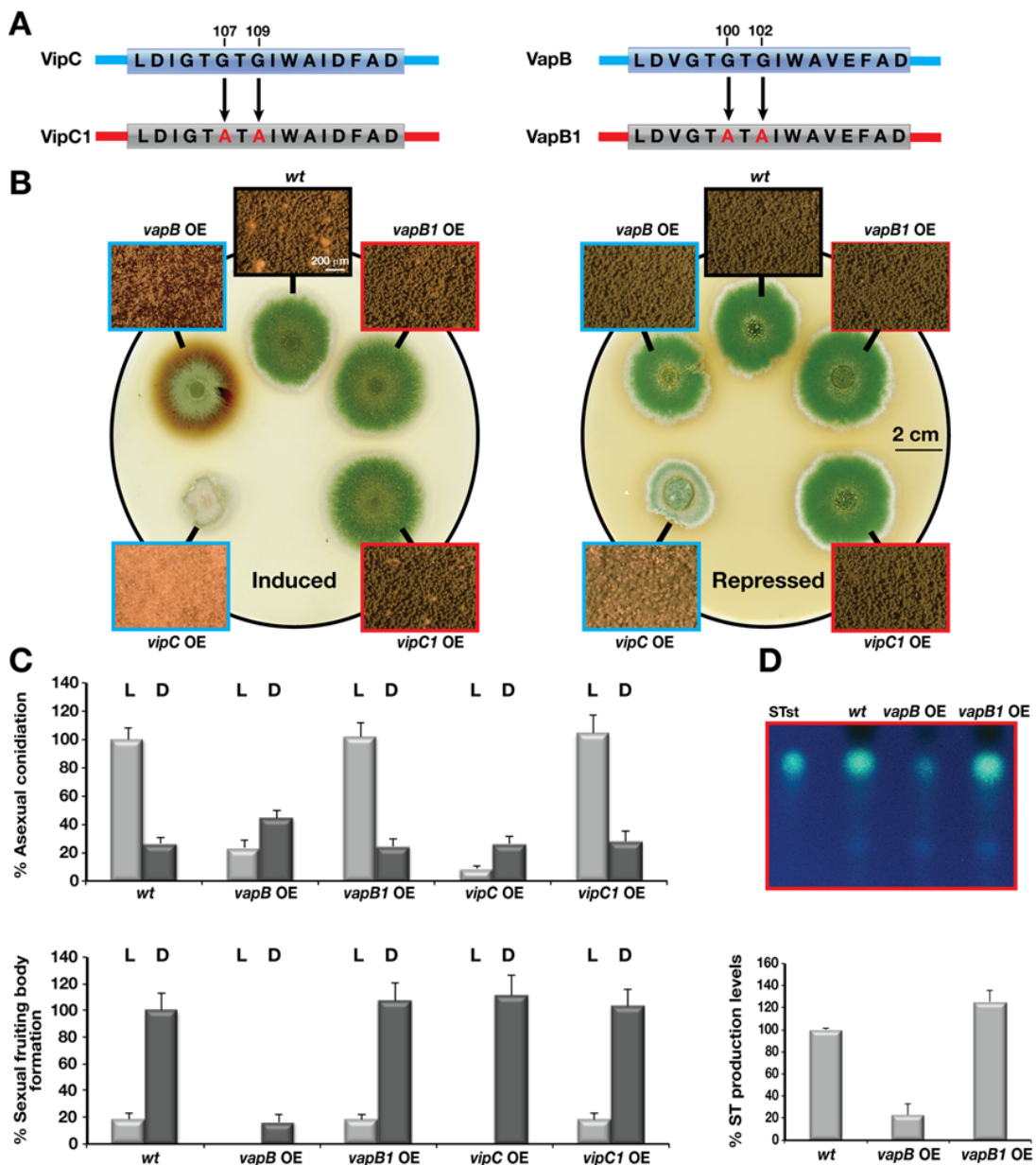
Figure 25. The influence of SAM binding domain on development and secondary metabolism. A. Schematic depiction of the SAM binding motif on VipC and VapB proteins. Two repetitive glycine amino acids ($G^{100}TG^{102}$ in VapB, $G^{107}TG^{109}$ in VipC) were changed to alanine (A). Mutant versions are indicated as new alleles *vipC1* and *vapB1,* respectively. **B.** Growth of the strains expressing the *wt* and mutated alleles on inducing and repressing medium in the light. Small squares show the close-up pictures of the colonies made with stereomicroscope. Brown pigment secretion of *vapB* and slow growth phenotypes of *vipC* overproductions disappear in *vapB1* and *vipC1* mutant allele overexpressions. **C.** Quantified light-dependent conidiation and sexual fruiting body formation by the *wild-type*, *vipC(1)* and *vapB(1)* overexpression strains on induction medium (B). Conidia produced in the light and sexual fruiting bodies generated in the dark by the *wild-type* strain serve as 100%. **D.** Mycotoxin ST productivity of the strains from (B). STs: Sterigmatocystin standard. Overexpression of *vapB1* allele is able to produce ST as does the *wild-type*.
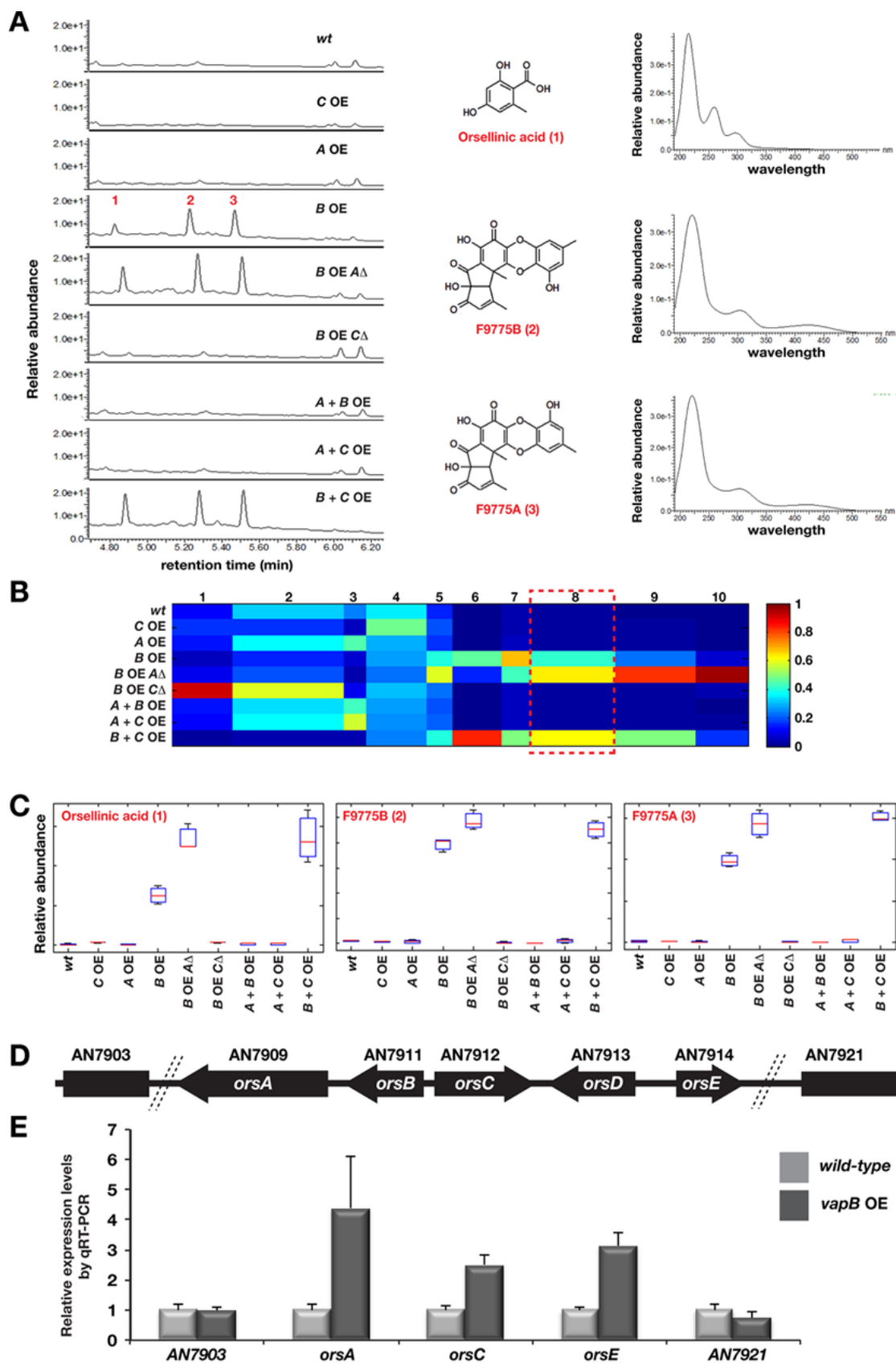
Figure 26. UPLC PDA TOF MS based metabolite fingerprinting of supernatants of the *wild-type* and overexpression strains. A. UPLC chromatograms detected by UV/VIS analysis (190 – 800 nm). Signals (1-3) were identified as orsellinic acid (1), F9775B (2), F9775A (3). **B**. 1D-SOM matrix with 10 prototypes after metabolite-based clustering of 1197 marker candidates (FDR < 10^{-6}) from data sets of the positive and negative ionization mode. The data set includes analysis of three biological replicates. The vertical axis represents the nine analyzed strains. The horizontal axis corresponds to the prototypes numbers. The intensities were normalized and color-coded according to the indicated scale. The compounds 1-3 are represented by prototype 8. **C.** Box-Whisker plots showing relative abundance of orsellinic acid, F9775B and F9775A. **D.** Schematic drawing of the orsellinic acid gene cluster. **E.** Expressional analysis of the orsellinic acid gene cluster by qRT-PCR. Orsellinic acid gene cluster is upregulated in *vapB* overexpression strain. The expression of the genes lying in upstream and downstream of the cluster are not severely affected.

A detailed metabolic examination of the overexpression strains revealed that the products of the cryptic orsellinic acid and its derivatives F9775A and F9775B were accumulated in *vapB* overexpression in a *vipC* dependent manner (Figure 26). This is apparently due to the negative effect of *vapB* on the *veA* gene expression, because a recent study showed that the deletion of *veA* results in an elevation in the expression of orsellinic acid gene cluster (Bok et al., 2013).

These results underline that VapA functions antagonistically against the VipC-VapB methyltransferase heterodimers apparently by excluding them from the nucleus. When protein levels are increased, the ratio between membrane-associated VapA-VipC-VapB and nuclear VipC-VapB complex does not only balance asexual and sexual development but has also an impact on fungal secondary metabolism.

3.2.7. VeA nuclear import is supported by membrane-associated VapA and inhibited by the VipC-VapB methyltransferases

VipC protein physically interacts with VeA and in addition, the methyltransferases VipC-VapB affect *veA* expression. VeA also serves as a bridge between the transcription factor VelB and the methyltransferase LaeA. The controlled-import of VeA into the nucleus sets a threshold for coordination of development and secondary metabolism. Deletion of the *vapA* ZF gene prompts a drastic decrease in fruiting body formation and an increase in asexual conidiation. In contrast, strains lacking the methyltransferases show opposite phenotypes with elevated sexual but reduced asexual development. We addressed the nuclear import of VeA in the corresponding deletion strains.
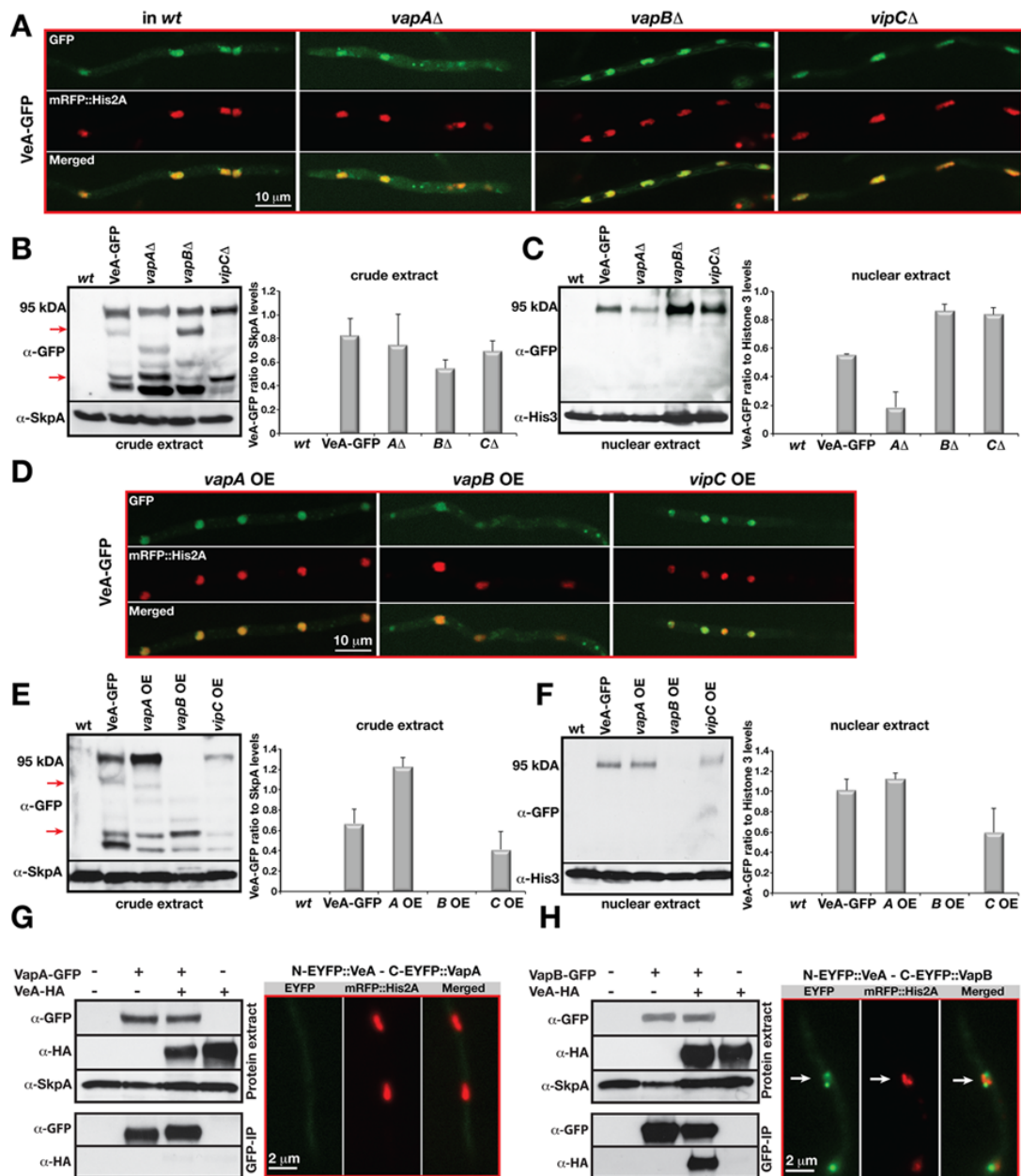
Figure 27. Impact of VapA and the methyltransferases VipC-VapB on subcellular localization and nuclear import of the VeA protein. A. Confocal microscopic images of functional VeA-GFP fusion in *wild-type* (*wt*), *vapA*, *vapB,* or *vipC* deletions. Cytoplasmic subpopulation of VeA in *vapA* deletion mutant strain increases. **B**. Protein levels of VeA-GFP fusion in crude extracts of indicated mutant strains. Red arrows mark degradation products of VeA-GFP. *AΔ*, *BΔ*, and *CΔ* represent *vapA*, *vapB* and *vipC* deletions. Vertical lines on the graphs show standard deviations (SD) from two biological replicates. **C**. Nuclear subpopulations of the VeA-GFP protein from the enriched nuclear extracts of *wild-type* and mutant strains. Nuclear import of VeA is reduced in the absence of *vapA* and increased in *vapB* or *vipC* mutant strains. **D**. Confocal images of VeA-GFP fusion in the respective overexpression strains. VeA-GFP localization in the nucleus is affected if VapB is in excess. VeA protein levels in crude (**E**) or nuclear (**F**) extracts of *wild-type* and and respective overexpressions (OE). Excessive *vapB* causes less *veA* transcripts and also less VeA-GFP levels in crude or nuclear extracts. **G**. Lack of an *in vivo* interaction between VapA-VeA protein by the Co-IP and BIFC method. **H**. An *in vivo* physical interaction of VapB MT and VeA by CoIP and BIFC. In both Co-IPs, GFP-TRAP was used for immunoprecipitations. VapB-VeA proteins interact in the nucleus and at the edge of the nucleus.

Subcellular localization of the functional VeA-GFP fusion expressed under the native promoter was monitored in the absence of VapA, VipC or VapB. VeA-GFP was mostly targeted to the nucleus in *wild-type* strains (Figure 27A). Lack of membrane-associated VapA decreased VeA nuclear intake and increased cytoplasmic signals, suggesting that VapA favors for VeA nuclear import. In contrast, when both VipC and VapB were absent, VeA was enriched in the nucleus. This indicates a negative effect of the VipC-VapB on the nuclear import of the VeA protein (Figure 27A). These findings were substantiated by monitoring protein levels of the VeA protein in the respective mutants. VeA is equally expressed in *wild-type* or mutant strains (Figure 27B). Immunoblotting of enriched nuclear extracts further revealed that the VeA nuclear import was reduced in the *vapA* mutant, but increased in *vapB* and *vipC* mutant in comparison to *wild-type* (Figure 27C).

VeA nuclear entry was further investigated in overexpression strains. Especially *vapB* overexpression had negative effect on *veA* transcript levels resulting in decreased sexual development and impaired ST production. Overexpression of *vapB* resulted in reduced VeA nuclear localization (Figure 27D) but there was hardly any VeA-GFP protein present in the cell (Figure 27E, F). VeA was predominantly found in nuclei when *vapA* or *vipC* were overexpressed but the protein level of VeA was reduced in *vapB* overexpression.

Together these data demonstrate that membrane-associated VapA supports the nuclear entry of VeA probably by keeping VipC and VapB at the membrane. VipC and especially VapB have the opposite effect and impair VeA nuclear import and probably also VeA protein stability. This molecular mechanism contributes to the opposing effects of VapA and VipC-VapB on fungal developmental programs and coordinated secondary metabolism.

3.2.8. VeA physically interacts with VapB methyltransferase

The initial finding of this study was the novel physical interaction of VipC to VeA. VapB impairs cellular VeA protein levels as well as nuclear import, whereas VapA has a positive effect on VeA nuclear entry. We analyzed whether there is any physical interaction between the membrane-associated VapA or VapB methyltransferase and VeA. We examined the *in vivo* interactions between VapA-VeA, and VapB-VeA by Co-IP and BIFCs. VapA did not interact with VeA in Co-IP and also did not result in

a split yellow fluorescent signal in the microscope (Figure 27G). However, the second methyltransferase VapB co-precipitated with VeA protein similar to VipC *in vivo.* The localization of the interaction signal in the BIFC was intriguing because it was not only within the nucleus but also at the border of the nucleus (Figure 27H). These results demonstrate that both VipC and VapB physically interact with the VeA protein. The impact of membrane bound VapA on VeA is indirect through binding of the two methyltransferases VipC-VapB. After release from VapA, VipC and VapB presumably interfere at nuclear and perinuclear physical contact sites with import and stability of VeA.

3.2.9. VapB counteracts histone 3 lysine 9 trimethylation and controls heterochromatin distribution in the nucleus

Nuclear VipC-VapB affects sexual development and when overexpressed also secondary metabolism presumably by interfering with VeA location and stability. The additional impact on asexual development might be due to an additional nuclear methyltransferase function. Histone proteins are the possible targets of the heteromer. Especially histone 3 undergoes extensive PTM, which includes methylation of various residues (Berger, 2007). Methylation regulates the chromatin state together with other PTMs and is part of the epigenetic control of gene expression. In a first approach histone modifications were investigated in deletion strains of the VapA-VipC-VapB complex. Single and double mutants did not lead to any changes in major histone marks, including H3K9 me3 (repression), H3K4 me2 (activation), H3K9/K14 acetylation (activation). A significant effect was achieved by overexpression strains. Intriguingly, VapB overexpression resulted in a 50% reduction of H3K9 me3 marks (Figure 28A). In contrast, other histone modifications did not alter significantly. Previous experiments showed that the VapB SAM binding domain was essential for the molecular function of this methyltransferase (Figure 25). Consistently, the VapB1 variant carrying an amino acid substituion in the SAM domain could not decrease H3K9 me3 marks. This corroborates that the SAM binding motif is crucial for H3K9 me3 reduction and the corresponding developmental function.

Heterochromatin protein (HP1 in Human, HepA in *A. nidulans*) recognizes and binds to H3K9 me3 marks on histones in order to establish the facultative heterochromatin (Maison and Almouzni, 2004). Since VapB overexpression leads to

decreased H3K9 trimethylation, HepA distribution was investigated by using HepA::GFP fusions (Figure 28B). HepA formed in *wild-type* 2-4 distinct heterochromatin foci. In contrast, *vapB* overexpression resulted in a significantly different distribution of HepA signals that were diffused to the entire nucleus.
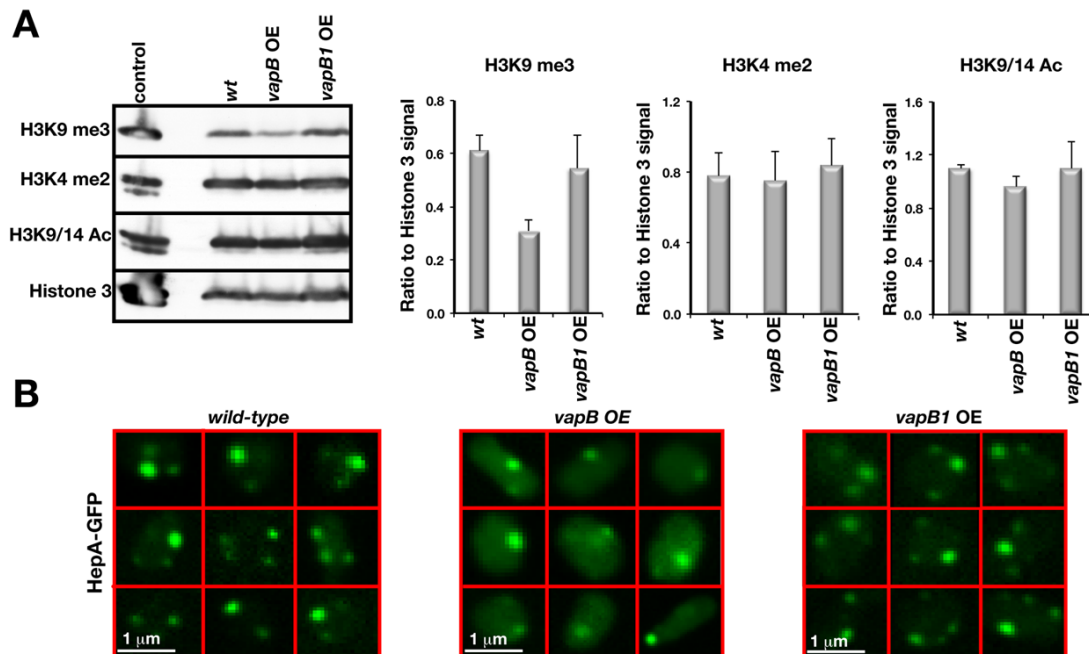
Figure 28. VapB mediated posttranslational histone 3 modifications. A. Influence of VapB overexpression on posttranslational modifications of histone 3. Immunoblotting of the enriched nuclei from *wild-type*, *vapB,* and *vapB1* overexpression strains with specific antibodies against H3K9 trimethylation, H3K4 dimethylation, H3K9/14 acetylation, and unmodified histone 3. Quantifications of two biological immunoblotting replicates. Vertical bars represent standard deviation from two quantifications. Enriched nuclei of chicken erythrocytes were used as control for modifications. **B.** Nuclear distribution of heterochromatin (HepA::GFP) protein. HepA::GFP protein was expressed under endogenous promoter in *wild-type*, *vapB*, and *vapB1*. Enlarged confocal images of nine different nuclei from these strains.

These data imply that there is an additional nuclear function besides the VapB-VipC effect on the sexual program by impairing VeA nuclear import and protein stability through direct physical interaction. Our data suggest that a subpopulation of nuclear VapB methyltransferase is involved in counteracting H3K9 me3 modification. This epigenetic control function of VapB is presumably required for the observed activation of the regulatory genes for asexual conidiation. This supports a tight and mutual even physically interplay between fungal developmental transcription factors including velvet domain proteins as VeA and epigenetic histone methyltransferases as VapB.

4. Discussion

4.1. LaeA control of velvet family regulatory proteins for light-dependent development and fungal cell-type specificity

4.1.1. The velvet family of fungal regulatory proteins of cell fate

The velvet family regulatory proteins are fungus-specific and highly conserved among ascomycetes and basidiomycetes (Ni and Yu, 2007). Structural studies revealed that the velvet domain shows similarities to the fold of the <u>R</u>el <u>h</u>omology <u>d</u>omain (RHD) proteins of mammalian immune response (Ahmed et al., 2013). Fungi represent one of the largest groups of eukaryotic organisms on earth with an estimated 5 million, mostly unknown, species including human and plant pathogens (Hawksworth and Rossman, 1997, Taylor et al., 2001, Strange and Scott, 2005, Normile, 2010, Godfray et al., 2010). The understanding of the molecular mechanisms of the VeA family proteins function might play a key role to understand fungal development. The VeA family includes VeA, VelB, VelC and VosA. VeA, as the first identified light regulator of this family (Kaefer, 1965), regulates morphological development coupled with secondary metabolism (Li et al., 2006, Dreyer et al., 2007, Bayram et al., 2008d, Duran et al., 2007, Calvo, 2008). VosA is not only able to repress asexual development in *A. nidulans*, but is also essential to link sporogenesis and trehalose biogenesis (Ni and Yu, 2007). VelB was discovered by its ability to interact with VeA and characterized as a light-dependent developmental regulator (Bayram et al., 2008c). In this study, we identified VelB-VosA as the second VelB complex. The appearance of VelB correlates with the VosA protein. VelB and VosA seem to share at least parts of their functions, because overexpression of the dimer represses asexual development and the *velB*Δ strain exhibits similar reduced survival rates as the *vosA* deletion. The genetic data suggest that VelB and VosA are inter-dependent in executing trehalose biogenesis, spore maturation and long-term viability. This may be associated with the formation of the nuclear VelB-VosA heterodimeric complex. Therefore, VelB has dual functions within asexual as well as sexual development.

The roles of VelB and VosA in spore maturation are similar to those found in other filamentous fungi including *A. fumigatus* and *Histoplasma capsulatum*. In *H. capsulatum*, Ryp2 and Ryp3, are homologs of VosA and VelB, respectively, and play

a role in regulation of sporulation and inter-dependent expression of the *RYP* genes (Webster and Sil, 2008, Beyhan et al., 2013). In *A. fumigatus*, the deletion of *vosA* and *velB* caused ~50% reduction of the spore trehalose content and viability (Park et al., 2012). Preliminary functional studies of *velC* in *A. nidulans* indicate that this fourth member of the velvet family positively functions in sexual development (Park et al, unpublished).

4.1.2. The protein complexes: VosA-VelB, VelB-VelB and VelB-VeA-LaeA

Heteromeric proteins play vital roles in the development of fungi, plants or animals. Fungal examples involved in the development of sex-specific cells include the heterodimeric a2-a1 complex which represses haploid specific gene expression or the a2-MCM1 complex which turns off alpha-specific genes in yeast cells (Madhani, 2007). Combinations of bE (*E*ast) and bW (*W*est) heterodimeric complexes promote the switch from the haploid yeast phase to the pathogenic dikaryotic phase of the corn smut fungus *Ustilago maydis* (Schulz et al., 1990). Our studies demonstrated that the velvet family proteins form a novel class of fungal regulators that also establish heteromeric complexes and have interdependent functions in determining cell fate.

The VeA-VelB heterodimeric complex of *A. nidulans* presumably forms in the cytoplasm and serves as the major pathway for the VelB entry into the nucleus. The VeA nuclear transport is controlled during development by the light which increases the cytoplasmic fraction of VeA and reduces the nuclear population (Stinnett et al., 2007). The bipartite nuclear localization signal (NLS) is located at the N-terminus of the VeA protein and is disrupted in VeA1, which is derived from a truncation of 36 amino acids of the N-terminus of VeA. This results in the constitutive but reduced VeA nuclear import with reduced interaction with VelB without being controlled by illumination. Light control of VeA might be activated during development by a direct interaction of VeA to the phytochrome FphA. This light sensor is connected to the white collar homolog proteins LreB and LreA as additional light sensors (Purschwitz et al., 2008a). CryA, another fungal light sensing system, functions in a distinct way. It does not interact with VeA, but reduces *veA* mRNA accumulation and therefore reduces the VeA protein levels within the fungal cell during development (Bayram et al., 2008a). Whereas VelB can form homodimers in both cytoplasm and nucleus, VosA-VelB is preferentially located in the nucleus. If VeA provides the major nuclear

import pathway for VelB, this suggests that VeA can be exchanged for VosA or another VelB within the nucleus.

The VosA-VelB heterodimer complex appears to have multiple functions. It can repress asexual spore formation and also controls genes associated with trehalose biogenesis for the spore maturation. The VosA-VelB complex presumably acts as a transcription factor as the C-terminal domain of VosA has transcription activation domain and VosA protein binds to the promoter regions of various genes, including the asexual spore regulator *brlA* (Ni and Yu, 2007, Ahmed et al., 2013). It will be interesting to reveal the genes regulated by the VosA-VelB complexes among filamentous fungi including human or plant pathogens. While our *in vivo* biochemical studies never identified VelC as an interacting partner of the three velvet regulators, a YTH screen followed by GST pull-down assay suggested that VosA and VelC interact and form a heterodimer complex (Ni et al, unpublished data). It appears that *velC* might be expressed at very low levels under specific environmental or developmental conditions.
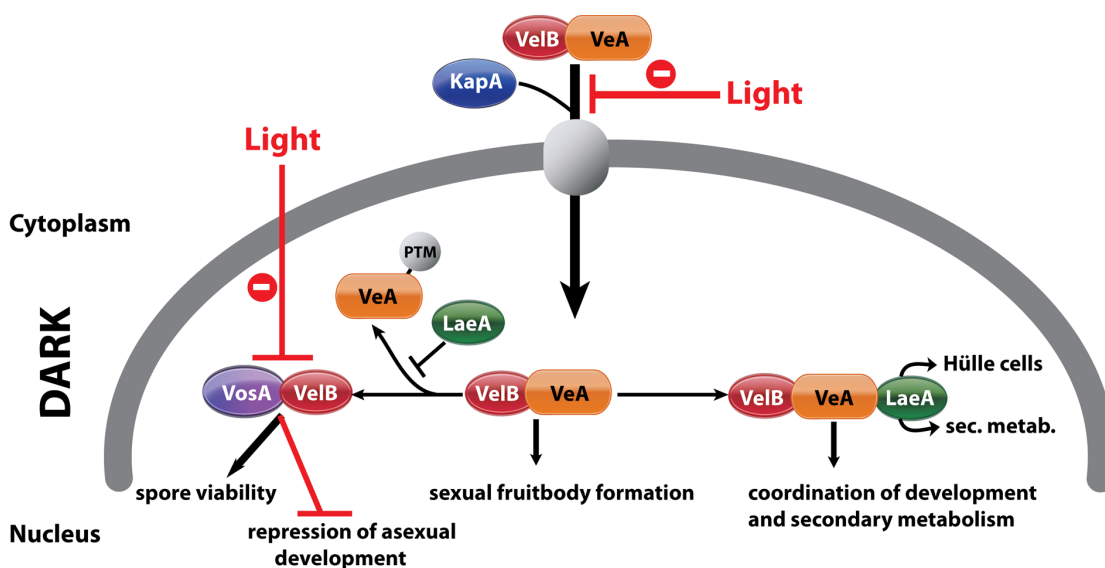
Figure 29. Complexes of velvet family regulatory proteins and LaeA during *A. nidulans* development. This model describes the fungal development in dark and the effect of light on nuclear entry and the formation of VosA/VelB. VelB primarily enters the nucleus together with VeA and alpha-importin KapA. Then, VelB can be distributed to two distinct complexes. The VosA-VelB dimer can repress asexual spore formation and controls spore maturation and trehalose biogenesis. VeA-VelB can associate to LaeA and the dimeric and/or the trimeric complex controls sexual development. The association of LaeA to the VelB-VeA complex links the secondary metabolism to the development. LaeA controls Hülle cell formation, secondary metabolism and protects VeA against posttranslational modification (PTM). VelB is part of the two complexes, VosA-VelB or VelB-VeA.

4.1.3. LaeA control of VosA and VelB protein levels requires an intact N-terminus of VeA

LaeA fulfills two distinct yet related functions within the fungal cell. One function includes the control of the amount of velvet family proteins and therefore the potential to form various complexes. We found here a specific regulatory role for LaeA for all three velvet family members. This novel regulatory role of LaeA for fungal development exceeds its previously reported function as a global regulator of secondary metabolism (Bok and Keller, 2004).

LaeA controls the amount of VosA and VelB in a light dependent manner. In the light the *wild-type* fungus would normally reduce the VosA-VelB complex to release asexual inhibition and to promote the asexual program. In parallel, the sexual program that also requires VelB is repressed. Without LaeA we find, even in the light, high amounts of VosA and VelB and consistent with the VosA-VelB complex, the asexual program is repressed and the sexual pathway is constitutively activated. It is not yet understood why the truncation of the N-terminus of the VeA1 mutant protein results in constitutively high asexual and low sexual development independent of illumination. Activation of sexual development by excessive amounts of the VelB-VosA dimers even under the light conditions further supports that a major function of the VelB-VosA complex after successful germination of spores is to repress fungal development during vegetative growth.

LaeA does not only control VosA and VelB protein levels but also controls simultaneously VeA protein levels and the formation of different VeA forms. VeA is constitutively expressed during different phases of fungal development and normally represents a 63 kDa protein. An additional higher molecular weight VeA of 72 kDa is inhibited in the light where asexual development is promoted, and is only detectable during vegetative growth or in the dark during sexual development. The increased amounts of VelB and VosA in the absence of *laeA* somehow correlate with an accumulation of the VeA-72 kDa version. This accumulation cannot be observed when the N-terminus is truncated as in the VeA1 mutant protein. The 72 kDa shift from VeA-63 kDa presumably represents a modification which is inhibited by LaeA in a light dependent manner. VeA is known to be a phosphoprotein (Purschwitz et al., 2008b) and phosphatase treatment does not affect VeA-63 kDa or the VeA1 mutant version but resulted in a partial reduction in the mobility of the 72 kDa version (not

shown). Furthermore α-phosphoserine and α-phosphothreonine recognized the immunoprecipitated phosphorylated 72 kDa VeA protein in the *laeA*Δ background supporting that the serine and threonine residues of VeA are phosphorylated (data not shown). However, the LaeA dependent VeA modification is even more complex and includes at least one yet unknown modification. LaeA associates with the VelB-VeA dimer forming the heterotrimeric velvet complex. LaeA might protect VeA from modification by occupying the C-terminus of VeA, and thereby controlling the balance between VosA-VelB and VelB-VeA-LaeA (Figure 29). There might be another level of control that limits the overall VeA protein levels. It will be interesting to analyze whether LaeA is able to interfere with the interaction of VeA to the light receptor complex FphA-LreA-LreB (Fischer, 2008) to confer its light control function.

4.1.4. The global regulator of secondary metabolism LaeA is part of the control of Hülle cell formation

Further LaeA regulatory functions are independent of the N-terminus of VeA. It is tempting to speculate that the N-terminus dependent LaeA functions involve VosA and VelB, whereas the independent functions concern LaeA alone or in concert with VeA and/or VelB. The LaeA-VeA1 complex can at least partially fulfill the LaeA control of secondary metabolism, which has been investigated in *veA1* laboratory strains (Bok and Keller, 2004, Keller et al., 2005).

In a striking contrast to the *veA* and *velB* mutants, loss of LaeA does not abolish the potential to form fruiting bodies. We found it remarkable that without LaeA almost no Hülle cells can be formed, and hardly any expression of the Hülle cell specific *mut*A gene occurs. The function of Hülle cells are proposed to protect and nourish the maturating nests, which are the primitive structures of cleistothecia (Braus et al., 2002). Consistently to the proposed nursing function the fungal fruiting bodies of a *laeA* deficient strain are only one fifth of the normal size. The size of an average cleistothecium is around 200 μm. In literature there are few genes affecting the size of cleistothecia including tryptophan auxotrophic mutants (Eckert et al., 1999), *hisB* gene deletion (Busch et al., 2001) as well as *sumO* mutant. SumO is a small ubiquitin like modifier of *A. nidulans* (Wong et al., 2008). The *laeA* deletion mutant constitutively produces these high amounts of small cleistothecia, even in the

presence of light, further corroborating the key role that LaeA plays in light dependent fungal development.

Another remarkable finding is that the expression of the transcriptional regulatory genes *steA* (Vallim et al., 2000) and *nosA* are LaeA dependent during vegetative growth. Both genes are involved in the sexual pathway. Without SteA there are no fruiting bodies (Vallim et al., 2000). Even more interesting is that *nosA* mRNA is completely absent in vegetative cells of *laeA*Δ. Deletion of *nosA* gene also results in very small cleistothecia which are about 30 μm in size but still containing fertile ascospores (Vienken and Fischer, 2006). *nosA*Δ strain has almost no Hülle cells, a phenotype similar to *laeA*Δ strains. It is therefore likely that LaeA dependent expression of *nosA* during the vegetative stage is required for Hülle cell formation. This is further supported by the findings that overexpression of *nosA* under nitrate inducible *niiA* promoter in *laeA*Δ partially rescued the lack of Hülle cells, small cleistothecia and ascospore production (Figure 16). This results in abundant expression of NosA in vegetative cells in a *laeA* deletion (Figure 16D). The reason why the rescue is only partial might be due to the fact that some other regulators acting in the parallel pathway with *nosA* for Hülle cell formation are still less expressed or misregulated in a *laeA*Δ. It will be interesting to examine whether and how this LaeA dependent temporal control of transcription factor genes like *nosA* depends on the members of the velvet family.

4.1.5. LaeA: cell-type regulator and master of secondary metabolism

The parental generation of multicellular organisms normally has to provide nourishment as well as protection for the next generation. Hülle cells of the mold *A. nidulans* are associated with cleistothecia and provide this function for the fungal fruiting body. Our major finding here is that LaeA in combination with the velvet family of related regulatory proteins is involved in both lines of support for the next generation. LaeA was first discovered to be the global regulator of secondary metabolite genes including ST, PN and many other compounds. All these chemicals might confer a certain advantage to the fungus during growth under substratum in the soil. *Aspergillus* produces asexual conidiation on the surface of the soil, but sexual development takes place under substratum where numerous eukaryotic or prokaryotic organisms compete for nutrients and represent a threat to vulnerable sexual fruiting

bodies. Carcinogenic ST might protect fungal cleistothecia against eukaryotic competitors. Consistently, *laeAΔ* strains are the preferred food source of insect larvae in comparison to a *wild-type* strain (Rohlfs et al., 2007).

Similarly, penicillin might help to defend against various bacteria in the soil. All these responses regulated by LaeA might be considered as the chemical protection of fruiting bodies. At the same time, LaeA is essential for the Hülle cells and therefore controls feeding of the fruiting bodies by providing these cells. Thus, LaeA promotes both the production of chemicals to protect fruiting bodies and the production of nourishing cells for developing fruiting bodies.

The LaeA functions exerted on maturating cleistothecia in combination with the heteromeric protein complexes of the velvet family represent an unexpected scenario in fungal development. It will be interesting to see how much convergent evolution there is and whether there are molecular counterparts of LaeA in other higher organisms, which are involved in the protective as well as the nutritional function for preparing the next generation for future life.

4.2. The membrane-bound VapA-VipC-VapB methyltransferase complex guides signal transduction for epigenetic and transcriptional control of fungal development

S-adenosyl methionine is the second most frequently utilized enzyme cofactor in the cell after ATP. The biochemical reactions where SAM-dependent methyltransferases are involved include the methylation of proteins, DNA, RNA, lipids, polysaccharides, and small molecules. Protein and DNA methylations provide the fundamental mechanisms for epigenetic control of gene expression in eukaryotes. Here, we discovered a novel fungal heterotrimeric protein complex that includes the FYVE-like zinc finger protein VapA and the methyltransferase heteromer VipC-VapB. VapA is a positive regulator of sexual development as long as it tethers the methyltransferases to the membrane. When VipC-VapB are released from the membrane to the nucleus they reduce nuclear VeA levels which results in repression of sexual development and secondary metabolism. Nuclear methyltransferase VapB influences heterochromatin distribution by decreasing histone 3 lysine 9 trimethylation. This promotes the asexual differentiation program.

4.2.1. Comparison of two trimeric complexes VelB-VeA-LaeA and VapA-VipC-VapB

VapA-VipC-VapB and the velvet complex VelB-VeA-LaeA share the presence of methyltransferase subunits within a trimeric complex. The nuclear velvet complex includes the two velvet domain transcription factors VeA-VelB, and the SAM-dependent methyltransferase LaeA, whereas the novel membrane-associated trimeric complex contains a zinc finger protein VapA and two SAM-dependent methyltransferases VipC-VapB. Without external signal this complex is preassembled at the plasma membrane. VapA attaches the VipC-VapB methyltransferase heteromers to the plasma membrane (Figure 30). Velvet complex formation requires that the cytoplasmic VeA-VelB heterodimer is imported into the nucleus where it recruits the methyltransferase LaeA. Both trimeric complexes are required to promote sexual development and coordinated secondary metabolism preferentially in the absence of light. Illumination impairs both trimeric complexes. The VapA-VipC-VapB complex dissociates the methyltransferase dimer from the plasma membrane, resulting in reduced velvet complex formation because the VipC-VapB dimer impairs

VeA nuclear entry and protein stability. The VipC-VapB heterodimer counteracts the trimethylation of H3K9, which in turn affects gene expression and activates asexual development.
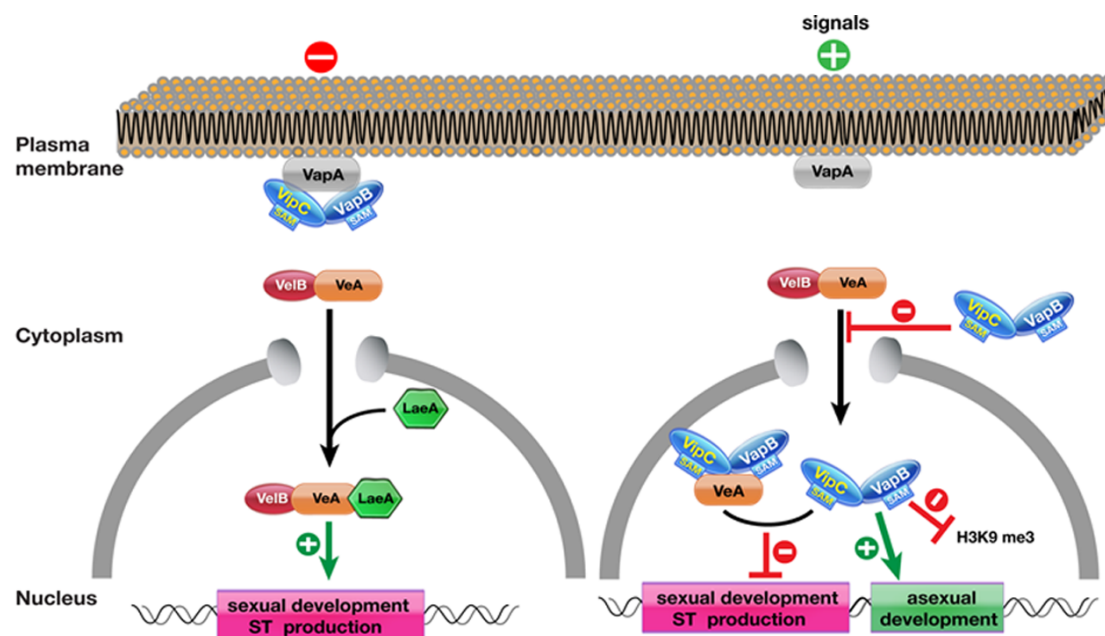
Figure 30. Interplay between trimeric VapA-VipC-VapB and VelB-VeA-LaeA methylase complexes. A model for the control of development and sterigmatocystin production by the novel VapA-VipC-VapB methyltransferase complex is depicted. In the absence of a respective signal (e.g. light) physically interacting trimeric complex VapA-VipC-VapB assembles at the plasma membrane. VeA-VelB heterodimer enters into the nucleus and recruits the methyltransferase LaeA. The assembly of the velvet complex allows the coordination of sexual development and ST production. Presence of the signal leads to release of VipC-VapB methyltransferase heterodimer that inhibits nuclear import of VeA. Nuclear fraction of VipC-VapB heterodimer associates with VeA, and either this association (VipC-VeA-VapB) or VipC-VapB represses sexual development and induces asexual conidiation. In VipC-VapB dimer, VapB counteracts H3K9 trimethylation with an unknown mechanism. A balance between these complexes is required for a proper development and natural product biosynthesis.

The number of described membrane-tethered methyltransferases is limited and a nuclear shuttling has to our knowledge not yet been described. Transmembrane methyl-accepting chemotaxis receptor proteins (MCPs) are sensors in bacteria. They are controlled by the cytoplasmic methyltransferase and demethylase pair CheR/CheB resulting in methylation or demethylation (Kentner and Sourjik, 2009). CheR homologs also control biofilm formation of pathogenic bacteria (Garcia-Fontana et al., 2013). Catechol O-methyltransferases are membrane-bound and contribute to O-methylation of catecholamine neurotransmitters as dopamine and norepinephrine in the human brain (Rivett et al., 1983). Protein arginine methyltransferases (PRMTs) of mammalian cells are associated with the plasma membrane. PRMT8 is directly

tethered to the plasma membrane by amino-terminal myristoylation (Lee et al., 2005). Some mammalian PRMTs interact with various transmembrane receptors such as interferon-a-receptor 1 (IFNR1), B cell antigen receptor (BCR), or epidermal growth factor receptor (EGFR) (Yang and Bedford, 2013). There are also a few crosstalks between methyltransferase and MAPK mediated signal transduction mechanisms. For example, arginine methyltransferase PRMT5 influences the RAS-ERK signal transduction by methylating the RAF proteins, which reduces the catalytic activity of CRAF and BRAF by enhancing their degradation (Andreu-Perez et al., 2011).

4.2.2. Regulation of the VeA nuclear import and development by the VipC-VapB methyltransferase complex

The crosstalk between the fungal MAPK pathway and the VipC-VapB methyltransferases focuses on VeA. This includes the ratio between nuclear and cytoplasmic VeA distribution, VeA stability and VeA phosphorylation which makes it prone to interact to VelB. All these parameters affect the VeA function in the control of fruiting body formation and secondary metabolism. The L̲aeA-l̲ike m̲ethyltransferase LlmF represents a cytoplasmic methyltransferase that reduces the VeA nuclear import by an unknown mechanism (Palmer et al., 2013). The VipC-VapB methyltransferase interacts with the VeA protein inside as well as at the border of nucleus, indicating a possible interaction just during nuclear entry. In the absence of VipC-VapB, nuclear accumulation of VeA is greatly enhanced. VeA nuclear import is decreased in the *vapA* mutant where VapB or VipC prevent nuclear VeA accumulation. Consistently, increased levels of VapB cause an impairment of sexual development and secondary metabolism. VeA interacts with numerous proteins including other velvet domain proteins that act as transcription factors. Therefore, an increased interaction of the methyltransferases VapB-VipC will allow VeA partners to participate in different complexes and also affect asexual development. This might be a reason why VeA also contributes to the expression of major asexual regulatory genes as *brlA* (Kim et al., 2002, Kato et al., 2003). VeA also acts as a strong repressor of orsellinic acid gene cluster and therefore reduced VeA as in the VapB overexpression strains leads even to an accumulation of orsellinic acid and its derivatives F9775A and F9775B.

4.2.3. Epigenetic functions of the VipC-VapB methyltransferase dimers

A second nuclear function of the VipC-VapB methyltransferases includes histone modification as part of an epigenetic control mechanism. Methylation and acetylation of histone 3 lysine 4 (H3K4) vs. lysine 9 (H3K9) are in a dynamic competition, where acetylation turns on gene expression. Methylation of histones is widespread and has opposing functions depending on where the methylation occurs. Methylation of H3K4 is most often correlated with active transcription, whereas methylation of H3K9 results in gene silencing and therefore heterochromatin accumulation (Maison and Almouzni, 2004). Increased VapB protein levels cause a reduction in the repressive histone 3 lysine 9 trimethylation mark. It is yet unknown whether the influence of the VipC-VapB heteromer on histone modification is mediated by interfering with the H3K9 methyltransferase ClrD activity or enhancing specific demethylases for H3K9 residues.

Understanding the regulation of fungal development and natural product biosynthesis is essential to explore the fungal potential to produce novel bioactive compounds and to control fungal growth and development of human or plant pathogens. The discovery of the novel VapA-VipC-VapB complex identifies a new layer of regulation for transmission of extracellular signals into the regulatory network of the fungal specific *velvet* domain family. It will be interesting to analyze the exact molecular mechanism how the VipC-VapB methyltransferases interfere with VeA nuclear import and stability. The interconnection between the methyltransferase and the MAPK signaling module of *A. nidulans* will be another focus of future research. It will be appealing to know whether this type of signal transduction is also conserved in other members of the fungal kingdom or other eukaryotes and what kind of roles they play during development, pathogenesis and secondary metabolite production.

4.3. Future outlook

LaeA protein controls secondary metabolism as well as the development of the fungus *A. nidulans*. Protein levels as well as posttranslational modifications of the velvet family proteins are influenced by LaeA. Especially, yet unknown posttranslational modifications of the VeA protein were influenced by LaeA. In future studies, it will be essential to identify the dynamics of the posttranslational modifications of the VeA protein at the molecular level. The presence of a PEST region on VeA protein suggests that it is a target for ubiquitination. Immunoprecipitation of the VeA protein and detailed mass spectrometry analyses will give more insights into the nature of these PTMs. Furthermore, to see whether these modifications take place at the cytoplasmic or nuclear fraction of the cell, VeA protein lacking the nuclear localization signal (NLS) can be used in the presence or absence of the LaeA protein. The velvet protein family represents the fungal specific novel transcription domain proteins. Therefore, it will be intriguing to reveal whether the binding sites of VeA, VelB and VosA are affected by the LaeA protein. ChIP experiments combined with next-generation sequencing will yield more insights into this direction.

The VapA-VipC-VapB complex plays an important role by connecting the membrane associated signal transduction to the epigenetic control of secondary metabolism. The complex influences the development by interfering with the nuclear import of the VeA protein, which needs to be further elucidated. VipC-VapB proteins might inhibit the interaction of the VeA with the α-importin KapA. Therefore, this phenomenon can be analyzed by checking VeA-KapA interaction *in vivo* as well as *in vitro* in the presence or absence of VapB/VipC methyltransferases. It will be also interesting too to see how VapA-VipC-VapB complex influences the complete transcriptome of *A. nidulans*. In connection with expression studies, ChIP experiments with VapB-VipC methyltransferases might also lead to mechanistic information into the function of these nuclear methyltransferases. Since the VapA-VapB-VipC complex is located at the plasma membrane, there could be a possible cross talk between the MAPK pathways and the trimeric complex. It is appealing to study whether any of the complex components interacts with the MAPK module components SteC-SteD-MkkB-MpkB.

.

References

ADAMS, T. H., DEISING, H. & TIMBERLAKE, W. E. 1990. *brlA* requires both zinc fingers to induce development. *Mol Cell Biol,* 10**,** 1815-1817.

ADAMS, T. H., WIESER, J. K. & YU, J. H. 1998. Asexual sporulation in *Aspergillus nidulans*. *Microbiol Mol Biol Rev,* 62**,** 35-54.

AHMED, Y. L., GERKE, J., PARK, H., BAYRAM, O., NEUMANN, P., NI, M., DICKMANNS, A., KIM, S., YU, J., GH, B. & FICNER, R. 2013. The Velvet family of fungal regulators contains a DNA-binding domainstructurally similar to NF-kB. *PloS biology*.

ANDREU-PEREZ, P., ESTEVE-PUIG, R., DE TORRE-MINGUELA, C., LOPEZ-FAUQUED, M., BECH-SERRA, J. J., TENBAUM, S., GARCIA-TREVIJANO, E. R., CANALS, F., MERLINO, G., AVILA, M. A. & RECIO, J. A. 2011. Protein arginine methyltransferase 5 regulates ERK1/2 signal transduction amplitude and cell fate through CRAF. *Sci Signal,* 4**,** ra58.

ANDRIANOPOULOS, A. & TIMBERLAKE, W. E. 1994. The *Aspergillus nidulans abaA* gene encodes a transcriptional activator that acts as a genetic switch to control development. *Mol Cell Biol,* 14**,** 2503-2515.

AXELROD, D. E., GEALT, M. & PASTUSHOK, M. 1973. Gene control of developmental competence in *Aspergillus nidulans*. *Dev Biol,* 34**,** 9-15.

BADEAUX, A. I. & SHI, Y. 2013. Emerging roles for chromatin as a signal integration and storage platform. *Nature reviews. Molecular cell biology,* 14**,** 211-24.

BAYRAM, O., BAYRAM, O. S., AHMED, Y. L., MARUYAMA, J., VALERIUS, O., RIZZOLI, S. O., FICNER, R., IRNIGER, S. & BRAUS, G. H. 2012a. The *Aspergillus nidulans* MAPK module AnSte11-Ste50-Ste7-Fus3 controls development and secondary metabolism. *PLoS Genet,* 8**,** e1002816.

BAYRAM, O., BAYRAM, O. S., VALERIUS, O., JOHNK, B. & BRAUS, G. H. 2012b. Identification of protein complexes from filamentous fungi with tandem affinity purification. *Methods Mol Biol,* 944**,** 191-205.

BAYRAM, O., BIESEMANN, C., KRAPPMANN, S., GALLAND, P. & BRAUS, G. H. 2008a. More than a repair enzyme: *Aspergillus nidulans* photolyase-like CryA is a regulator of sexual development. *Mol Biol Cell,* 19**,** 3254-62.

BAYRAM, O. & BRAUS, G. H. 2012. Coordination of secondary metabolism and development in fungi: the velvet family of regulatory proteins. *FEMS Microbiol Rev,* 36**,** 1-24.

BAYRAM, O., BRAUS, G. H., FISCHER, R. & RODRIGUEZ-ROMERO, J. 2010. Spotlight on *Aspergillus nidulans* photosensory systems. *Fungal Genet Biol,* 47**,** 900-8.

BAYRAM, O., KRAPPMANN, S., NI, M., BOK, J., HELMSTAEDT, K., VALERIUS, O., BRAUS-STROMEYER, S., KWON, N., KELLER, N., YU, J. & BRAUS, G. 2008b. VelB/VeA/LaeA complex coordinates light signal with fungal development and secondary metabolism. *Science,* 320**,** 1504-1506.

BAYRAM, O., KRAPPMANN, S., NI, M., BOK, J. W., HELMSTAEDT, K., VALERIUS, O., BRAUS-STROMEYER, S., KWON, N. J., KELLER, N. P., YU, J. H. & BRAUS, G. H. 2008c. VelB/VeA/LaeA complex coordinates light signal with fungal development and secondary metabolism. *Science,* 320**,** 1504-6.

BAYRAM, O., KRAPPMANN, S., SEILER, S., VOGT, N. & BRAUS, G. H. 2008d. Neurospora crassa ve-1 affects asexual conidiation. *Fungal Genet Biol,* 45**,** 127-38.

BAYRAM, O., SARI, F., BRAUS, G. H. & IRNIGER, S. 2009. The protein kinase *ImeB* is required for light-mediated inhibition of sexual development and for mycotoxin production in *Aspergillus nidulans*. *Mol Microbiol,* 71**,** 1278-95.

BERGER, S. L. 2007. The complex language of chromatin regulation during transcription. *Nature,* 447**,** 407-12.

BEYHAN, S., GUTIERREZ, M., VOORHIES, M. & SIL, A. 2013. A temperature-responsive network links cell shape and virulence traits in a primary fungal pathogen. *PLoS biology,* 11**,** e1001614.

BHAUMIK, S. R., SMITH, E. & SHILATIFARD, A. 2007. Covalent modifications of histones during development and disease pathogenesis. *Nature structural & molecular biology,* 14**,** 1008-16.

BI, Q., WU, D., ZHU, X. & GILLIAN TURGEON, B. 2013. *Cochliobolus heterostrophus* Llm1 - a Lae1-like methyltransferase regulates T-toxin production, virulence, and development. *Fungal Genet Biol,* 51**,** 21-33.

BLACKWELL, M. 2011. The fungi: 1, 2, 3 ... 5.1 million species? *Am J Bot,* 98**,** 426-38.

BLUMENSTEIN, A., VIENKEN, K., TASLER, R., PURSCHWITZ, J., VEITH, D., FRANKENBERG-DINKEL, N. & FISCHER, R. 2005. The *Aspergillus nidulans* phytochrome FphA represses sexual development in red light. *Curr Biol,* 15**,** 1833-8.

BOK, J. W., CHIANG, Y. M., SZEWCZYK, E., REYES-DOMINGUEZ, Y., DAVIDSON, A. D., SANCHEZ, J. F., LO, H. C., WATANABE, K., STRAUSS, J., OAKLEY, B. R., WANG, C. C. & KELLER, N. P. 2009. Chromatin-level regulation of biosynthetic gene clusters. *Nat Chem Biol,* 5**,** 462-4.

BOK, J. W., HOFFMEISTER, D., MAGGIO-HALL, L. A., MURILLO, R., GLASNER, J. D. & KELLER, N. P. 2006. Genomic mining for Aspergillus natural products. *Chem Biol,* 13**,** 31-7.

BOK, J. W. & KELLER, N. P. 2004. LaeA, a regulator of secondary metabolism in *Aspergillus spp. Eukaryot Cell,* 3**,** 527-35.

BOK, J. W., SOUKUP, A. A., CHADWICK, E., CHIANG, Y. M., WANG, C. C. & KELLER, N. P. 2013. VeA and MvlA repression of the cryptic orsellinic acid gene cluster in *Aspergillus nidulans* involves histone 3 acetylation. *Mol Microbiol.*

BOND, U., AGELL, N., HAAS, A. L., REDMAN, K. & SCHLESINGER, M. J. 1988. Ubiquitin in stressed chicken embryo fibroblasts. *The Journal of biological chemistry,* 263**,** 2384-8.

BORGIA, P. T., MIAO, Y. & DODGE, C. L. 1996. The *orlA* gene from *Aspergillus nidulans* encodes a trehalose-6-phosphate phosphatase necessary for normal growth and chitin synthesis at elevated temperatures. *Molecular microbiology,* 20**,** 1287-96.

BRAKHAGE, A. A. 2013. Regulation of fungal secondary metabolism. *Nat Rev Microbiol,* 11**,** 21-32.

BRAUS, G. H., KRAPPMANN, S. & ECKERT, S. E. 2002. Sexual Development in Ascomycetes - Fruit Body Formation of *Aspergillus nidulans. In:* OSIEWACZ, H. D. (ed.) *Molecular Biology of Fungal Development.* New York, Basel: Marcel Dekker, Inc.

BROWN, D. W., YU, J. H., KELKAR, H. S., FERNANDES, M., NESBITT, T. C., KELLER, N. P., ADAMS, T. H. & LEONARD, T. J. 1996. Twenty-five coregulated transcripts define a sterigmatocystin gene cluster in *Aspergillus nidulans. Proc Natl Acad Sci U S A,* 93**,** 1418-22.

BROWN, T. & MACKEY, K. 1997. Analysis of RNA by Northern and slot blot hybridization. *Current protocols in molecular biology.* New York, NY: John Wiley and Sons Inc.

BROWNELL, J. E., ZHOU, J., RANALLI, T., KOBAYASHI, R., EDMONDSON, D. G., ROTH, S. Y. & ALLIS, C. D. 1996. Tetrahymena histone acetyltransferase A: a homolog to yeast Gcn5p linking histone acetylation to gene activation. *Cell,* 84**,** 843-51.

BUSBY, T. M., MILLER, K. Y. & MILLER, B. L. 1996. Suppression and enhancement of the *Aspergillus nidulans* medusa mutation by altered dosage of the bristle and stunted genes. *Genetics,* 143**,** 155-63.

BUSCH, S., ECKERT, S. E., KRAPPMANN, S. & BRAUS, G. H. 2003. The COP9 signalosome is an essential regulator of development in the filamentous fungus *Aspergillus nidulans. Mol Microbiol,* 49**,** 717-30.

BUSCH, S., HOFFMANN, B., VALERIUS, O., STARKE, K., DUVEL, K. & BRAUS, G. H. 2001. Regulation of the Aspergillus nidulans hisB gene by histidine starvation. *Curr Genet,* 38**,** 314-22.

BUSCH, S., SCHWIER, E. U., NAHLIK, K., BAYRAM, O., HELMSTAEDT, K., DRAHT, O. W., KRAPPMANN, S., VALERIUS, O., LIPSCOMB, W. N. & BRAUS, G. H. 2007. An eight-subunit COP9 signalosome with an intact JAMM motif is required for fungal fruit body formation. *Proc Natl Acad Sci U S A,* 104**,** 8089-94.

CABALLERO ORTIZ, S., TRIENENS, M. & ROHLFS, M. 2013. Induced fungal resistance to insect grazing: reciprocal fitness consequences and fungal gene expression in the Drosophila-Aspergillus model system. *PloS one,* 8**,** e74951.

CALVO, A. M. 2008. The VeA regulatory system and its role in morphological and chemical development in fungi. *Fungal Genet Biol,* 45**,** 1053-61.

CAO, R., WANG, L., WANG, H., XIA, L., ERDJUMENT-BROMAGE, H., TEMPST, P., JONES, R. S. & ZHANG, Y. 2002. Role of histone H3 lysine 27 methylation in Polycomb-group silencing. *Science,* 298**,** 1039-43.

CHI, P., ALLIS, C. D. & WANG, G. G. 2010. Covalent histone modifications--miswritten, misinterpreted and mis-erased in human cancers. *Nature reviews. Cancer,* 10**,** 457-69.

D'ENFERT, C. & FONTAINE, T. 1997. Molecular characterization of the Aspergillus nidulans treA gene encoding an acid trehalase required for growth on trehalose. *Mol Microbiol,* 24**,** 203-16.

DOLL, K., CHATTERJEE, S., SCHEU, S., KARLOVSKY, P. & ROHLFS, M. 2013. Fungal metabolic plasticity and sexual development mediate induced resistance to arthropod fungivory. *Proceedings. Biological sciences / The Royal Society,* 280**,** 20131219.

DREYER, J., EICHHORN, H., FRIEDLIN, E., KURNSTEINER, H. & KUCK, U. 2007. A homologue of the Aspergillus velvet gene regulates both cephalosporin C biosynthesis and hyphal fragmentation in Acremonium chrysogenum. *Appl Environ Microbiol,* 73**,** 3412-22.

DURAN, R. M., CARY, J. W. & CALVO, A. M. 2007. Production of cyclopiazonic acid, aflatrem, and aflatoxin by Aspergillus flavus is regulated by veA, a gene necessary for sclerotial formation. *Appl Microbiol Biotechnol,* 73**,** 1158-68.

DYER, P. S. & O'GORMAN, C. M. 2012. Sexual development and cryptic sexuality in fungi: insights from Aspergillus species. *FEMS Microbiol Rev,* 36**,** 165-92.

ECKERT, S. E., HOFFMANN, B., WANKE, C. & BRAUS, G. H. 1999. Sexual development of *Aspergillus nidulans* in tryptophan auxotrophic strains. *Arch Microbiol,* 172**,** 157-66.

ETXEBESTE, O., GARZIA, A., ESPESO, E. A. & UGALDE, U. 2010. *Aspergillus nidulans* asexual development: making the most of cellular modules. *Trends Microbiol,* 18**,** 569-76.

FENG, Q., WANG, H., NG, H. H., ERDJUMENT-BROMAGE, H., TEMPST, P., STRUHL, K. & ZHANG, Y. 2002. Methylation of H3-lysine 79 is mediated by a new family of HMTases without a SET domain. *Curr Biol,* 12**,** 1052-8.

FERNANDES, M., KELLER, N. P. & ADAMS, T. H. 1998. Sequence-specific binding by *Aspergillus nidulans* AflR, a C6 zinc cluster protein regulating mycotoxin biosynthesis. *Mol Microbiol,* 28**,** 1355-65.

FILLINGER, S., CHAVEROCHE, M. K., VAN DIJCK, P., DE VRIES, R., RUIJTER, G., THEVELEIN, J. & D'ENFERT, C. 2001. Trehalose is required for the acquisition of tolerance to a variety of stresses in the filamentous fungus *Aspergillus nidulans*. *Microbiology,* 147**,** 1851-62.

FISCHER, R. 2008. Developmental biology. Sex and poison in the dark. *Science,* 320**,** 1430-1.

FISCHLE, W. 2012. One, two, three: how histone methylation is read. *Epigenomics,* 4**,** 641-53.

FLOERL, S., MAJCHERCZYK, A., POSSIENKE, M., FEUSSNER, K., TAPPE, H., GATZ, C., FEUSSNER, I., KUES, U. & POLLE, A. 2012. *Verticillium longisporum* infection affects the leaf apoplastic proteome, metabolome, and cell wall properties in *Arabidopsis thaliana*. *PLoS One,* 7**,** e31435.

GALAGAN, J. E., CALVO, S. E., CUOMO, C., MA, L. J., WORTMAN, J. R., BATZOGLOU, S., LEE, S. I., BASTURKMEN, M., SPEVAK, C. C., CLUTTERBUCK, J., KAPITONOV, V., JURKA, J., SCAZZOCCHIO, C., FARMAN, M., BUTLER, J., PURCELL, S., HARRIS, S., BRAUS, G. H., DRAHT, O., BUSCH, S., D'ENFERT, C., BOUCHIER, C., GOLDMAN, G. H., BELL-PEDERSEN, D., GRIFFITHS-JONES, S., DOONAN, J. H., YU, J., VIENKEN, K., PAIN, A., FREITAG, M., SELKER, E. U., ARCHER, D. B., PENALVA, M. A., OAKLEY, B. R., MOMANY, M., TANAKA, T., KUMAGAI, T., ASAI, K., MACHIDA, M., NIERMAN, W. C., DENNING, D. W., CADDICK, M., HYNES, M., PAOLETTI, M., FISCHER, R., MILLER, B., DYER, P., SACHS, M. S., OSMANI, S. A., BIRREN, B. W., ECKERT, S. E. & KRAPPMANN, S. 2005. Sequencing of *Aspergillus nidulans* and comparative analysis with *A. fumigatus* and *A. oryzae*. *Nature,* 438**,** 1105-15.

GARCIA-FONTANA, C., REYES-DARIAS, J. A., MUNOZ-MARTINEZ, F., ALFONSO, C., MOREL, B., RAMOS, J. L. & KRELL, T. 2013. High Specificity in CheR Methyltransferase Function: CheR2 of Pseudomonas putida is essential for chemotaxis, whereas CheR1 is involved in biofilm formation. *J Biol Chem,* 288**,** 18987-99.

GAULLIER, J. M., SIMONSEN, A., D'ARRIGO, A., BREMNES, B., STENMARK, H. & AASLAND, R. 1998. FYVE fingers bind PtdIns(3)P. *Nature,* 394**,** 432-3.

GAVRIAS, V., ANDRIANOPOULOS, A., GIMENO, C. J. & TIMBERLAKE, W. E. 1996. Saccharomyces cerevisiae TEC1 is required for pseudohyphal growth. *Mol Microbiol,* 19**,** 1255-63.

GILLOOLY, D. J., SIMONSEN, A. & STENMARK, H. 2001. Cellular functions of phosphatidylinositol 3-phosphate and FYVE domain proteins. *Biochem J,* 355**,** 249-58.

GODFRAY, H. C., BEDDINGTON, J. R., CRUTE, I. R., HADDAD, L., LAWRENCE, D., MUIR, J. F., PRETTY, J., ROBINSON, S., THOMAS, S. M. & TOULMIN, C. 2010. Food security: the challenge of feeding 9 billion people. *Science,* 327**,** 812-8.

GREWAL, S. I. & ELGIN, S. C. 2007. Transcription and RNA interference in the formation of heterochromatin. *Nature,* 447**,** 399-406.

GUTIERREZ, R. M. & HNILICA, L. S. 1967. Tissue specificity of histone phosphorylation. *Science,* 157**,** 1324-5.

HAN, K. H., HAN, K. Y., YU, J. H., CHAE, K. S., JAHNG, K. Y. & HAN, D. M. 2001. The *nsdD* gene encodes a putative GATA-type transcription factor necessary for sexual development of *Aspergillus nidulans*. *Mol Microbiol,* 41**,** 299-309.

HAN, K. H., SEO, J. A. & YU, J. H. 2004. Regulators of G-protein signalling in Aspergillus nidulans: RgsA downregulates stress response and stimulates asexual sporulation through attenuation of GanB (Galpha) signalling. *Mol Microbiol,* 53**,** 529-40.

HANAHAN, D., JESSEE, J. & BLOOM, F. R. 1991. Plasmid transformation of Escherichia coli and other bacteria. *Methods Enzymol,* 204**,** 63-113.

HARTING, Y., BAYRAM, O., LAUBINGER, K., VALERIUS, O. & BRAUS, G. H. 2013. Interplay of the fungal sumoylation network for control of multicellular development. *Mol Microbiol*.

HAWKSWORTH, D. L. & ROSSMAN, A. Y. 1997. Where are all the undescribed fungi? *Phytopathology,* 87**,** 888-91.

HAYAKAWA, A., HAYES, S., LEONARD, D., LAMBRIGHT, D. & CORVERA, S. 2007. Evolutionarily conserved structural and functional roles of the FYVE domain. *Biochem Soc Symp***,** 95-105.

HAYAKAWA, A., HAYES, S. J., LAWE, D. C., SUDHARSHAN, E., TUFT, R., FOGARTY, K., LAMBRIGHT, D. & CORVERA, S. 2004. Structural basis for endosomal targeting by FYVE domains. *J Biol Chem,* 279**,** 5958-66.

HEBBES, T. R., THORNE, A. W. & CRANE-ROBINSON, C. 1988. A direct link between core histone acetylation and transcriptionally active chromatin. *EMBO J,* 7**,** 1395-402.

HELMSTAEDT, K., SCHWIER, E. U., CHRISTMANN, M., NAHLIK, K., WESTERMANN, M., HARTING, R., GROND, S., BUSCH, S. & BRAUS, G. H. 2011. Recruitment of the inhibitor Cand1 to the cullin substrate adaptor site mediates interaction to the neddylation site. *Mol Biol Cell,* 22**,** 153-64.

HOFFMANN, B., VALERIUS, O., ANDERMANN, M. & BRAUS, G. H. 2001. Transcriptional autoregulation and inhibition of mRNA translation of amino acid regulator gene *cpcA* of filamentous fungus *Aspergillus nidulans*. *Mol Biol Cell,* 12**,** 2846-57.

HOFFMANN, B., WANKE, C., LAPAGLIA, S. K. & BRAUS, G. H. 2000. c-Jun and RACK1 homologues regulate a control point for sexual development in *Aspergillus nidulans*. *Mol Microbiol,* 37**,** 28-41.

KAEFER, E. 1965. Origins of translocations in *Aspergillus nidulans*. *Genetics,* 52**,** 217-232.

KAEVER, A., LANDESFEIND, M., POSSIENKE, M., FEUSSNER, K., FEUSSNER, I. & MEINICKE, P. 2012. MarVis-Filter: ranking, filtering, adduct and isotope correction of mass spectrometry data. *J Biomed Biotechnol,* 2012**,** 263910.

KAEVER, A., LINGNER, T., FEUSSNER, K., GOBEL, C., FEUSSNER, I. & MEINICKE, P. 2009. MarVis: a tool for clustering and visualization of metabolic biomarkers. *BMC Bioinformatics,* 10**,** 92.

KARVE, T. M. & CHEEMA, A. K. 2011. Small changes huge impact: the role of protein posttranslational modifications in cellular homeostasis and disease. *Journal of amino acids,* 2011**,** 207691.

KATO, N., BROOKS, W. & CALVO, A. M. 2003. The expression of sterigmatocystin and penicillin genes in *Aspergillus nidulans* is controlled by *veA*, a gene required for sexual development. *Eukaryot Cell,* 2**,** 1178-86.

KELLER, N. P., TURNER, G. & BENNETT, J. W. 2005. Fungal secondary metabolism - from biochemistry to genomics. *Nat Rev Microbiol,* 3**,** 937-47.

KENTNER, D. & SOURJIK, V. 2009. Dynamic map of protein interactions in the Escherichia coli chemotaxis pathway. *Mol Syst Biol,* 5**,** 238.

KIM, H., HAN, K., KIM, K., HAN, D., JAHNG, K. & CHAE, K. 2002. The *veA* gene activates sexual development in *Aspergillus nidulans*. *Fungal Genet Biol,* 37**,** 72-80.

KIM, H. R., CHAE, K. S., HAN, K. H. & HAN, D. M. 2009. The *nsdC* gene encoding a putative C2H2-type transcription factor is a key activator of sexual development in *Aspergillus nidulans*. *Genetics,* 182**,** 771-83.

KOZBIAL, P. Z. & MUSHEGIAN, A. R. 2005. Natural history of S-adenosylmethionine-binding proteins. *BMC Struct Biol,* 5**,** 19.

KRAPPMANN, S., JUNG, N., MEDIC, B., BUSCH, S., PRADE, R. A. & BRAUS, G. H. 2006. The *Aspergillus nidulans* F-box protein GrrA links SCF activity to meiosis. *Mol Microbiol,* 61**,** 76-88.

KROGAN, N. J., DOVER, J., KHORRAMI, S., GREENBLATT, J. F., SCHNEIDER, J., JOHNSTON, M. & SHILATIFARD, A. 2002. COMPASS, a histone H3 (Lysine 4) methyltransferase required for telomeric silencing of gene expression. *J Biol Chem,* 277**,** 10753-5.

KUENG, S., OPPIKOFER, M. & GASSER, S. M. 2013. SIR Proteins and the Assembly of Silent Chromatin in Budding Yeast. *Annual review of genetics*.

KWON, N. J., GARZIA, A., ESPESO, E. A., UGALDE, U. & YU, J. H. 2010a. FlbC is a putative nuclear C2H2 transcription factor regulating development in *Aspergillus nidulans*. *Mol Microbiol,* 77**,** 1203-19.

KWON, N. J., SHIN, K. S. & YU, J. H. 2010b. Characterization of the developmental regulator FlbE in Aspergillus fumigatus and *Aspergillus nidulans*. *Fungal Genet Biol,* 47**,** 981-93.

LARA-ORTIZ, T., RIVEROS-ROSAS, H. & AGUIRRE, J. 2003. Reactive oxygen species generated by microbial NADPH oxidase NoxA regulate sexual development in *Aspergillus nidulans*. *Mol Microbiol,* 50**,** 1241-55.

LEE, D. W., FREITAG, M., SELKER, E. U. & ARAMAYO, R. 2008. A cytosine methyltransferase homologue is essential for sexual development in *Aspergillus nidulans*. *PLoS One,* 3**,** e2531.

LEE, J., SAYEGH, J., DANIEL, J., CLARKE, S. & BEDFORD, M. T. 2005. PRMT8, a new membrane-bound tissue-specific member of the protein arginine methyltransferase family. *J Biol Chem,* 280**,** 32890-6.

LEJEUNE, E., BAYNE, E. H. & ALLSHIRE, R. C. 2010. On the connection between RNAi and heterochromatin at centromeres. *Cold Spring Harbor symposia on quantitative biology,* 75**,** 275-83.

LI, S., MYUNG, K., GUSE, D., DONKIN, B., PROCTOR, R. H., GRAYBURN, W. S. & CALVO, A. M. 2006. FvVE1 regulates filamentous growth, the ratio of microconidia to macroconidia and cell wall formation in Fusarium verticillioides. *Mol Microbiol,* 62**,** 1418-32.

LIMA, J. F., MALAVAZI, I., VON ZESKA KRESS FAGUNDES, M. R., SAVOLDI, M., GOLDMAN, M. H., SCHWIER, E., BRAUS, G. H. & GOLDMAN, G. H. 2005. The csnD/csnE signalosome genes are involved in the Aspergillus nidulans DNA damage response. *Genetics,* 171**,** 1003-15.

LIVAK, K. J. & SCHMITTGEN, T. D. 2001. Analysis of relative gene expression data using real-time quantitative PCR and the 2(-Delta Delta C(T)) Method. *Methods,* 25**,** 402-8.

LOW, D. A. & CASADESUS, J. 2008. Clocks and switches: bacterial gene regulation by DNA adenine methylation. *Curr Opin Microbiol,* 11**,** 106-12.

LUGER, K., MADER, A. W., RICHMOND, R. K., SARGENT, D. F. & RICHMOND, T. J. 1997. Crystal structure of the nucleosome core particle at 2.8 A resolution. *Nature,* 389**,** 251-60.

MADHANI, H. D. 2007. *From a to α: yeast as a model for cellular differentiation.,* Cold Spring Harbod, NY, Cold Spring Harbor Press.

MAISON, C. & ALMOUZNI, G. 2004. HP1 and the dynamics of heterochromatin maintenance. *Nat Rev Mol Cell Biol,* 5**,** 296-304.

MIN, J., FENG, Q., LI, Z., ZHANG, Y. & XU, R. M. 2003. Structure of the catalytic domain of human DOT1L, a non-SET domain nucleosomal histone methyltransferase. *Cell,* 112**,** 711-23.

MURO-PASTOR, M. I., GONZALEZ, R., STRAUSS, J., NARENDJA, F. & SCAZZOCCHIO, C. 1999. The GATA factor AreA is essential for chromatin remodelling in a eukaryotic bidirectional promoter. *Embo J,* 18**,** 1584-97.

NAGY, P. L., GRIESENBECK, J., KORNBERG, R. D. & CLEARY, M. L. 2002. A trithorax-group complex purified from *Saccharomyces cerevisiae* is required for methylation of histone H3. *Proc Natl Acad Sci U S A,* 99**,** 90-4.

NAHLIK, K., DUMKOW, M., BAYRAM, O., HELMSTAEDT, K., BUSCH, S., VALERIUS, O., GERKE, J., HOPPERT, M., SCHWIER, E., OPITZ, L., WESTERMANN, M., GROND, S., FEUSSNER, K., GOEBEL, C., KAEVER, A., MEINICKE, P., FEUSSNER, I. & BRAUS, G. H. 2010. The COP9 signalosome mediates transcriptional and metabolic response to hormones, oxidative stress protection and cell wall rearrangement during fungal development. *Mol Microbiol,* 78**,** 964-79.

NATHAN, D., INGVARSDOTTIR, K., STERNER, D. E., BYLEBYL, G. R., DOKMANOVIC, M., DORSEY, J. A., WHELAN, K. A., KRSMANOVIC, M., LANE, W. S., MELUH, P. B., JOHNSON, E. S. & BERGER, S. L. 2006. Histone sumoylation is a negative regulator in Saccharomyces cerevisiae and shows dynamic interplay with positive-acting histone modifications. *Genes Dev,* 20**,** 966-76.

NAYAK, T., SZEWCZYK, E., OAKLEY, C. E., OSMANI, A., UKIL, L., MURRAY, S. L., HYNES, M. J., OSMANI, S. A. & OAKLEY, B. R. 2006. A versatile and efficient gene-targeting system for Aspergillus nidulans. *Genetics,* 172**,** 1557-66.

NGUYEN, A. T. & ZHANG, Y. 2011. The diverse functions of Dot1 and H3K79 methylation. *Genes & development,* 25**,** 1345-58.

NI, M., FERETZAKI, M., SUN, S., WANG, X. & HEITMAN, J. 2011. Sex in fungi. *Annual review of genetics,* 45**,** 405-30.

105

NI, M., RIERSON, S., SEO, J. A. & YU, J. H. 2005. The *pkaB* gene encoding the secondary protein kinase A catalytic subunit has a synthetic lethal interaction with *pkaA* and plays overlapping and opposite roles in *Aspergillus nidulans*. *Eukaryot Cell,* 4**,** 1465-76.

NI, M. & YU, J. H. 2007. A novel regulator couples sporogenesis and trehalose biogenesis in Aspergillus nidulans. *PLoS One,* 2**,** e970.

NORMILE, D. 2010. Spoiling for a fight with mold. *Science,* 327**,** 807.

NUTZMANN, H. W., REYES-DOMINGUEZ, Y., SCHERLACH, K., SCHROECKH, V., HORN, F., GACEK, A., SCHUMANN, J., HERTWECK, C., STRAUSS, J. & BRAKHAGE, A. A. 2011. Bacteria-induced natural product formation in the fungus *Aspergillus nidulans* requires Saga/Ada-mediated histone acetylation. *Proc Natl Acad Sci U S A,* 108**,** 14282-7.

O'BRIEN, H. E., PARRENT, J. L., JACKSON, J. A., MONCALVO, J. M. & VILGALYS, R. 2005. Fungal community analysis by large-scale sequencing of environmental samples. *Appl Environ Microbiol,* 71**,** 5544-50.

PALMER, J. M. & KELLER, N. P. 2010. Secondary metabolism in fungi: does chromosomal location matter? *Curr Opin Microbiol,* 13**,** 431-6.

PALMER, J. M., PERRIN, R. M., DAGENAIS, T. R. & KELLER, N. P. 2008. H3K9 methylation regulates growth and development in *Aspergillus fumigatus*. *Eukaryot Cell,* 7**,** 2052-60.

PALMER, J. M., THEISEN, J. M., DURAN, R. M., GRAYBURN, W. S., CALVO, A. M. & KELLER, N. P. 2013. Secondary metabolism and development is mediated by LlmF control of VeA subcellular localization in *Aspergillus nidulans*. *PLoS Genet,* 9**,** e1003193.

PAOLETTI, M., SEYMOUR, F. A., ALCOCER, M. J., KAUR, N., CALVO, A. M., ARCHER, D. B. & DYER, P. S. 2007. Mating type and the genetic basis of self-fertility in the model fungus Aspergillus nidulans. *Curr Biol,* 17**,** 1384-9.

PARK, H. S., BAYRAM, O., BRAUS, G. H., KIM, S. C. & YU, J. H. 2012. Characterization of the velvet regulators in *Aspergillus fumigatus*. *Molecular microbiology,* 86**,** 937-53.

PARK, H. S. & YU, J. H. 2012. Genetic control of asexual sporulation in filamentous fungi. *Curr Opin Microbiol,* 15**,** 669-77.

PATANANAN, A. N., PALMER, J. M., GARVEY, G. S., KELLER, N. P. & CLARKE, S. G. 2013. A novel automethylation reaction in the *Aspergillus nidulans* LaeA protein generates S-methylmethionine. *J Biol Chem,* 288**,** 14032-45.

PERRIN, R. M., FEDOROVA, N. D., BOK, J. W., CRAMER, R. A., WORTMAN, J. R., KIM, H. S., NIERMAN, W. C. & KELLER, N. P. 2007. Transcriptional regulation of chemical diversity in *Aspergillus fumigatus* by LaeA. *PLoS Pathog,* 3**,** e50.

PÖGGELER, S., NOWROUSIAN, M. & KÜCK, U. 2006. Fruiting-Body Development in Ascomycetes. *In:* FISCHER, K. (ed.) *The Mycota I   Growth, Differentiation and Sexuality.* Heidelberg: Springer-Verlag.

PRABAKARAN, S., LIPPENS, G., STEEN, H. & GUNAWARDENA, J. 2012. Post-translational modification: nature's escape from genetic imprisonment and the basis for dynamic information encoding. *Wiley interdisciplinary reviews. Systems biology and medicine,* 4**,** 565-83.

PUNT, P. J. & VAN DEN HONDEL, C. A. 1992. Transformation of filamentous fungi based on hygromycin B and phleomycin resistance markers. *Methods Enzymol,* 216**,** 447-57.

PURSCHWITZ, J., MULLER, S. & FISCHER, R. 2009. Mapping the interaction sites of *Aspergillus nidulans* phytochrome FphA with the global regulator VeA and the White Collar protein LreB. *Mol Genet Genomics,* 281**,** 35-42.

PURSCHWITZ, J., MULLER, S., KASTNER, C., SCHOSER, M., HAAS, H., ESPESO, E. A., ATOUI, A., CALVO, A. M. & FISCHER, R. 2008. Functional and physical interaction of blue- and red-light sensors in *Aspergillus nidulans*. *Curr Biol,* 18**,** 255-9.

RASPOR, P. & ZUPAN, J. 2006. Yeasts in extreme environments. *In:* ROSA, C. & GABOR, P. (eds.) *Biodiversity and ecophysiology of yeasts.* Berlin, Germany: Verlag.

REUTER, G., GIARRE, M., FARAH, J., GAUSZ, J., SPIERER, A. & SPIERER, P. 1990. Dependence of position-effect variegation in Drosophila on dose of a gene encoding an unusual zinc-finger protein. *Nature,* 344**,** 219-23.

REYES-DOMINGUEZ, Y., BOK, J. W., BERGER, H., SHWAB, E. K., BASHEER, A., GALLMETZER, A., SCAZZOCCHIO, C., KELLER, N. & STRAUSS, J. 2010. Heterochromatic marks are associated with the repression of secondary metabolism clusters in *Aspergillus nidulans*. *Mol Microbiol,* 76**,** 1376-86.

RIVETT, A. J., FRANCIS, A. & ROTH, J. A. 1983. Localization of membrane-bound catechol-O-methyltransferase. *J Neurochem,* 40**,** 1494-6.

ROBINSON, P. J., FAIRALL, L., HUYNH, V. A. & RHODES, D. 2006. EM measurements define the dimensions of the "30-nm" chromatin fiber: evidence for a compact, interdigitated structure. *Proceedings of the National Academy of Sciences of the United States of America,* 103**,** 6506-11.

RODRIGUEZ-ROMERO, J., HEDTKE, M., KASTNER, C., M¸LLER, S. & FISCHER, R. 2010. Fungi, hidden in soil or up in the air: light makes a difference. *Annu Rev Microbiol,* 64**,** 585-610.

RODRIGUEZ-URRA, A. B., JIMENEZ, C., NIETO, M. I., RODRIGUEZ, J., HAYASHI, H. & UGALDE, U. 2012. Signaling the induction of sporulation involves the interaction of two secondary metabolites in *Aspergillus nidulans*. *ACS Chem Biol,* 7**,** 599-606.

ROGUEV, A., SCHAFT, D., SHEVCHENKO, A., PIJNAPPEL, W. W., WILM, M., AASLAND, R. & STEWART, A. F. 2001. The *Saccharomyces cerevisiae* Set1 complex includes an Ash2 homologue and methylates histone 3 lysine 4. *EMBO J,* 20**,** 7137-48.

ROHLFS, M., ALBERT, M., KELLER, N. P. & KEMPKEN, F. 2007. Secondary chemicals protect mould from fungivory. *Biol Lett,* 3**,** 523-5.

SAIKI, R. K., BUGAWAN, T. L., HORN, G. T., MULLIS, K. B. & ERLICH, H. A. 1986. Analysis of enzymatically amplified beta-globin and HLA-DQ alpha DNA with allele-specific oligonucleotide probes. *Nature,* 324**,** 163-6.

SAMBROOK, J., MANIATIS, T. & FRITSCH, E. F. 1989. *Molecular cloning : a laboratory manual,* Cold Spring Harbor, N.Y., Cold Spring Harbor Laboratory Press.

SANCHEZ, J. F., CHIANG, Y. M., SZEWCZYK, E., DAVIDSON, A. D., AHUJA, M., ELIZABETH OAKLEY, C., WOO BOK, J., KELLER, N., OAKLEY, B. R. & WANG, C. C. 2010. Molecular genetic analysis of the orsellinic acid/F9775 gene cluster of Aspergillus nidulans. *Mol Biosyst,* 6**,** 587-93.

SARIKAYA BAYRAM, O., BAYRAM, O., VALERIUS, O., PARK, H. S., IRNIGER, S., GERKE, J., NI, M., HAN, K. H., YU, J. H. & BRAUS, G. H. 2010. LaeA control of velvet family regulatory proteins for light-dependent development and fungal cell-type specificity. *PLoS Genet,* 6**,** e1001226.

SASSONE-CORSI, P., MIZZEN, C. A., CHEUNG, P., CROSIO, C., MONACO, L., JACQUOT, S., HANAUER, A. & ALLIS, C. D. 1999. Requirement of Rsk-2 for epidermal growth factor-activated phosphorylation of histone H3. *Science,* 285**,** 886-91.

SCHOTTA, G., LACHNER, M., SARMA, K., EBERT, A., SENGUPTA, R., REUTER, G., REINBERG, D. & JENUWEIN, T. 2004. A silencing pathway to induce H3-K9 and H4-K20 trimethylation at constitutive heterochromatin. *Genes Dev,* 18**,** 1251-62.

SCHROECKH, V., SCHERLACH, K., NUTZMANN, H. W., SHELEST, E., SCHMIDT-HECK, W., SCHUEMANN, J., MARTIN, K., HERTWECK, C. & BRAKHAGE, A. A. 2009. Intimate bacterial-fungal interaction triggers biosynthesis of archetypal polyketides in *Aspergillus nidulans*. *Proc Natl Acad Sci U S A,* 106**,** 14558-63.

SCHULZ, B., BANUETT, F., DAHL, M., SCHLESINGER, R., SCHAFER, W., MARTIN, T., HERSKOWITZ, I. & KAHMANN, R. 1990. The b alleles of *U. maydis*, whose combinations program pathogenic development, code for polypeptides containing a homeodomain-related motif. *Cell,* 60**,** 295-306.

SEILER, S., VOGT, N., ZIV, C., GOROVITS, R. & YARDEN, O. 2006. The STE20/Germinal Center Kinase POD6 Interacts with the NDR Kinase COT1 and Is Involved in Polar Tip Extension in *Neurospora crassa*. *Mol Biol Cell,* 17**,** 4080-92.

SELKER, E. U., TOUNTAS, N. A., CROSS, S. H., MARGOLIN, B. S., MURPHY, J. G., BIRD, A. P. & FREITAG, M. 2003. The methylated component of the *Neurospora crassa* genome. *Nature,* 422**,** 893-7.

SEO, J. A., HAN, K. H. & YU, J. H. 2005. Multiple roles of a heterotrimeric G-protein gamma-subunit in governing growth and development of *Aspergillus nidulans*. *Genetics,* 171**,** 81-9.

SEWALL, T. C., MIMS, C. W. & TIMBERLAKE, W. E. 1990. *abaA* controls phialide differentiation in *Aspergillus nidulans*. *Plant Cell,* 2**,** 731-9.

SHEN, X., YU, L., WEIR, J. W. & GOROVSKY, M. A. 1995. Linker histones are not essential and affect chromatin condensation in vivo. *Cell,* 82**,** 47-56.

SHIIO, Y. & EISENMAN, R. N. 2003. Histone sumoylation is associated with transcriptional repression. *Proc Natl Acad Sci U S A,* 100**,** 13225-30.

SHIMIZU, K., HICKS, J. K., HUANG, T. P. & KELLER, N. P. 2003. Pka, Ras and RGS protein interactions regulate activity of AflR, a Zn(II)2Cys6 transcription factor in *Aspergillus nidulans*. *Genetics,* 165**,** 1095-104.

SHWAB, E. K., BOK, J. W., TRIBUS, M., GALEHR, J., GRAESSLE, S. & KELLER, N. P. 2007. Histone deacetylase activity regulates chemical diversity in Aspergillus. *Eukaryot Cell,* 6**,** 1656-64.

SMITH, M. & MARCH, J. 2001. *March's advanced organic chemistry : reactions, mechanisms, and structure,* New York, John Wiley & Sons.

SMITH, Z. D. & MEISSNER, A. 2013. DNA methylation: roles in mammalian development. *Nature reviews. Genetics,* 14**,** 204-20.

SOHN , K. T. & YOON, K. S. 2002. Ultrastructural Study on the Cleistothecium Development in *Aspergillus nidulans. Mycobiology,* 30**,** 117-127.

SOUTHERN, E. M. 1975. Detection of specific sequences among DNA fragments separated by gel electrophoresis. *J Mol Biol,* 98**,** 503-17.

STINNETT, S. M., ESPESO, E. A., COBENO, L., ARAUJO-BAZAN, L. & CALVO, A. M. 2007. *Aspergillus nidulans* VeA subcellular localization is dependent on the importin alpha carrier and on light. *Mol Microbiol,* 63**,** 242-55.

STRAHL, B. D., GRANT, P. A., BRIGGS, S. D., SUN, Z. W., BONE, J. R., CALDWELL, J. A., MOLLAH, S., COOK, R. G., SHABANOWITZ, J., HUNT, D. F. & ALLIS, C. D. 2002. Set2 is a nucleosomal histone H3-selective methyltransferase that mediates transcriptional repression. *Mol Cell Biol,* 22**,** 1298-306.

STRANGE, R. N. & SCOTT, P. R. 2005. Plant disease: a threat to global food security. *Annu Rev Phytopathol,* 43**,** 83-116.

STRAUSS, J. & REYES-DOMINGUEZ, Y. 2010. Regulation of secondary metabolism by chromatin structure and epigenetic codes. *Fungal Genet Biol,* 48**,** 62-9.

STRUCK, A. W., THOMPSON, M. L., WONG, L. S. & MICKLEFIELD, J. 2012. S-adenosyl-methionine-dependent methyltransferases: highly versatile enzymes in biocatalysis, biosynthesis and other biotechnological applications. *Chembiochem : a European journal of chemical biology,* 13**,** 2642-55.

STRUHL, K. & SEGAL, E. 2013. Determinants of nucleosome positioning. *Nature structural & molecular biology,* 20**,** 267-73.

SZEWCZYK, E., NAYAK, T., OAKLEY, C. E., EDGERTON, H., XIONG, Y., TAHERI-TALESH, N., OSMANI, S. A. & OAKLEY, B. R. 2006. Fusion PCR and gene targeting in Aspergillus nidulans. *Nat Protoc,* 1**,** 3111-20.

TAYLOR, L. H., LATHAM, S. M. & WOOLHOUSE, M. E. 2001. Risk factors for human disease emergence. *Philos Trans R Soc Lond B Biol Sci,* 356**,** 983-9.

TODD, R. B., HYNES, M. J. & ANDRIANOPOULOS, A. 2006. The *Aspergillus nidulans rcoA* gene is required for *veA*-dependent sexual development. *Genetics,* 174**,** 1685-8.

TSITSIGIANNIS, D. I., KOWIESKI, T. M., ZARNOWSKI, R. & KELLER, N. P. 2004. Endogenous lipogenic regulators of spore balance in *Aspergillus nidulans. Eukaryot Cell,* 3**,** 1398-411.

TSITSIGIANNIS, D. I., KOWIESKI, T. M., ZARNOWSKI, R. & KELLER, N. P. 2005. Three putative oxylipin biosynthetic genes integrate sexual and asexual development in *Aspergillus nidulans. Microbiology,* 151**,** 1809-21.

TUNCHER, A., REINKE, H., MARTIC, G., CARUSO, M. L. & BRAKHAGE, A. A. 2004. A basic-region helix-loop-helix protein-encoding gene (*devR*) involved in the development of *Aspergillus nidulans. Mol Microbiol,* 52**,** 227-41.

VALLIM, M. A., MILLER, K. Y. & MILLER, B. L. 2000. Aspergillus SteA (sterile12-like) is a homeodomain-C2/H2-Zn+2 finger transcription factor required for sexual reproduction. *Mol Microbiol,* 36**,** 290-301.

VIENKEN, K. & FISCHER, R. 2006. The Zn(II)2Cys6 putative transcription factor NosA controls fruiting body formation in *Aspergillus nidulans. Mol Microbiol,* 61**,** 544-54.

WEBSTER, R. H. & SIL, A. 2008. Conserved factors Ryp2 and Ryp3 control cell morphology and infectious spore formation in the fungal pathogen Histoplasma capsulatum. *Proc Natl Acad Sci U S A,* 105**,** 14573-8.

WEI, H., REQUENA, N. & FISCHER, R. 2003. The MAPKK kinase SteC regulates conidiophore morphology and is essential for heterokaryon formation and sexual development in the homothallic fungus *Aspergillus nidulans. Mol Microbiol,* 47**,** 1577-88.

WEI, H., SCHERER, M., SINGH, A., LIESE, R. & FISCHER, R. 2001. Aspergillus nidulans alpha-1,3 glucanase (mutanase), mutA, is expressed during sexual development and mobilizes mutan. *Fungal Genet Biol,* 34**,** 217-27.

WIESER, J. & ADAMS, T. H. 1995. *flbD* encodes a Myb-like DNA-binding protein that coordinates initiation of *Aspergillus nidulans* conidiophore development. *Genes Dev,* 9**,** 491-502.

WIESER, J., LEE, B. N., FONDON, J., 3RD & ADAMS, T. H. 1994. Genetic requirements for initiating asexual development in *Aspergillus nidulans*. *Curr Genet,* 27**,** 62-9.

WONG, K. H., TODD, R. B., OAKLEY, B. R., OAKLEY, C. E., HYNES, M. J. & DAVIS, M. A. 2008. Sumoylation in Aspergillus nidulans: sumO inactivation, overexpression and live-cell imaging. *Fungal Genet Biol,* 45**,** 728-37.

WU, J. & MILLER, B. L. 1997. Aspergillus asexual reproduction and sexual reproduction are differentially affected by transcriptional and translational mechanisms regulating stunted gene expression. *Mol Cell Biol,* 17**,** 6191-201.

YANG, Y. & BEDFORD, M. T. 2013. Protein arginine methyltransferases and cancer. *Nat Rev Cancer,* 13**,** 37-50.

YU, J. H., WIESER, J. & ADAMS, T. H. 1996. The Aspergillus FlbA RGS domain protein antagonizes G protein signaling to block proliferation and allow development. *EMBO J,* 15**,** 5184-90.

Abbreviations

ATP	....	Adenosine triphosphate
BIFC	....	Bimolecular fluorescence complementation
BSA	....	Bovine serum albumin
C-terminus	....	Carboxy-terminus
CBP	....	Calmodulin binding peptide
ChIP	....	Chromatin immunoprecipitation
Co-IP	....	Coimmunoprecipitation
CpG	....	Cytosine-phosphate-Guanine
DAPI	....	4´-6´-Diamidino-2-phenylindol
ddH$_2$O	....	double distilled H$_2$O
DIC	....	Differential interference contrast
DIG	....	Digoxigenin
DNA	....	Deoxyribonucleic acid
DTT	....	DL-dithiothreitol
E-YFP	....	Enhanced yellow fluorescent protein
EDTA	....	Ethylenediaminetetraacetic acid
FYVE	....	Fab1, YOTB, Vac1, EEA1
GFP	....	Green fluorescent protein
GMM	....	Glucose Minimal Medium
gpdA	....	Glyceraldehyde-3-phosphate dehydrogenase
h	....	Hour
H3K27 me3	....	Histone 3 Lysine 27 trimethylation
H3K36 me3	....	Histone 3 Lysine 36 trimethylation
H3K4 me2	....	Histone 3 Lysine 4 dimethylation
H3K4 me3	....	Histone 3 Lysine 4 trimethylation
H3K79 me3	....	Histone 3 Lysine 79 trimethylation
H3K9 me2	....	Histone 3 Lysine 9 dimethylation
H3K9 me3	....	Histone 3 Lysine 9 trimethylation
H4K20 me3	....	Histone 4 Lysine 20 trimethylation
HAT	....	Histone acetyltransferase
HDAC	....	Histone deacetylase
HMT	....	Histone methyltransferase
HP1	....	Heterochromatin protein 1
Kbp	....	Kilobase pairs
kDa	....	Kilodaltons
LaeA	....	loss of aflR expression A
MAPK	....	Mitogen activated protein kinase
min	....	Minute
mRNA	....	messenger RNA
N-terminus	....	(NH$_2$) Amino-terminus
natR	....	nourseothricin resistance gene
NLS	....	Nuclear localization signal

nm	....	nanometer
OA	....	Orsellinic acid
OE	....	Overexpression
ORF	....	Open reading frame
PCR	....	Polymerase chain reaction
PEB	....	Protein extraction buffer
PN	....	Penicillin
PNK	....	Polynucleotide kinase
PRC	....	Polycomb repressive complex
PRMT	....	Protein arginine methyltransferase
PTM	....	Posttranslational modification
ptrA	....	Pyrithiamine resistance gene A
RFP	....	Red fluorescent protein
RGS	....	Regulator of G-protein signaling
RNA	....	Ribonucleic acid
ROS	....	Reactive oxygen species
RT	....	Room temperature
Ryp	....	Required for yeast phase
SAM	....	S-adenosyl-L-methionine
SDS	....	Sodium dodecylsulfate
SET	....	Supressor enhancer of zeste trithorax
ST	....	Sterigmatocystin
SUMO	....	Small ubiquitin-like modifier
TAP	....	Tandem affinity purification
TBS	....	Tris buffered saline
TLC	....	Thin layer chromatography
TQ	....	Terrequinone
UTR	....	Untranslated region
UVA	....	Ultraviolet A
VapA,B	....	VipC associated proteins
Vip	....	Velvet interacting protein
Wt	....	*wild-type*
YTH	....	Yeast two-hybrid
ZF	....	Zinc Finger
μm	....	micrometer

Acknowledgments

I would like to thank Prof. Dr. Gerhard H. Braus for supporting my research starting from my early diploma years in Biology and providing his department to do my doctoral work.

Special thanks to Prof. Dr. Stefanie Pöggeler and Prof. Dr. Heike Krebber for being in my doctoral thesis committee as well as supporting my research with various helpful suggestions and advice. I thank PD Dr. Stefan Irniger, PD Dr. Marko Rohlfs and PD Dr. Michael Hoppert for kindly accepting to be in my examination board.

I am indebted to Dr. Özgür Bayram for his supervision in molecular biology methods, and his constant support outside the lab. I would also like to thank Dr. Fatih Sari and Dr. Tanja Kuczera for their help during my initial years of diploma studies.

I am also grateful to Göttingen Graduate School for Neurosciences, Biophysics, and Molecular Biosciences (GGNB) for financing me with their "excellence-stipend" and providing me with "travel grants" to present my results in various national as well as international conferences. I am thankful to the GGNB office especially, Mrs. Christin Fischer, Mrs. Christina Bach, Mrs. Kirsten Pöhlker, Mrs. Simone Pairan and Dr. Steffen Burkhardt for their continuous support.

For metabolite fingerprinting and detailed analysis of the secondary metabolites, I would like to thank Dr. Kirstin Feussner and Mr. Alexander Kaever. Many thanks to Dr. Van Tuan Tran and Mrs. Gertrud Stahlhut for important tips for qRT-PCR and Dr. Oliver Valerius for mass spectrometry identifications of the protein complexes. I thank Dr. Kangkan Halder for proofreading my thesis.

I have been very influenced by two very friendly Japanese postdocs Dr. Jun-Ichi Maruyama and Dr. Satoshi Suzuki, who taught me valuable experimental methods. I also thank Mrs. Maria Meyer for her friendly support and coffe-chats on Fridays and Mrs. Nicole Scheiter as well as Mrs. Heidi Northemann for their help with reagents and numerous official matters. I also thank the members of my lab Basti and Karl.

My deepest thanks go to my father-in-law Mr. Bayram Ali Bayram, my mother-in-law Mrs. Hatice Bayram and sister-in-law Mrs. Nilgün Bayram for their endless support during my doctoral studies.

Finally, my heartfull appreciation and thanks go to my beloved mother, Mrs. Gülten Sarikaya, who devoted her life to her children and unfortunately left us too early.

Curriculum vitae

Personal details

Özlem Sarikaya Bayram

born on January 13th, 1982

in Istanbul, Turkey

Education

1988 – 1996   **Primary and secondary education**, Sabiha Hanim Primary and Secondary School in Sakarya, Turkey.

1996 – 2000   **High school education,** Bursa Kiz Lisesi (Girl´s High School) in Bursa, Turkey

Scientific background

2000 – 2004   **Study of Biology (BSc)** at the Uludag University in Bursa, Turkey

2004 – 2006   Study of English and German Language in Bursa, Turkey and Göttingen, Germany

2006 – 2008   **Study of Diploma in Biology** at the Georg-August University in Göttingen. Subjects: Microbiology, Genetics and Botany

2008 – 2009   **Diploma thesis** „Role of methyltransferases in development and coordinated secondary metabolism in the filamentous fungus *Aspergillus nidulans*" at the Department of Molecular Microbiology and Genetics at the Georg-August University in Göttingen (Prof. Dr. Gerhard H. Braus).

2010 -   Member of the "Göttingen Graduate School for Neurosciences and Molecular Biosciences" (GGNB).

2010 - 2014   **Research assistant and doctoral student** at the Department of Molecular Microbiology and Genetics at the Georg-August University in Göttingen (Prof. Dr. Gerhard H. Braus).